CENTRELINE SEGREGATION IN CONTINUOUSLY CAST STEEL BILLETS

by

Rajesh Kumar Goyal

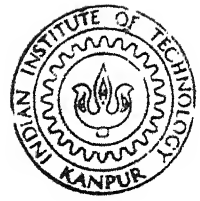

DEPARTMENT OF METALLURGICAL ENGINEERING

INDIAN INSTITUTE OF TECHNOLOGY KANPUR

November, 1991

CENTRELINE SEGREGATION IN CONTINUOUSLY CAST STEEL BILLETS

A Thesis Submitted
In Partial Fulfilment of the Requirements
for the Degree of
MASTER OF TECHNOLOGY

by

Rajesh Kumar Goyal

to the

DEPARTMENT OF METALLURGICAL ENGINEERING
INDIAN INSTITUTE OF TECHNOLOGY KANPUR

November, 1991

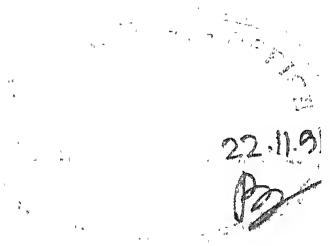

CERTIFICATE

This is to certify that the work **"Centreline Segregation in Continuously Cast Steel Billets"** has been carried out by **Mr. Rajesh Kumar Goyal** under my supervision and that it has not been submitted elsewhere for a degree.

(**A. Ghosh**)
Professor
Department of Metallurgical Engineering
Indian Institute of Technology
KANPUR

ACKNOWLEDGEMENTS

It is a great pleasure in expressing my sense of profound gratitude and indebtedness to Professor Ahindra Ghosh for his able guidance and constant encouragement during the course of this work.

The present work is a part of the project sponsored by National Mission of Iron and Steel, Department of Steel, Government of India. Their financial support as well as necessary help by Research and Development Centre for Iron and Steel, Ranchi are duly acknowledged.

My thanks are due to Management of Haryana Concast Ltd., Hisar, Haryana for providing continuously cast billet sections and other help rendered by them during plant data collection.

Thanks are also due to Management of National Metallurgical Laboratory, Jamshedpur for the timely help in using their Automatic Carbon and Sulphur Determinator and other help provided by Mr.K.G. Sengupta during carbon and sulphur analysis.

I am very much indebted to Dr.D.Bandyopadhyay for his nice hospitality and encourgement recieved during my visit to National Metallurgical Laboratory.

I express my heartfelt thanks to Mr.S.K. Choudhary, Mr.T.K. Roy, Mr.K.K. Singh and Mr.S.K. Dutta for helping me at various stages of experimental work as well as valuable suggestions rendered by them in the present study. My sincere thanks are also due to Mr.A. Sharma for his active help during this study.

I render my acknowledgements to Mr.V.P. Vohra, Mr.R.C. Sharma of Metallurgical Engineering Work Shop, IIT Kanpur, for

their help in the sample preparation work. Thanks are due to Mr.K.P. Mukherjee for his help in photography work, and Mr.S.R. Chaurasia for his help in the analytical work.

I express my sincere appreciation to Mr.B.D. Biswas for his sincere efforts in excellent typing and Mr.B.K. Jain for tracing the figures.

I am thankful to family members of Prof.A. Ghosh for rendering me homelike environment during my stay in the campus.

I would like to express my heartfelt thanks to Prakash, Praveen, Kirshna Mohan, and Sanjeev for their help during my thesis work.

I offer my sincere thanks to my beloved family members and Grandpa, Kaabil, Banshi, Nirmal, Sarit and Mittal for their inspiration and encouragement in this study.

Rajesh Kumar Goyal

CONTENTS

LIST OF TABLES

LIST OF FIGURES

ABSTRACT

Centreline segregation (i.e. axial segregation) is a principal defect in continuously cast products of steel. In this investigation, a total of 11 samples of carbon steel billets, 100x100 mm. sq. and 125x125 mm. sq. section size and 150 to 250 mm. in length, obtained from Tata Steel and Haryana Concast, were studied. Each billet was sliced longitudinally along its axial plane. Since segregation and morphology of cast products are interrelated, one slice was employed for sulphur printing and physical examination. The other slice was used for chemical analysis of carbon and sulphur at various locations on the centreline.

Interpretations are mostly qualitative. Tundish superheat is the only variable that could be taken into consideration. Comparisons were made with literature findings wherever possible. Also attempts were made to correlate segregation profiles with the corresponding sulphur prints.

Important observations were as follows.

(1) Sulphur prints without preetching of samples were superior to those where preetching were done with nitric acid.

(2) Photocopies of sulphur prints were superior to the original prints in revealing segregation patterns.

(3) All features of central segregated zone, such as V- bands, V- lines, U- bands, porosity etc., were observed in this investigation too.

(4) Increasing tundish superheat tended to enlarge columnar zone as well as made the positive segregation zone along centreline less wide and more prominent.

(5) Centreline segregation profiles exhibited typical fluctuating nature. Maximum segregation ratios were 2.4 and 2.2 respectively for carbon and sulphur.

(6) Relationship between segregation ratios for sulphur and carbon showed approximate agreement with literature for low carbon steels but not for medium/high carbon steels.

CHAPTER 1

INTRODUCTION

1.1 Objective

Continuous casting, popularly known as CONCAST, is a process by which semifinished products such as billet, bloom or slab can be made continuously from liquid metal. Fig.1.1 shows the CONCAST machine schematically(1). This process has the ability to continuously produce material in sizes and shapes appropriate to a wide range of subsequent processing steps. Greater cost effectiveness has been achieved through improved productivity, quality, yield, safety, operational reliability, flexibility, and reduced labour.

Hence ingot casting in most of the steel plants in various countries has been largely replaced by continuous casting over the last three decades, and all new plants are being provided with continuous casting facility. According to an International Iron and Steel Institute (IISI) study, in 1974 the CONCAST ratio in the world as a whole was 11.1%(2). In 1986, 60% of the world's steel was cast using continuous casting, twice as much as in 1980(3). By 2000 this ratio is expected to reach 95% according to a recent IISI study(2).

Although continuous casting made inroads commercially in the Indian steel industry in the sixties, even in 1986-87 only around 27% of the total steel (including mini steel plants

and integrated steel plants) was cast continuously in India(4). Fig.1.2 shows future trends of CONCAST in integrated steel plants in India(5). It may be noted that considerable expansion of CONCAST facility is visualized in the near future.

Although continuously cast (CC) products are superior in metallurgical quality, most defects of cast products made by ingot casting are commonly found in CC products also, though of course not to the same extent. The general level of macrosegregation in CC steel is less than that in steel ingots in both longitudinal and transverse directions(6-10). Macrosegregation refers to non-uniformity in composition over large distances in a cast product. However, wrought billets produced by the ingot route have less macrosegregation along the centreline (i.e.axis) as compared to that in CC billets(7-9). This is known as "centreline segregation" or "axial segregation", and is considered to be a major defect in CC products. Centreline segregation is also connected with central porosity(11).

It is very difficult to eliminate macrosegregation even after prolonged annealing at elevated temperature. This often poses quality problems in CC products. For example, in steel, centrally segregated regions are responsible for inconsistent mechanical properties in finished products due to formation of low ductility structures such as network structure of cementite or hard martensite. This may cause fracture during wire drawing. Centreline segregation of elements like sulphur leads to hot-shortness during hot working of CC products. Extensive research has been carried out to understand the causes of centreline segregation and casting conditions responsible for it,

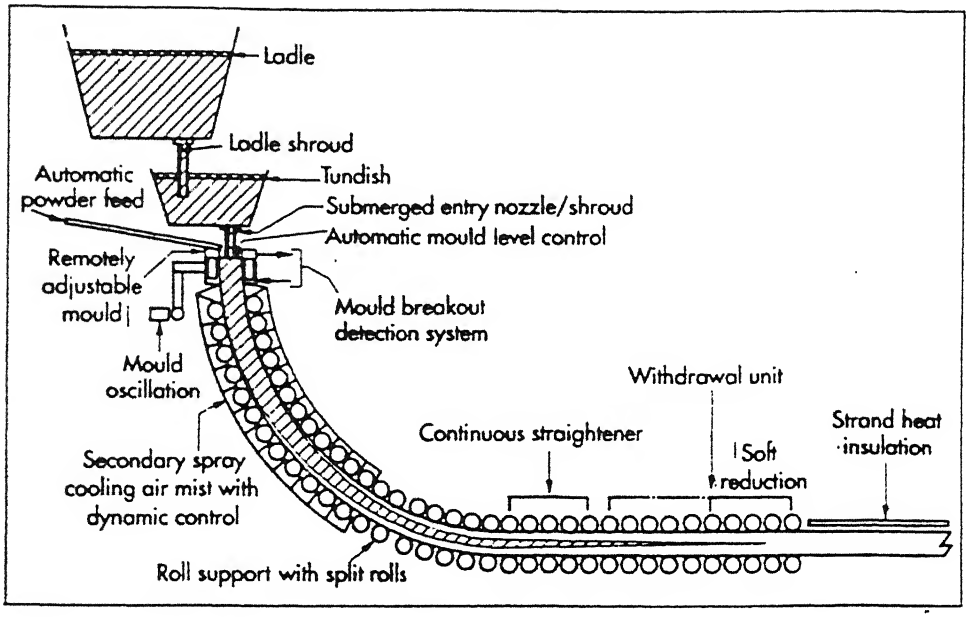

Fig.1.1 Schematic diagram of continuous casting machine

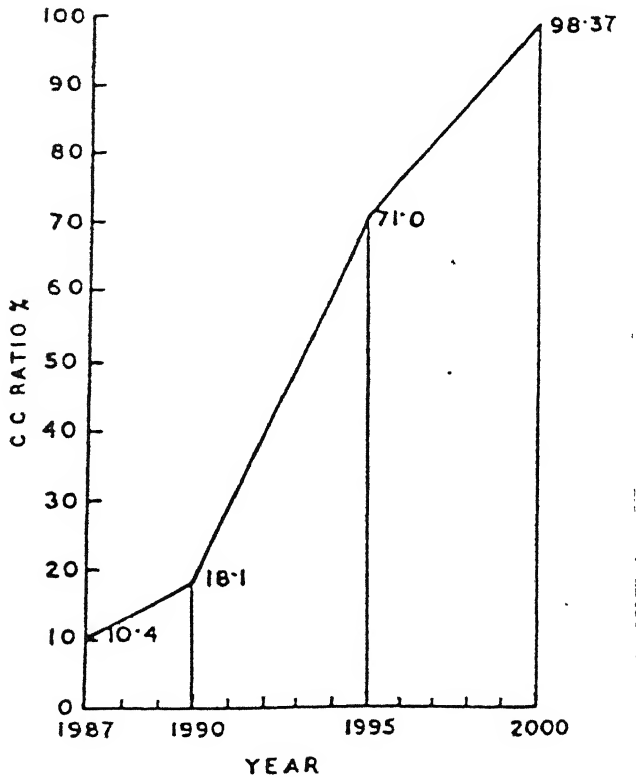

Fig.1.2 Future trends of continuous casting in

as well as to minimise its severity.

The prime objective of the present investigation was to study macrosegregation of sulphur and carbon along the centrelines of longitudinal sections of CC billets collected from different plants in India. Since macrosegregation and morphology are inter-related the latter was also included in the program of study. Very few studies of this type on Indian steel plants could be found in the published literature. Roy(12) carried out measurements on transverse sections of CC billets but not on longitudinal sections. Therefore, this investigation is complementary to that of Roy(12). Centreline segregation is a complex phenomenon and depends on a number of operating parameters. Hence it is somewhat specific to the practices employed at the plant. Therefore, it is necessary that such studies are carried out on billets produced in Indian steel plants to generate the necessary data base. So it is expected that this study will contribute towards better understanding of the nature and extent of macrosegregation in CC billets produced at Indian steel plants.

1.2 Plan of Work

(i) Literature review on macrosegregation and morphology specifically on longitudinal sections

(ii) Collection of billet samples and related shop floor data

(iii) Preparation of longitudinal sections of billets by cutting, grinding, and polishing

(iv) Sulphur printing of longitudinal sections including trials

(v) Trials with the existing evolution method for analysis of sulphur

(vi) Search for availability of carbon and sulphur determinator elsewhere

(vii) Selection of proper drilling scheme to generate drill samples for quantitative study of centreline segregation

(viii) Chemical analysis of drill samples either for both carbon and sulphur by automatic carbon and sulphur determinator or just for sulphur by modified evolution method, whichever is available

(ix) Presentation of results and discussions.

CHAPTER 2

LITERATURE REVIEW

2.1 Macrosegregation - Introductory Remarks

Macrosegregation refers to solute concentration variation over large distances in a cast product. It occurs over distances several times as large as a grain diameter, as compared to microsegregation which is a variation of solute concentration across a single dendrite arm. Macrosegregation is a consequence of movements of solid and liquid during solidification. It cannot be removed by annealing because homogenization would require much larger times than are economically acceptable under production conditions. Macrosegregation poses quality problems. For example, segregated regions are responsible for the formation of unwanted transformation products in steels such as martensite, and non-uniform composition during the subsequent operations. This gives rise to non-uniform mechanical properties in the finished products.

A solute element has lower solubility when in the solid state than when in the liquid state. This is the basic cause of segregation. As a result, a liquid rejects solutes continuously at liquid-solid interface during solidification. In alloys, this interface is of considerable thickness and is called "mushy zone" in which solid and liquid coexist during solidification. Movement of highly segregated phases, such as

inter-dendritic liquid in the mushy zone during solidification, leads to macrosegregation(13). The flow of interdendritic liquid, caused by temperature gradient, solidification shrinkage, and concentration differences, appears to be by far the most important and general cause of macrosegregation. Some macrosegregation can be attributed to the settling or floating of solid crystals, as in the early stages of equiaxed solidification. Based on some assumptions, a basic tool used to describe macrosegregation quantitatively is the "Local Solute Redistribution Equation" together with Darcy's Law(13). In a simple situation of plane front solidification with no diffusion in solid and complete mixing in liquid, the extent of segregation can be calculated from Scheil's equation(10),

$$C_l = C_o \, (1 - f_s)^{K_e - 1} \qquad \ldots 2.1$$

where,

C_l = Concentration of solute(say species i) in liquid during solidification,

C_o = Concentration of a solute i in the liquid before solidification begins,

f_s = Fraction of solid in total amount of melt,

and K_e = Equilibrium partition coefficient of solute i between solid and liquid phases.

In a situation with no diffusion in solid and incomplete mixing in the liquid of finite amount, macrosegregation may be calculated from Burton's equation(10) as follows.

$$C_l = C_o (1 - f_s)^{K_{eff}-1} \qquad ...2.2$$

Eq.2.2 incorporates several simplifying assumptions such as plane front solidification, no bulk movement of solid etc.K_{eff} is an effective partition coefficient and is defined as

$$K_{eff} = \frac{K_e}{K_e + (1 - K_e) \exp(-R/k_m)} \qquad ...2.3$$

where,

R = Linear rate of advance of solidification front,

and k_m = Boundary layer mass transfer coefficient in liquid for solute i.

K_{eff} is an important parameter for deciding segregation. Smaller the K_{eff} more is the extent of segregation(10).

Eq.(2.3) shows that segregation in general would depend upon parameters, K_e and R/k_m. However in the real castings, macrosegregation patterns are much more complex since solidification process mostly exhibits a dendritic front, and morphological features such as extent of columnar and equiaxed zones influence macrosegregation in a major way. Actually macrostructure and macrosegregation are closely interlinked.

Other influencing factors are:

(i) extent of chemical reactions during freezing, i.e. formation of oxides, sulphides and oxysulphides, and

(ii) nature of fluid flow in the solidifying castings and movement of free crystals.

Due to different values of K_e for each solute, the extent of macrosegregation of different solutes would not be the same.

However since factors such as (i) and (ii) are common, some relationship can be expected. Moore and Hamilton(14) have presented a correlation amongst centreline segregation of several elements in continuously cast steel billet based on Kawamoto's studies (Fig.2.1).

2.2 Macrosegregation in Killed Steel Ingots

Macrosegregation is a particularly distinctive phenomenon in large castings and ingots. In the area of steel casting, many pioneering studies were carried out on ingots. In order to understand macrosegregation in continuously cast products, a brief discussion of the same from the ingot area is described. Specially relevent for CONCAST is the behaviour of killed steel ingots. Fig.2.2 shows macrosegregation patterns in a killed steel ingot(10). These have been classified as centreline segregation (i.e. positive segregation near the centre of the ingots), bottom cone of negative segregation, inverse segregation, banding etc.

The centreline solute concentration of the ingot is usually higher than the overall average. Often macroetched sections show streaks, or channel segregates, arranged in V-pattern and associated with porosity. These channel segregates are known in their various manifestations as "freckles", "A" segregates and "V" segregates (see Fig.2.2). They are a consequence of the flow of liquid through interdendritic channels. This flow is upward because the inter-dendritic liquid is richer in solute and hence lighter. When the liquid is very

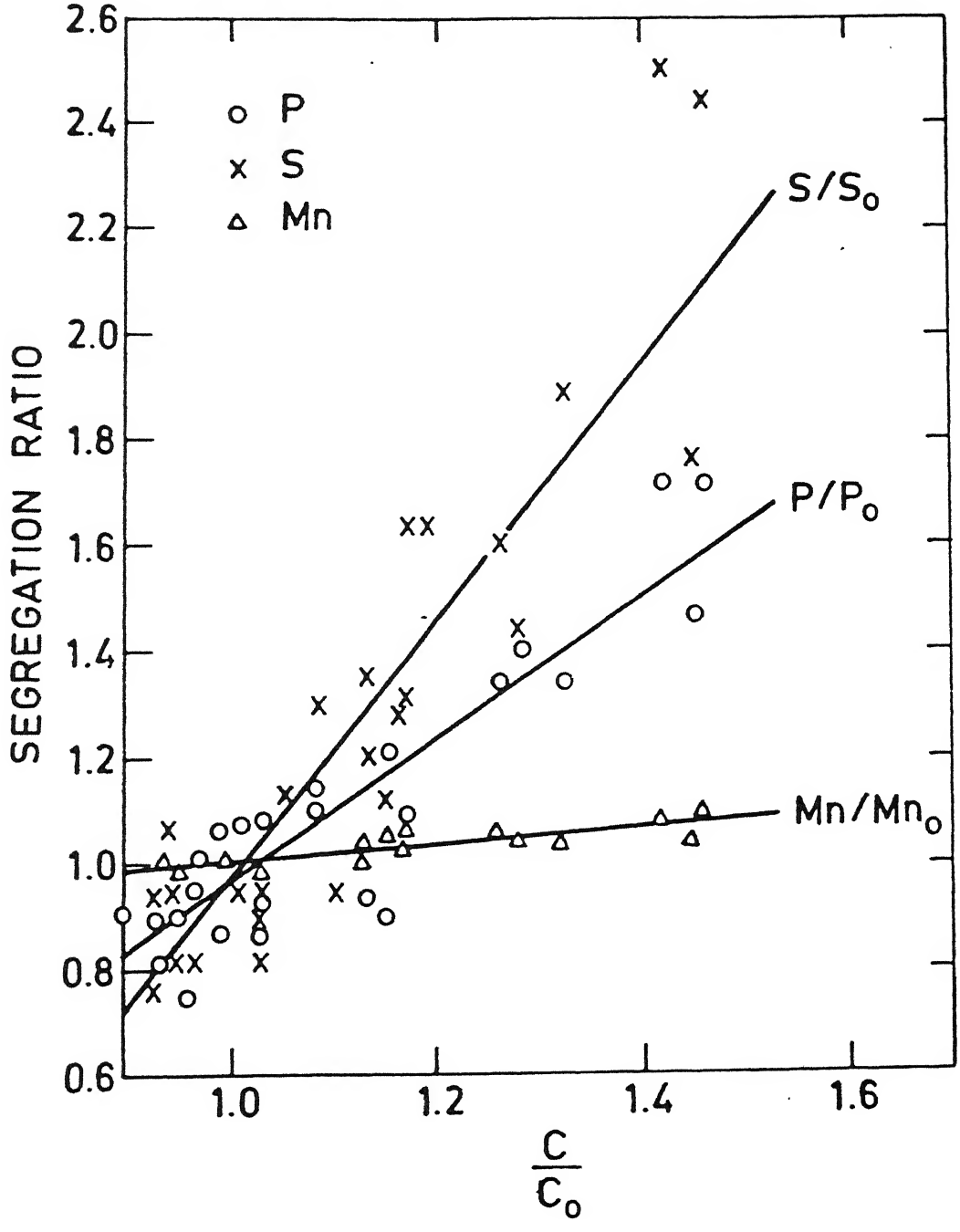

Fig.2.1 Relationship between segregationratios of S, P and Mn with that of carbon (ratio of axial to average concentration) in continuously cast steel billet(14)

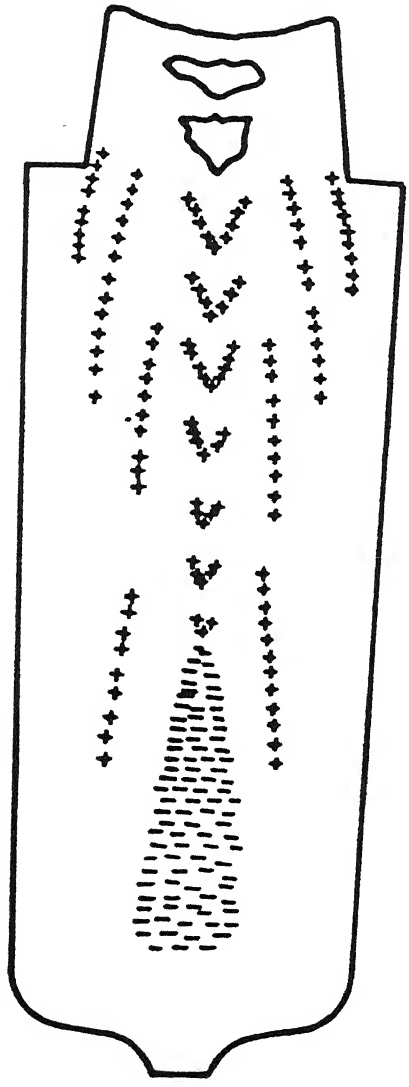

Fig.2.2 Macrosegregation patterns in a killed steel ingot; + denotes regions of positive segregation;- denotes regions of negative segregation(10)

enriched or hot, then it causes local melting of dendrites. Such melting decreases the resistance to flow and so more fluid flows through this path, thereby gradually creating channels(10). Similarly, Bennon and Incropera showed the channel formation and resultant macrosegregation in an ingot of NH_4Cl - 70 wt.% H_2O. They observed higher upward velocities within these channels formed by local remelting and therefore, higher permeability in the channel region(15).

A cone of negative segregation is present at the bottom of the ingot. Due to strong thermal convection in the central liquid pool, there occurs a downward velocity at the solid-liquid interface. This liquid carries detached crystals of metal downwards. The crystals being purer and heavier than the liquid tend to settle at the bottom and also cause formation of negative cone of segregation at the bottom(10). Ohno and Sōda(16) investigated solidification of aluminium and Al-Cu alloys in graphite moulds under static and vibrating conditions. Based on their experimental results, they proposed a formation machanism of negative segragation, inverted-V segregation and V-segregation in large steel ingots (Fig.2.3).

Flemings and Nereo(17) did experiments on solidification of Al-Cu alloy ingots and observed that centreline segregation occured during the last stages of solidification when significant liquid flow occurs parallel to isotherms within the liquid-solid zone. Thermal contraction of the fully solid region of a solidifying ingot increases the fluid flow parallel to isotherms and accentuates the centreline segregation. However, the extent

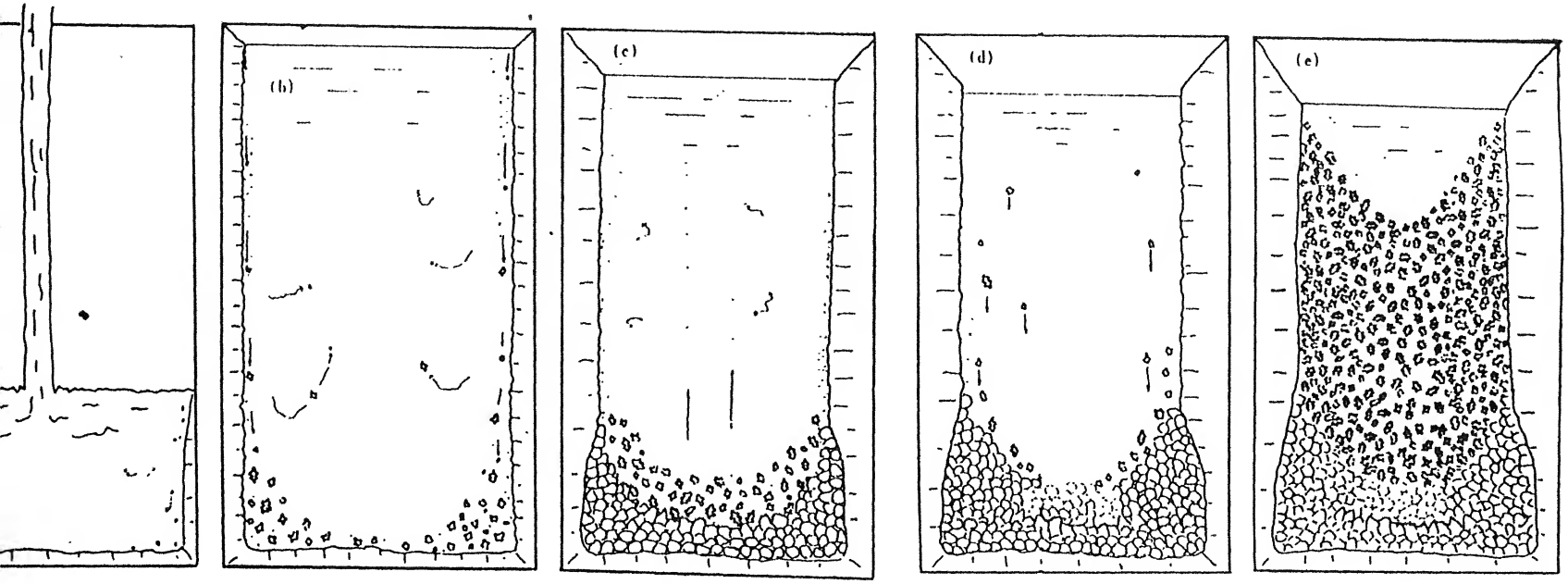

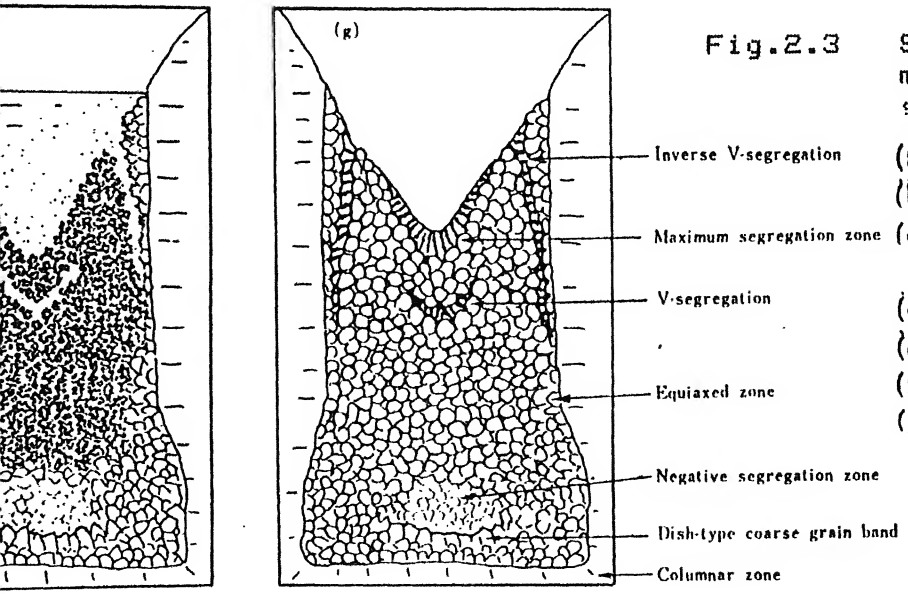

Fig.2.3 Schematic representation of the formation mechanism of macrosegregation in large steel ingots(16)

(a) Pouring
(b) Initial precipitation
(c) No precipitation, formation of dish-type band of coarse grains
(d) Secondary precipitation
(e) V-mount of equiaxed crystals
(f) Settling and formation of tears
(g) Formation of V-segregation, inverted V-segregation, maximum segregation zone, and pipe

of segregated zone resulting from this contraction was small compared with that resulting from contractions occuring within the liquid-solid zone.

Suzuki and Miyamoto(18) explained their experimental results on sand cast ingots by the theory of suction due to volume shrinkage of molten steel during the solidification. Again, according to Ameling et al(19),macrosegregation is connected with suction currents and temperature difference in the residual melt during final solidification.

2.3 Centreline Segregation in Continuous Casting

2.3.1 Introductory remarks

There is general agreement that the overall level of macrosegregation in continuously cast (CC) products is less than what is typically found in statically cast ingots along both the longitudinal and transverse directions(6-10). However, the segregation along the centreline in the former tends to be more severe than that in the latter(7-9) and is a major defect of CC products such as billets, slabs and blooms.

In some finished shapes after rolling it does not pose significant quality problems, but there are some others where it does. For example, in high carbon steels, martensite may exist as a defect along the centreline in wire rods if the degree of segregation is such that there is significant increase in the hardenability of the steel(20). Positive segregation of sulphur along the centreline of longitudinal sections of billets leads to subsequent difficulties during hot working due to presence of low

melting FeS phase.

As noted in Sec.2.1, macrosegregation depends significantly on morphology of the castings. It also depends on the nature of fluid motion during solidification as well as the movement of free crystals. These are going to be briefly discussed now.

2.3.2 Effect of morphology on centreline segregation

The extent of equiaxed zone, expressed as percentage area of cross section of the continuously cast products,is an important factor affecting centreline segregation. The segregation in an alloy is a result of continuous solute rejection at the dendrite tips and its redistribution into the bulk of liquid by convection and diffusion processes(14). Therefore, growth of columnar crystals tend to enrich the remaining liquid in solute. The extent of segregation may be established by employing Burton's equation (Eq.2.3) if simplifying assumptions are valid(10). Qualitatively speaking this continuous enrichment makes the final liquid freezing around the central axis of the CC products very impure, thus giving rise to a high degree of centreline segregation.

A large equiaxed zone is conducive to reduction of this axial segregation. Equiaxed zone stops the growth of columnar zone and thus does not allow the zone refining action to aggrevate(7-8,10,14,19-25). Equiaxed zone with its more evenly distributed microsegregation have been found to reduce the degree of axial segregation(7,10,14). Increased proportion of equiaxed crystals were observed by Ohashi et al(25) to reduce centreline segregation in CC slabs. They also developed a relation (Fig.2.4) between the proportion of equiaxed crystals at upper

side of the slab and segregation ratios of different solutes. An equiaxed structure is preferred over columnar structure for preventing internal cracks and centreline porosity also as discussed later. Miyamura et al(26) reported that the fineness of network structure of equiaxed zone not only supresses the central segregation but also V-shape segregation in CC slabs. Fig.2.5 shows the relationship between the level of central segregation and the fineness of network structure(26). A similar observation was made by Mori et al(6) in CC billets. In their study of autoradiographs, they reported that multilayered V-segregation lines were observed inside or in the vicinity of large equiaxed crystals which were densely intermingled, whereas V-bands were observed in the regions of very small and evenly distributed equiaxed crystals.

For the equiaxed crystal zone to form,there must be a sufficient number of seed crystals in the melt(6). Moreover, the melt temperature should be at freazing point so that the seed crystals can grow. Several studies have been done on mechanism of equiaxed zone formation during solidification of metals. It has been proposed that such seed crystals are crystals broken away from chill or columnar zone either due to impact of fluid or by remelting. Critical reviews are available in literature(10,23).

Sometimes the columnar zone extends right upto the centreline of CC products. This produces solidification bridges at various positions along the axis, thereby resulting in the formation of "mini-ingots". This has been discussed in several reviews(7,10,14,21,23) elaborately. Stages of mini-ingot

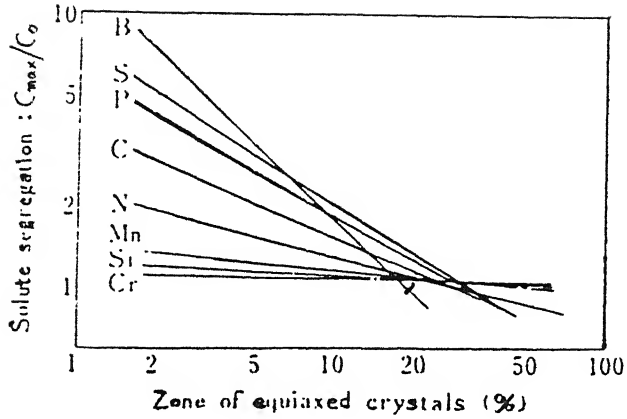

Fig.2.4 Influence of proportion of equiaxed zone on centreline segregation of various elements in steel slab(25)

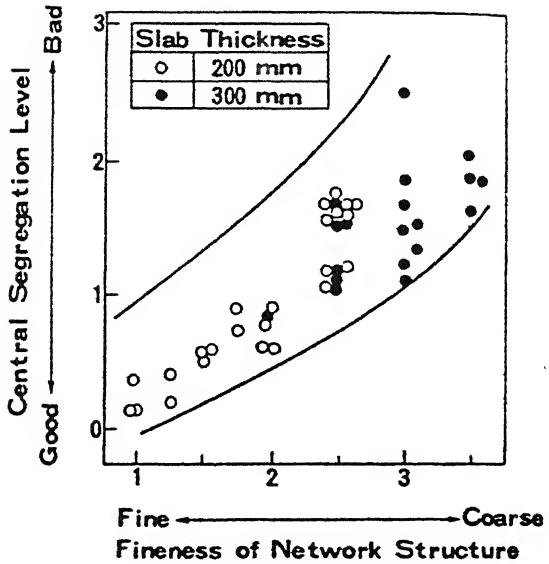

Fig.2.5 Relation between the central segregation level and the fineness of network structure(26)

formation are shown in Fig.2.6(14). Such bridges do not allow feeding of liquid metal into cavities below, resulting from solidification shrinkage. This has the following effects(10):

(i) The impure liquid from the interdendritic region of columnor zone gets sucked into the axial region, thereby increasing the axial segregation

(ii) Zone refining action becomes more severe due to the lack of feeding of fresh liquid

(iii)Centreline porosity develops if feeding is not complete.

All the effects above aggravate the problem of centreline segregation and porosity. In their study of autoradiographs, Mori et al(6) discovered the presence of centreline segregation at positions where columnar or branched columnar crystals had grown upto the central axis of CC billets.

2.3.3 Fluid flow, bulging and centreline segregation

Fluid flow plays an important role in the development of cast structure and macrosegregation as already mentioned in Secs.2.1 and 2.2. Fluid flow in continuous casting has been discussed elaborately by many investigators(11,15,25,27) and reviewed by Lait et al(23). In continuous casting, the solidified shell exhibits bulging.The pressure of withdrawal rolls below the mould of CONCAST machine causes compression of the shell leading to bulging(24,28). According to Myoshi(11) bulging may be due to shrinkage from solidification, ferrostatic pressure of molten steel or misalignment of rolls. Schwerdtfeger mathematically analysed the bulging due to roll pressure and consequent centreline segregation(10). Such bulging creates

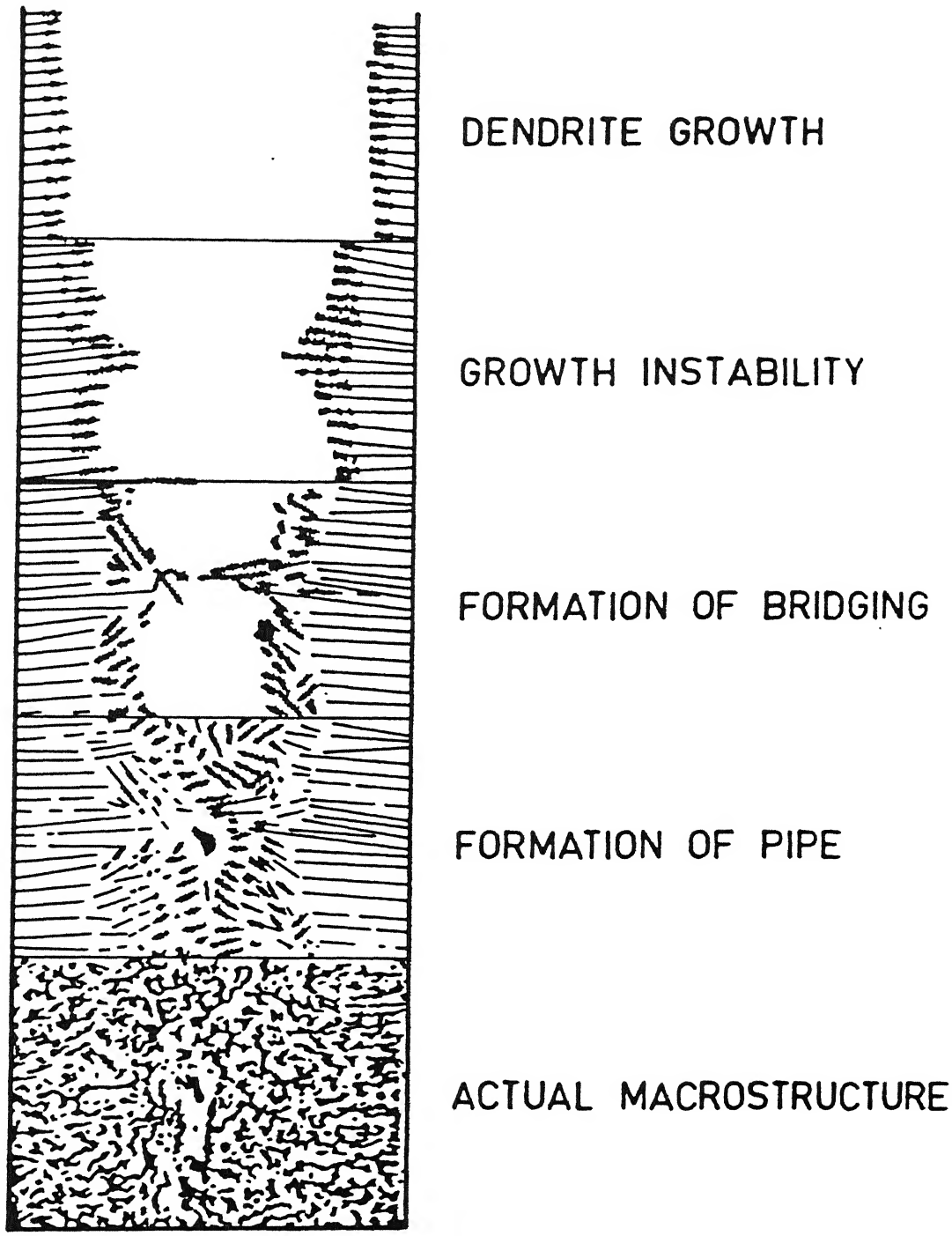

Fig.2.6 Formation of a mini-ingot in continuous casting(14)

cavity around the central axis of CC products. This causes suction of impure interdendritic liquid into the central region thus aggravating the centreline segregation.

Fig.2.7 schematically shows the effect of fluid flow pattern in the mushy zone on macrosegregation in continuous casting of steel(15). No segregation results if interdendritic flow lines are all vertical (Fig.2.7a). Negative segregation at mid-radius (i.e. somewhat off from axis) would result from the lines such as those of Fig.2.7b. Positive segregation at centreline would result from the flow lines such as those of Fig.2.7c, and this tendency is enhanced due to suction resulting from bulging of solidified shell.

Ohashi et al(25) mathematically calculated the flow of molten steel and its effect on the centreline segregation in CC slabs under various assumptions. Solidification rate was measured by radioactive gold(Au^{198}) in the form of Au-Pb alloy. They compared the fluid flow velocities due to nozzle flow, natural convection and bulging flow with the velocity obtained from the solute distribution at different distances from meniscus (Fig.2.8). Nozzle jet flow dominates at the start of solidification, natural convection at the middle of solidification, and fluid flow due to bulging at the end of solidification. The values of these flow velocities were estimated as 10 to 40, 1 to 1.25, and 2.0 to 4.0 cm sec^{-1}, respectively. The sum of these velocities was close to the distribution of flow velocity obtained from the solute redistribution. These three main types of flow varied with aspect

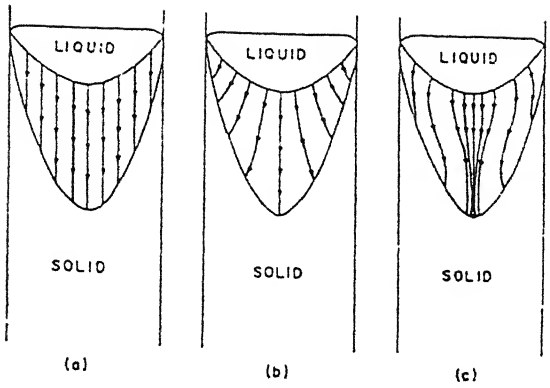

Fig.2.7 Interdendritic fluid flow in acontinuous casting (schematic) [a] no segregation, [b] negative segregation at mid-radius, [c] positive segregation at centreline(15)

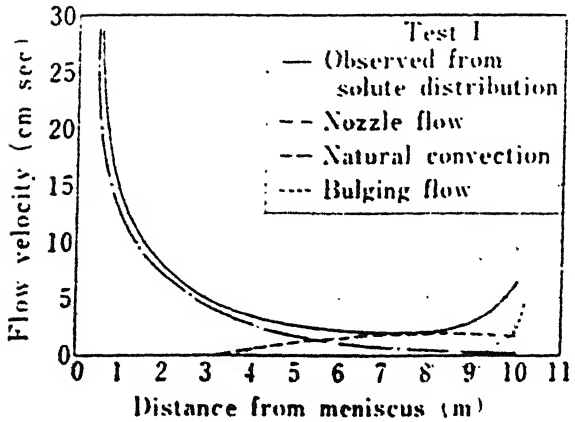

Fig.2.8 Flow velocity in continuously cast steel slab(25)

ratio of slab, shape of nozzle, casting speed, amount of bulging etc. In his study on slab segregation, Myoshi(11) observed the negative segregation at the vicinity of slab centre and positive segregation at the point of final solidification (i.e. the slab centre). From this finding, he pointed out that centreline segregation which was formed by the movement of enriched molten steel in the dendrites within the mushy zone at the crater bottom.

The effect of bulging on centreline segregation was studied by Myoshi(11), Marr(24), Ohashi et al(25),and Miyazawa and Schwerdtfeger(28), and a review was made by Ghosh(10). Fig.2.9 shows the effect of bulging on axial segregation(24). Miyazawa and Schwerdtfeger(28) studied the effect of bulging on interdendritic flow and resulting macrogregation of C and Mn. They proposed a schematic model of bulging and made a comparison of flow fields with and without bulging.Myoshi(11) pointed out that if bulging happens during the final stage of solidification, the enriched molten steel between the columnar crystals or equiaxed crystals solidifies and contracts or moves to the bulge thereby forming positive and negative zones in the slabs. A similar observation was also made by Ohashi et al(25). They also observed the change of solidification structures in the central region of test slabs. According to them, dendritic crystals occur in slabs without bulging and non-dendritic equiaxed crystals occur in slabs with bulging (Fig.2.10).

2.3.4 Centreline segregation and porosity

Centreline segregation and centreline

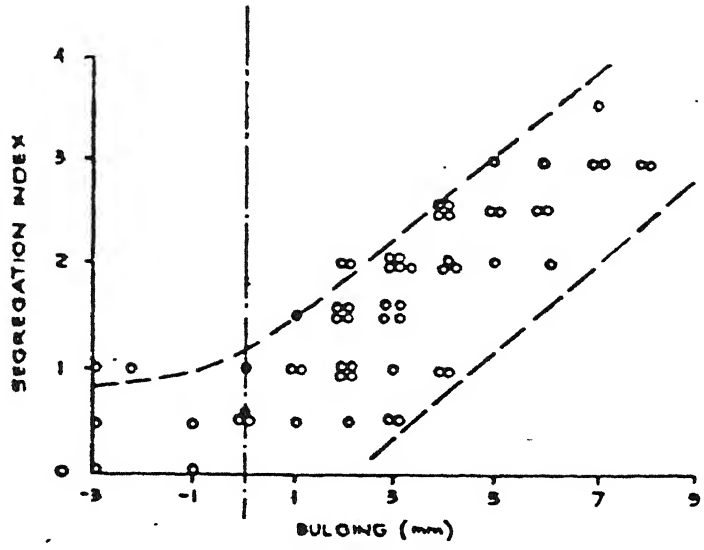

Fig.2.9 Effect of bulging on axial segregation(24)

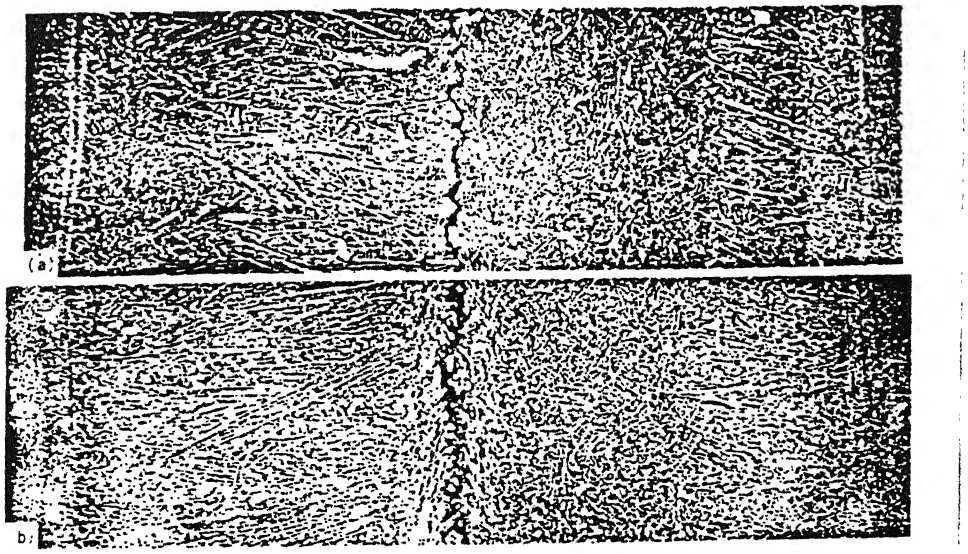

Fig.2.10 Effect of bulging on the solidification structures [a] without bulging [b] with

porosity are inter-related. Higher the porosity, higher is the segregation. The explanation is as follows. The axial region of CC products frezes at a depth several meters below the meniscus. The large ferrostatic pressure does not allow the formation of blowholes. Hence the centreline porosity is caused by solidification shrinkage and the inability of the molten pool situated above to feed it due to the solidification bridges etc. More of this happening, more is the chance of impure interdendritic liquid getting sucked into these cavities and hence more centreline segregation. X-ray examination of the porosities at the centre of slab width has revealed that more the centreline segregation was improved, the smaller and finer were the pores(11). However, it is to be kept in mind that segregation at the centre may be attacked so deeply during the etching that it may appear as a pipe or may be grouped in some fairly regular form about the centre(29). Therefore, the pores should be examined in unetched condition. A combined study of central segregation and porosity in plane carbon (0.1-0.85%C) steel billets and blooms was also carried out by Mori et al(6) using sulphur printing, macroething and autoradiography. Fredriksson and Rogberg(27) calculated that cooling rate at the centre was higher than that at the billet surface towards the end of solidification (Fig.2.11). From this calculation, they concluded that if the cooling rate at the centre is 6 times larger than at the surface at the end of solidification process, no shrinkage volume would occur in the central part and no macrosegregation will form. Ameling et al(19) identified five

characteristic types of shrinkage holes in the core region of the billet in longitudinal section by etching or X-ray technique. According to them, two different pipe formation mechanisms were:

(i) With equiaxed dendritic solidification, collision and linking of free flowing crystals form bridges which prevent feeding of liquid during solidification beneath the bridge.

(ii) During columnar dendritic solidification, the favourably oriented columnar crystals along the direction of steep temperature gradient grow faster and may meet at the centre, thus forming a bridge.

They also measured the volume of core porosity by analysing X-ray pictures of the billet core and by weighing the billet core with high accuracy to obtain the order of porosity and the effect of casting parameters on it. In their work on electromagnetic stirring of CC billets, Druzhinin et al(30) evaluated density of the axial zone by hydrostatic suspension method. The densities of the axial zone of billets produced with and without stirring were 7.72-7.78 and 7.35-7.52 g/cm^2 respectively.

2.3.5 Macrosegregation in transverse section of CC products

There have been several investigations on macrosegregation profile in transverse sections of CC products(7,10-11,14,18,27-28,31).Fig.2.12 shows a typical profile(10). It is this kind of profile which reveals high degree of segregation at the axis of the transverse section. Roy(32) investigated transverse sections of carbon steel billets

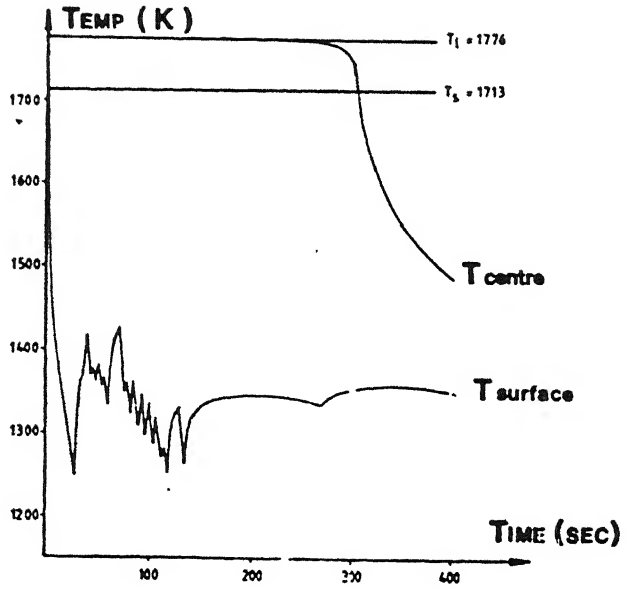

Fig.2.11 Temperature distribution at the surface and at the centre as a function of time for a billet of 140x140 mm sq.(27)

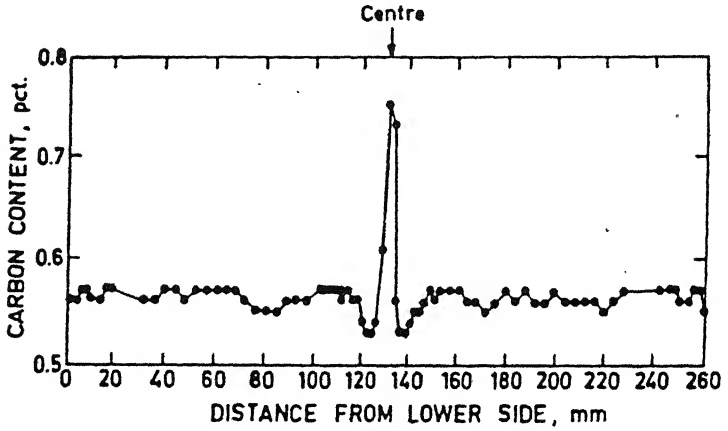

Fig.2.12 Typical concentration profile as

collected from steel plants in India. He carried out macroetching as well as chemical analysis of sulphur. Mecroetching with 50% hot hydrochloric acid solution in water was done to measure the fractions of chilled, equiaxed and columnar zones in transverse sections of billets of 100x100 mm. sq. and 125x125 mm. sq. cross sections. Observations were also made for central porosity, rhomboidity etc. in transverse sections before and after etching by the use of magnascope (an optical instrument with 3X magnification).To study the segregation profile of sulphur, drill samples were collected at various locations of the transverse section in a square grid pattern. Analysis of drill samples were done by a modified evolution method. Separate sulphur segregation profiles, one along the perpendicular to the edge of the billet and other along the diagonal of the billet, were determined. The various findings of his investigation are summarised below.

(i) Samples cast at a relatively low superheat generally revealed broad porous pattern or sponginess adjacent to the centre. In extreme cases, with increase in superheat, columnar crystals extended upto the centre and spongines near the centre took the form of central piping.

(ii) Area of equiaxed zone varied between 4 to 20 pct. of the billet area. It was mostly symmetric around the central axis of the billet. Decrease of pct. area of equiaxed zone with increase in superheat was observed.

(iii)Fluctuating segregation profiles were observed. Nature of profiles varied from billet to billet. Profiles

along diagonals also differed from those perpendicular to the edges of the billets.

(iv) A tendency of decreasing maximum segregation ratio with increasing area pct. of equiaxed zone was observed.

(v) Highest maximum sulphur segregation ratio was 1.8 in the centre of a 150 mm. sq. billet.

These findings are qualitatively consistent with observations reported by other investigators abroad.

2.4 Features of Macrosegregation in Longitudinal Sections of CC Products

Fig.2.13 shows random fluctuations in solute concentration along the axis of longitudinal section of a billet(10). Mini-ingot formation (see Sec.2.3.2), pulsations created by eddies of turbulent flow, fluctuating nature of heat transfer, and other flow fluctuations such as due to bulging, mould oscillations, jerky withdrawal etc. are the major factors responsible for these random oscillations(10).

When longitudinal sections are subjected to macroetching and sulphur printing, some features such as V-segregation bands, U-segregations bands, white bands etc. are observed (Fig.2.14). Formation mechanisms of these features were studied first in steel ingots(10,13,16,18). However, the solidification during continuous casting has some distinctive features as compared to those found during the solidification in ingot casting. Therefore, apart from the theories of formation of channel segregates and negative segregation as noted in Sec.2.2,

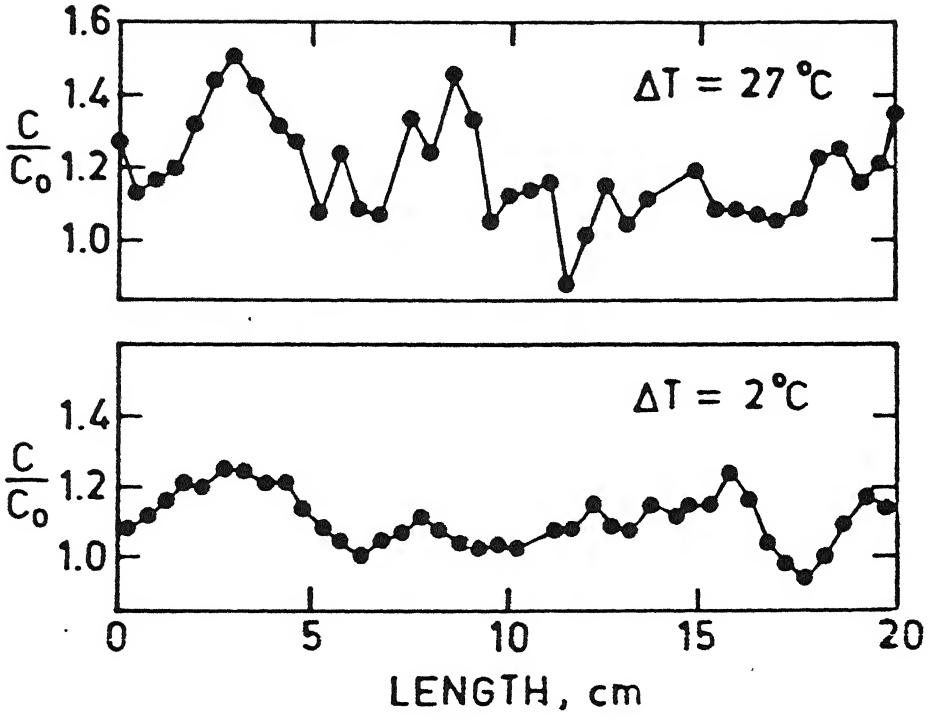

Fig.2.13 Typical concentration profile as observed in longitudinal section of a 0.8%C steel billet(10)

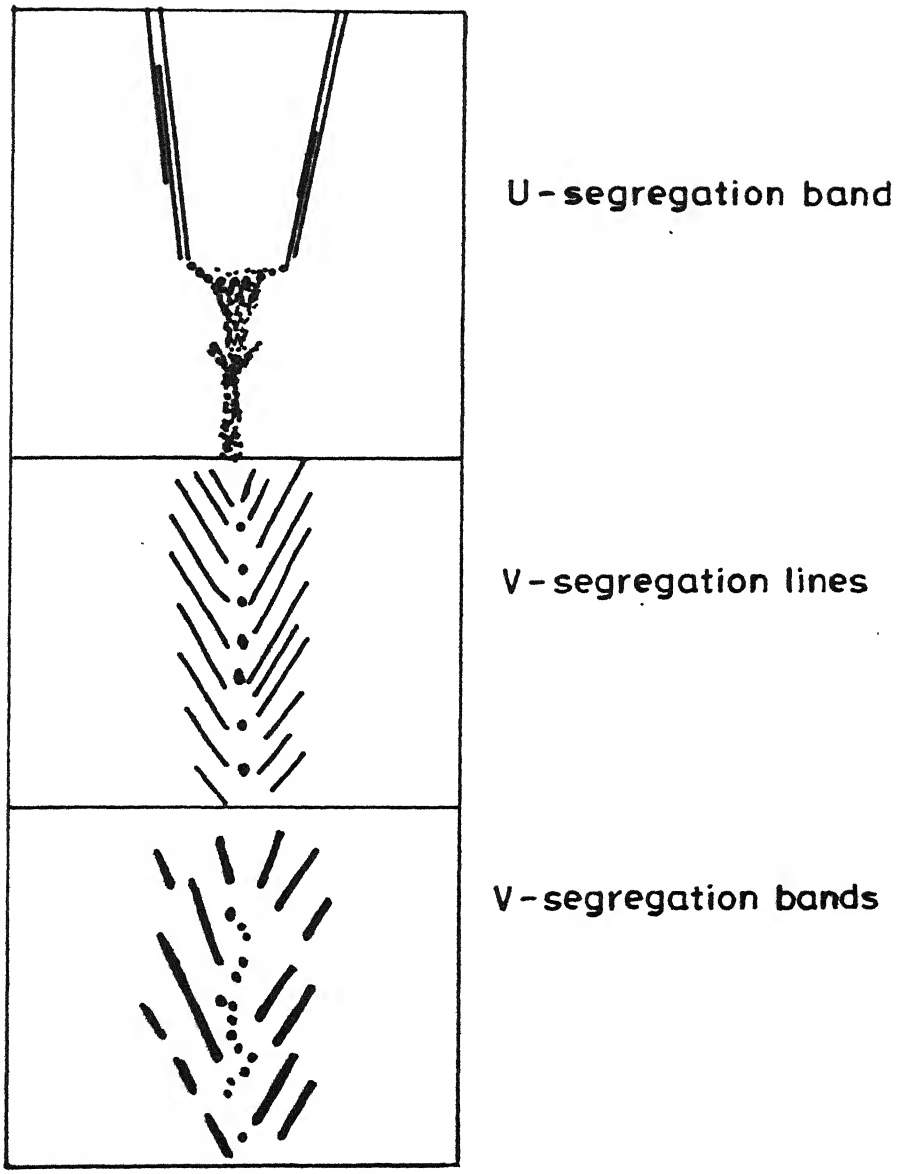

Fig. 2.14 Some features of macrosegregation in longitudinal section of CC products (schematic)

it is necessary to study these features in CONCAST as well.

Studies of formation mechanisms of V-segregation, positive and negative segregations in CC products were carried out by Mori et al(6), Myoshi(11), Fredriksson and Rogberg(27),and Tomono et al(33). Mori et al(6) discussed formation mechanism of various V-lines in CC steel billets such as "typical V-line" or U-line, major V-lines, multilayered V-lines etc. According to them V-type segregation is produced due to the downward flow, under gravity and convectional forces, of equiaxed crystals which nucleated and grew in the liquid steel ahead of the advancing columnar zone. This produces a counterbalancing upward movement of the solute enriched liquid which, on solidification, produces V-lines of positive segregation. Under conditions of few equiaxed crystals and extended columnar zone, U-segregation line forms. Bridge formation due to entrapment of equiaxed crystals between advancing columnar crystals results into higher resistance against flow of liquid metal. This bridge formation is a major cause of major V-lines and multilayerd V-lines, and V-shaped negative and positive segregations along with central porosity due to solidification shrinkage. Tomono et al(33) also observed V-shaped segregation within the equiaxed crystal zone in longitudinal section of CC blooms, instead of centreline segregation as found in slabs and billets. They concluded that it was due to easy formation of equiaxed zone in the central region of large section blooms.According to them, piling of equiaxed crystals as cohesive particles was the cause of the formation of V-shaped segregation. Birat et al(21) proposed a

model (Fig.2.15) of the mechanism of formation of centreline segregation in CC high carbon blooms. This model explains that segregation results from inter-dendritic flow in the mushy zone, which concentrates into channels and eventually leads to the formation of V-segregates and sometimes tubular centreline segregates.

The upward flow of enriched liquid was in agreement with Flemings(15), Ohno and Sōda(16), and Suzuki and Miyamoto(18). However, Fredriksson and Rogberg(27) observed downward flow around centre of billet from their nailing and sulphur print experiments. They also proposed the mechanism of formation of negative segregation, V-lines and pipe formation.

2.5 Influence of Process Variables on Centreline Segregation

The process variables, such as tundish superheat, steel composition, section size and shape, and casting speed, are known to affect the morphology, responsible for the changes in the extent of centreline segregation and porosity. The topic has been discussed in literature(6-7,14,22,34). These variables are independent but interrelated, and hence pose difficulties in interpretation of segregation and solidification in steel.

Increasing the tundish superheat enlarges the columnar zone and decreases the equiaxed zone causing more severe centreline segregation (see Figs.2.13) and porosity. This phenomenon has been observed by many investigators(6,21,31,35-36). Mori et al(6) reported that the

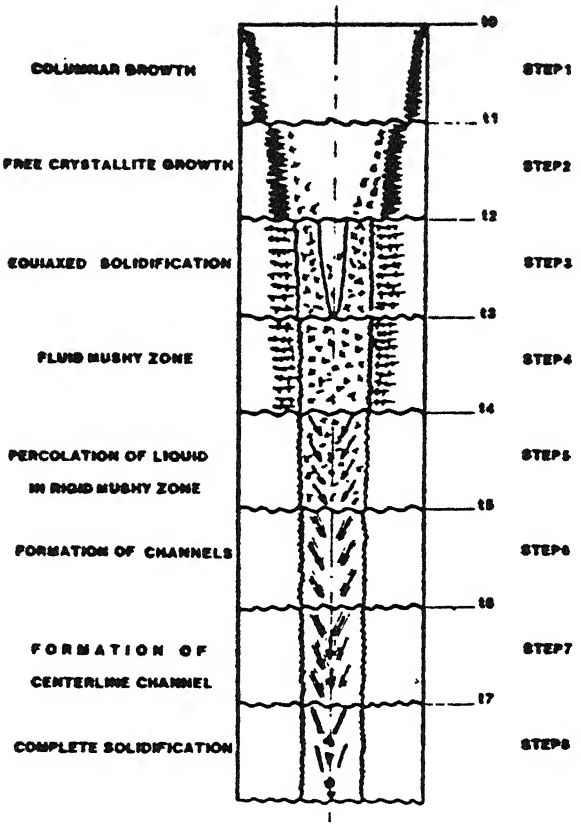

Fig.2.15 Model of solidification of a bloom made of steel exhibiting a large solidification interval(21)

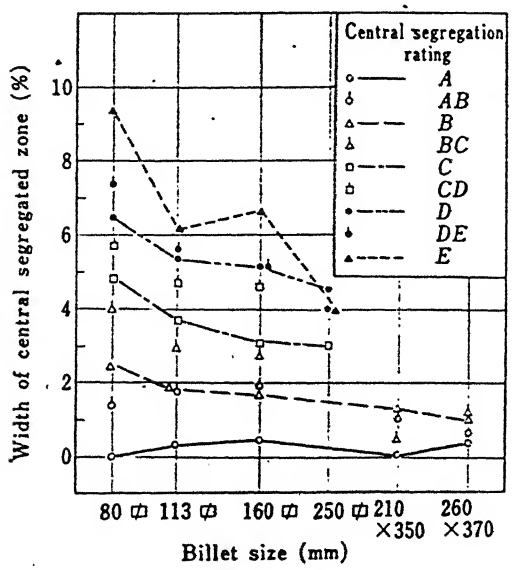

Fig.2.16 Relation between width of central segregated zone and billet size & shape; A= Best, E= Worst(6)

central porosity changed from a dispersed form of porosity to axially located pipes, and the form of V-type segregation turned from band to lines with the increase in casting superheat. This led to increase in the width of central segregation zone. Haggart et al(35) observed that increasing superheat helped to reduce the size and number of off centreline spots by promoting increased centreline macrosegregation. They also developed a mathematical relationship for the effect of superheat and carbon equivalent value on centreline macrosegregation, measured as percentage of centreline martensite, in slabs of high quality plate steel. In their evaluation of segregation by etch print method, Miyamura et al(26) obtained finer network structure of equiaxed crystals when tundish superheat dropped below $20^{o}C$ at constant slab thickness and casting speed. They also developed a mathematical equation to explain how the factors such as casting speed, secondary spray cooling and slab thickness affect the fineness of network structure at constant superheat. Moore(7) and Lait et al(23) have reviewed the effect of superheat on solidification and internal quality of continuously cast products.

Steel composition is another variable which influences centreline segregation and porosity. Severe centreline segregation was found in high carbon steel(6,14,21-22). Higher carbon content widens the freezing range thus causing this tendency. Benscoter(29) reported frequent presence of carbon spots, a type of segregation in carbon and alloy steels containing more than 0.40% carbon. The equiaxed zone is largest at medium carbon (0.3-0.4%C) steel and decreases as carbon

content is lowered(26). Therefore, it is clear that medium to high carbon steels are more prone towards segregation. According to Mori et al(6), the columnar zone increases in length as the carbon content changes from 0.3 to 0.1 and from 0.3 to 0.6% and the severity of segregation and porosity increases along with the tendency of occurance of V-line. Birat et al(21) presented a model which provides qualitative information about the effect of steel grades on centreline segragation. A regression equation has been proposed by Haggart et al(35) to calculate centreline macrosegration, measured as pct. of martensite along centreline, as a function of steel composition at different superheats. Revtov et al(34) have presented a relationship which shows that the width of the zone of columnar crystals increases as carbon pct. increases.

The section size and shape have been found to considerably influence the width of central equiaxed zone and the extent of axial segregation. Increasing the section size allows a longer solidification time, thereby helping to eliminate the superheat in the central part of the castings before complete solidification which reduces the relative length of the columnar zone, thus helping to form equiaxed crystals. Mori et al(6) studied the extent of segregation and porosity in square and rectangular billets and blooms. Fig.2.16 shows the relation between the width of segregation and billet size and shape, as averaged for central segregation rating(6). The absolute thickness of the central segregated zone increased as the section size increased, whereas the proportion of the cross section

occupied by the segregation decreased. They also observed that 160x160 mm. sq. billet exhibited the highest maximum segregation ratio followed by 250x250 mm. and 80x80 mm. square billets, where segregation ratio was defined as the ratio of concentration of solute i in a particular location to the nominal composition of the solute. At high casting temperature a 80x80 mm. square billet contained large V-line type defects with branched or columnar dendrites extending almost to the centre of the casting.

Calculations and experiments of Fredriksson and Rogberg(27) showed that a large square section decreased the macrosegregation in the central part whereas Bramfitt(37) observed that macrosegregation was more pronounced with increasing section size. The network structure of equiaxed crystals was finer in thick slab as compared to thin slab under the same casting conditions(26). A 50 mm. increase in slab thickness markedly reduced the number of cluster cracks and their openings, and caused uniform distribution of inclusions throughout the slab thickness(38). When the billet shape was changed from square to rectangular, Mori et al(6) observed that type of V-segregation changed from V-lines to V-bands with lesser width of the central segregated zone. Thus, rectangular sections had less segregation than a square section.

Casting speed is an important variable since it also influences solidification structure and hence the extent of segregation and porosity. Moore and Hamilton(14) reported that if casting speed is too high, the resulting liquid pool profile is greatly extended. The longer pool favours bridging associated

with large shrinkage cavities, central porosity, and increased axial segregation. The effect of casting speed on segregation was also examined by Fredriksson and Rogberg(27). They observed that a low casting speed decreased the macrosegregation in the central part. Higher casting speed increased columnar zone length which was also verified by Shah and Moore(22). For the slabs of same thickness cast at same superheat, the lower the casting speed, the finer was the network structure of equiaxed crystals(26). It seems that low casting rate reduces bulging by increasing solid shell stiffness(26).

Defects due to segregation on rods and wires drawn from concast billets have been studied by Iwata et al(31). Crack formation in continuous casting of steel is a problem which has been reviewed by Brimacombe and Sorimachi(39). Elements such as S and P worsen crack problem. The zones with sulphur rich material seemed to be responsible for midway or halfway cracks. Weinberg et al(40) showed that the interdentric segregation of sulphur was a major factor contributing to the hot-short fracture of the CC steel products during their working.

2.6 Measures to Reduce Centreline Segregation and Porosity

Application of electromagnetic stirring (EMS) is one of the most important process development in CONCAST technology for morphology control(10,35,41-46). Stirring assists in increasing equiaxed zone in two ways(10):

(i) dissipitation of heat of the liquid pool due to enhanced convective heat transfer,

(ii) control of fluid flow in inderdentric region of the columnar zone by inducing velocities in appropriate direction.

Turbulence sets in at higher velocity leading to remelting, breaking off of dendrite tips thus providing more seeds for growth of equiaxed crystals(10). Myoshi(11) observed that the slabs cast without stirring showed more columnar dendrite crystals in the region from the top surface to the centre, while those cast with stirring showed equiaxed crystals near the centre. Fig.2.17 presents the macrostructures of a small part of the transverse section of the slab around its axis. It may also be noted that white bands were prominent with EMS. According to Iwata et al(31), the EMS was shown to be more effective for segregation control when the casting temperature was higher(Fig.2.18). Investigation carried out by Birat et al(21) showed that EMS applied at different moments during solidification sequence can control centreline segregation, even in steels having a large solidification interval. Effect of stirrer locations on strand quality was examined by different investigators(10, 21,41,46-47). Komatsu et al(46), in their study of effect of EMS on solidification phenomenon of steel, found that stirring in both the mould and the upper part of secondary cooling zone successfully increased the amount of equiaxed crystals, but it also increased the strong V-segregation streaks due to reasons already discussed in Sec.2.3.6. They suggested that upward stirring just after the initiation of solidification at the centre of cast, and alternate stirring at

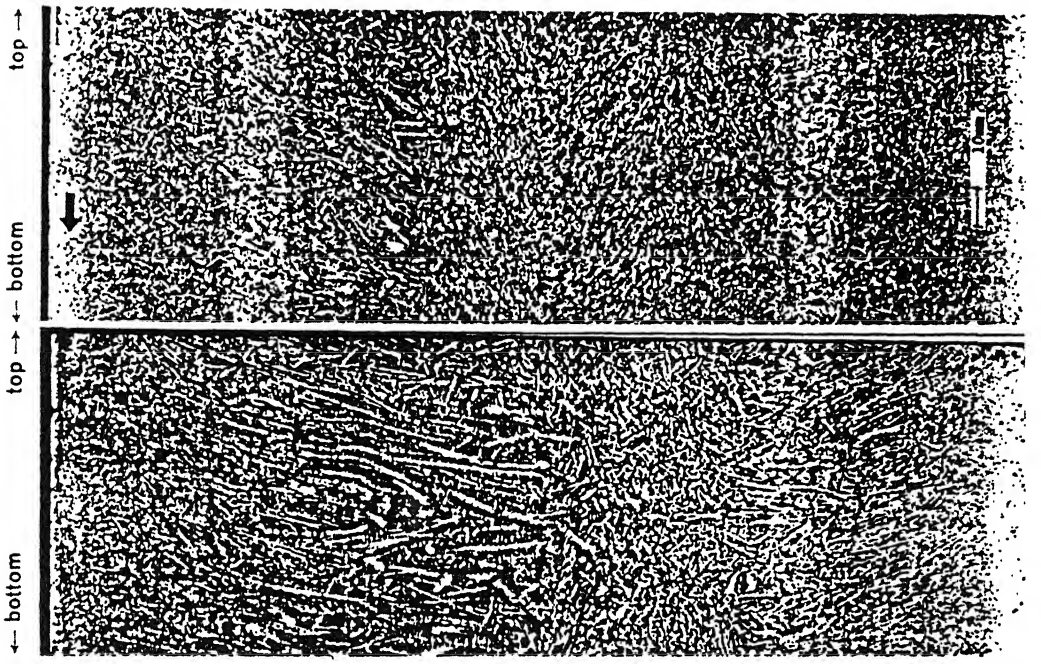

Fig.2.17 Comparison of casting structure of slabs [a] with EMS and [b] without EMS(11)

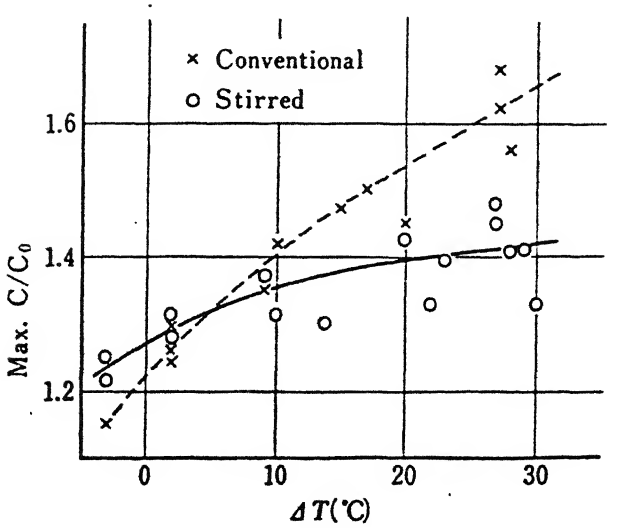

Fig.2.18 Effect of electromagnetic stirring and

the final stage of solidification were effective in better packing of equiaxed crystals in the axial zone of cast strands. Weak intensity stirring for a short duration was enough to eliminate V-segregation streaks in 150 mm. sq. steel ingots.

A considerable improvement was found in the absolute height of segregation peaks in longitudinal sections of 130 mm. sq. steel billets by Pochmarski et al(41). They also discussed the conditions to optimize the EMS process for steel billets. According to them, metallurgical effectiveness of stirring in reducing axial segregation, columnar zone and blow holes decreases with increasing carbon content. Haggart et al(35), reported that with optimised roll gap taper, the use of EMS leads to an increased centreline martensite level, but results in a reduction in the size of off centre semimacrosegregation in slabs. Radjai et al(42), from their work of evaluation of segregation by spectral analysis using Electron Probe Microanalyzer, observed that EMS supresses the centreline segregation but intensifies the intergranular segregation i.e. semimacrosegregation in the matrix surrounding the central region in slabs. A similar result was also found out by Sung et al(20) in their work on high carbon steel billets. They also found that the equiaxed structure formed by EMS was finer than the one formed as a result of lowered casting speed. Again, mould stirring along with the measure to improve castability by addition of CaSiMn (Mn/Si<2.5) was found to give excellent surface quality in high carbon steel billets, obviating the need to use aluminium wire feeding(43).

One problem with EMS is that it tends to increase the tendency of white band formation i.e. zone of negative segregation(10,20,22,30,44). Zavaras and Brody reported that the white band did not include any segregation or change in properties and was essentially an optical effect(20). Kor(44) and Druzhinin et al(30) discussed elaborately the formation of white bands and their elimination. The intensity of negative segregation due to EMS was found to depend on the carbon content of steel, even under identical conditions of solidification and stirring(46). The effect of EMS on centreline segregation has also been reviewed by Moore(7), Lait et al(23).

Addition of calcium has been found to reduce the extent of centreline segregation of sulphur and carbon by Kitamura et al(45),Radjai etal(42) and Nosochenko et al(48). Fig.2.19 shows the effect of calcium addition on centreline segregation of CC slab(45).Radjai et al reported reduced intensity of both intergranular segregation and centreline segregation by calcium treatment in slabs, but the segregation pattern remained almost unaffected. By their work of calcium treatment on CC tube billets, Nosochenko et al(48) observed improved macrostructure and globularization of oxide and sulphide inclusions. A 30-50% improvement in impact strength was obtained. According to Nosochenko et al(48), calcium being a surface active element, is adsorbed at the surface of the growing branches of the dendrites and causes retardation of their growth. It also leads to the growth of higher order branches and give rise to new centres of crystallization. A 10-15% increase in the rate of

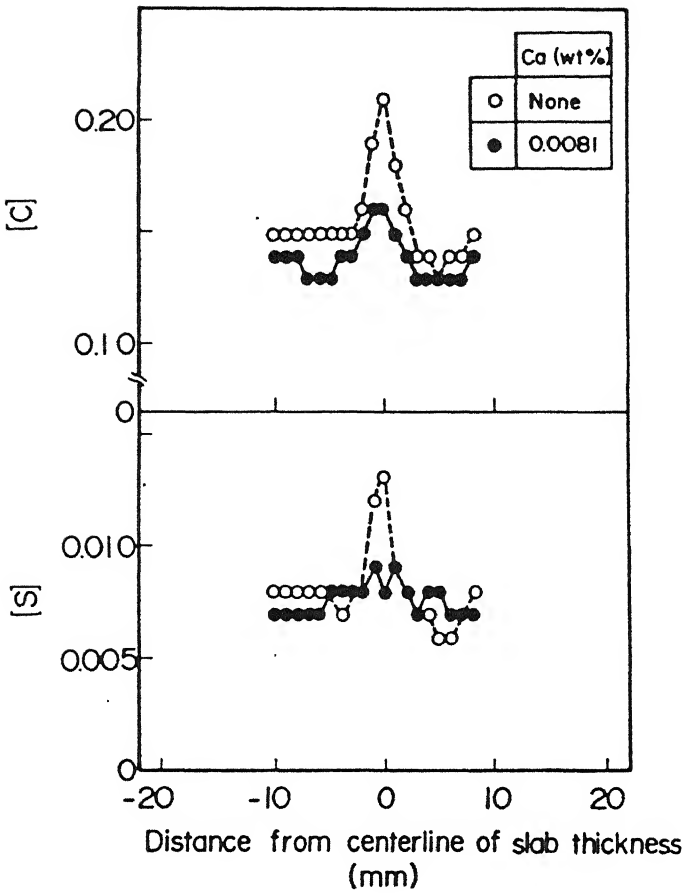

Fig.2.19 Effect of calcium addition on centreline segregation of continuously cast slab(45)

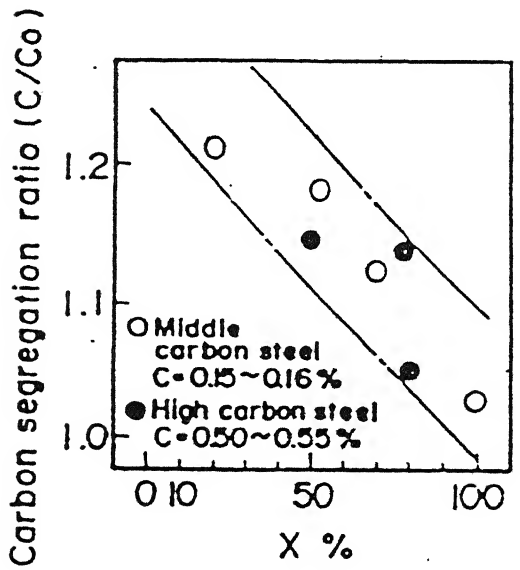

Fig.2.20 Relation between macrosegregation in continuously

crystallization was observed with the addition of calcium.

The application of rare earth metals (REM) to reduce the extent of centreline segregation of sulphur and carbon was reported by Kitamura et al(45),Miyamura et al(26) and Nosochenke et al(49). According to Miyamura et al(26), REM addition prevents the coarsening of network structure of equiaxed crystals in slab by promoting nucleation. Similarly sulphides and oxides of rare earth could act as heterogeneous nuclei assisting the rapid growth of equiaxed crystals(45). In production of 300 mm. thick carbon and low alloy steel slab, an improved macrostructure was obtained with less off centre segregation(49),central segregation and fine porosity by the addition of complex ferro alloy containing REM.

The introduction of roll gap taper to improve centreline segregation and off centre semimicrosegregation was studied by Haggart et al(35) and Bruce et al(50). Maximum improvement in centreline segregation, defined as percentage area of martensite, was obtained when taper encompassed the point of final solidification and a taper of 0.8 mm./m. was defined(35). In combination with EMS, roll gap taper was not so much effective when compared with roll gap taper alone. Haggert et al(35) suggested that this may be due to EMS altering the point of final solidification and proposed that taper reduces the fluid flow in the mushy zone before complete solidification. Thus, control of rate, extent and position of the roll gap taper are important parameters for this. Bruce et al(50) also studied the effect of increasing roll gap taper and its location with

respect to final solidification point on these segregations.

Soft reduction (SR) was studied by Flemings(15),Chaing(51), Masaoka et al(52), and Suzuki et al(53). SR significantly improved the centreline segregation in slabs by controlling the final stage of solidification(51). A drastic improvement in centreline segregation as well as in semi-microsegregation grain size was observed in slabs(52). A similar improvement was also noted by Suzuki et al(53) in macrostructure and centreline segregation, along with the absence of internal cracks in blooms of high carbon steels. A new technique named "controlled plane reduction" (CPR), when applied on CC slabs, improved centreline segregation to such a degree as comparable to that of interdendritic microsegregation(54). CPR completely prevents the movement of molten steel in the final stage of solidification by preventing bulging in slabs with flat bars and at the same time, by continuously compensating for the solidification shrinkage. Komai et al(55) pointed out that when slab was slightly reduced in thickness by short-pitch divided rolls, the amount of segregation was reduced a more than when the slab was supported only with short-pitch divided rolls. Flemings(15) pointed out that elimination of bulging plus slight amount of additional reduction (soft reduction) could reduce and even eliminate centreline segregation in continuous casting (Fig.2.20). To reduce the centreline segregation, it was important to establish a U-shaped, smooth, and orderly pool profile, in the direction of withdrawal of casting, over the entire slab width(11). Intensified secondary spray cooling improves the centreline

segregation as it prevents the bulging of slab due to increased stiffness(11,26).

Ultrasonic treatment of molten stream of ball bearing steel was applied during continuous casting of strand of 250x300 mm. sq. by Abramov et al(56). According to them, ultrasonic treatment lowers the temperature of the metal being poured before it enters the mould. This made it possible to increase the extent of equiaxed zone and hence improved axial segregation, porosity and carbide distribution. Water cooled immersible coolers were used by Revtov et al(34) and Parshin et al(57) in continuous casting of steel. Such coolers lowered the solidification period by 20-30%, reduced axial segregation and looseness, and extended the zone of equiaxed dendrites. This led to improved ductility and impact strength.

From the basic mechanism of macrosegregation and knowledge of effect of various factors on the same, the following conditions should be fulfilled to eliminate centreline segregation in CC products.

(i) Large equiaxed zone

(ii) Fine network structure of equiaxed crystals

(iii) Elimination of bulging caused by pressure of withdrawal rolls.

CHAPTER 3

PLANT DATA AND SAMPLE COLLECTION

The aim of present investigation was to study the centreline segregation in longitudinal sections of steel billets obtained from different steel plants in our country. The collection of samples cut from continuously cast(CC) billets and the corresponding shop floor data constituted an important part of this study. On the basis of various aspects of the science and technology of solidification and macrosegregation in CC steel products (discussed in chapter 2), the following scheme for sample collection was adopted.

(i) All samples should be from one strand in order to make comparative study easier.

(ii) Samples should be 150 to 250 mm long sections of billets. They should cover 2 to 3 columnar bridges.

(iii) Two samples from same heat, one at start of casting and other at end of casting should be collected to study effect of superheat.

(iv) Temperature of liquid steel should be measured in the tundish at the beginning and towards the end of casting in order to estimate tundish superheat.

(v) Samples should be preferably from billets of medium-to-high carbon steel. These grades are more susceptible to centreline segregation as well as development of adverse mechanical properties in final products.

Seven samples had already been selected according to the scheme above from the billet samples collected at Tata Steel, Jamshedpur. Table 3.1 presents the characteristics of CONCAST machine at Tata Steel. The specifications and casting details of the cut billet samples are presented in Table 5.1. More details of the process at Tata Steel are available elsewhere(12).

For some more samples from a different plant,Haryana Concast Limited, was selected. Haryana Concast agreed to provide the facility of tundish temperature measurement on request. A brief description about the facilities and operating conditions at Haryana Concast is recorded here.

3.1 Haryana Concast Limited

Haryana Concast Limited, located in Hisar (Haryana), is a Haryana Government Undertaking. Its only product is steel billets of various grades like Si-Mn spring steels, EN8, EN45a, 5S17, 65S17-Telco grade, Class -2 forge steel including mild steel billets (0.08 to 1.2%C). The annual capacity of billet production of all grades is 36000 tonnes.

The company produces billets of specific grades as per customers's requirements.The company purchases raw material (i.e. steel scrap etc.) from various sources. Liquid steel produced by direct electric arc furnace method is cast continuously in a two strand curved mould billet caster machine supplied by ISPL, India. Recently, rod and bar rolling mills are being set up. By having this facility, the company can also fulfil orders for rods and bars.

The plant has four major sections: (i) melting shop (ii) concast shop, (iii) laboratory, and (iv) maintenance shop

Table 3.1 : Characteristics of Continuous Casting Machine at Tata Steel, Jamshedpur(12)

Machine	
Supplier	CONCAST AG, W. Germany
Type	Curved Mould Billet Caster
Radius	6000 mm.
Ladle	
Capacity	130 tonnes
Refractory	Not Available
Teeming Modes	Slide Gate Valve with no Turret Facilit
Nozzle Diameter	45 mm.
Tundish	
Capacity	12 tonnes
Refractory	Garnex Board; Nozzle - Zirconia
Nozzle Diameter	12 mm. for 100x100 mm. sq. and 15 mm. for 125x125 mm. sq.
Strand	
Numbers	6
Centres	1100 mm.
Metallurgical Length	16.2 m./19.9 m.
Casting Speed	3.0 m./min. for 100x100 mm. sq. and 2.2 m./min. for 125x125 mm. sq.
Mould	
Material	Water Cooled Chromium Plated Copper
Sizes	100x100 mm. sq. and 125x125 mm. sq.

Table 3.1 (Contd.)

Tube Length	800 mm.
Lubricant	Rape Seed Oil
Stroke Length	Not Available
Oscillation Frequency	100 to 150 Cycles/min.
Water Flow Rate	504 m^3/hr.
Water Inlet/Outlet Temperatures	$45^oC/55^oC$
Secondary Cooling Zone	
Total Length	Not Available
Number of Zones	Zone I with 16 Spray Pipes
	Zone II with 48 Spray Pipes and Roller Apron
Water Flow Rate	324 m^3/hr.
Water Inlet/Outlet Temperature	$40^oC/60^oC$
Strand Straightening	Not Available
Billet	
Cut-off	Mechanical Pendulum Shears (360 tonnes capacity)
Length	5.5 m. to 13 m.
Cooling	Not Available
Sequence Casting	3 to 5 heats

including various kinds of stores for fire brick, steel scrap, electrodes, finished billets etc. A short description of first the two sections is given below:

(i) Melting Shop

There are two direct arc 3-phase electric furnaces each with a capacity of 15 tonnes and campaign life of 150-200 heats. Furnaces are lined first by a layer of high alumina (70% Al_2O_3) bricks followed by a second layer of magnesite bricks. A ramming mass of magnesite (80% MgO) is then used. The total thickness of lining is approximately 300 mm. Fettling is done by dolomite (18-25% MgO). All operations like adjustment of current and voltage, slagging-off, tapping, sliding of furnace roof etc. are performed through a control panel.

Charging of sorted scrap is done from the furnace top by an over head crane. Burnt lime stone and mill scale are added. Various deoxidisers employed are Fe-Si, Fe-Mn, coke and Al-Scrap. The total time for one heat is about 4-5 hours.

The chemical composition is checked by taking lolly-pop samples through the furnace slag hole. Temperature is measured by dipping consumable immersion-thermocouple connected to a dial meter. Molten steel is tapped at 1690-1700^{o}C (depending upon grade of steel) in a ladle pre-heated by oil burners. No shrouding facility is used for tapping. There is also no provision for measuring dissolved O, N and H. Only purging is carried out in ladle.

Sometimes composition is checked in the ladle. Plastic bags of rice-husk are thrown on top of the ladle to reduce heat loss by radiation. During transfer of ladle from melting shop to

concast shop, about 50 to 60°C temperature is lost.

(ii) The Continuous Casting Shop

At the CONCAST shop, first ladle purging is done either by N_2 gas for mild steel grade billets or by Ar gas in case of special steels such as spring steel and class- 2 forging grades. The main purpose of purging is to homogenize the melt for composition and to adjust the temperature to a value appropriate for teeming. Temperature is measured before and after the purging.

A mechanically operated slide gate valve is utilized to transfer the melt into the tundish. The cold garnex-board inside lining of the tundish is heated by an electric heater prior to teeming. In the tundish, sometimes oxygen lancing is carried out for temperature control and subsequently Ca-Si is added to control oxygen level in the melt. A cover of rice-husk is also maintained at the top of the tundish to reduce heat loss due to radiation from the upper surface of the molten steel.

From the tundish, liquid metal is fed continuously into the two oscillating moulds of the CONCAST machine. Aluminium wire is fed into the moulds continuously as a deoxidiser. There is no provision for measuring the tundish temperature on a routine basis. The specifications of the continuous casting machine at Haryana Concast Limited, are presented in Table 3.2. The casting stream from tundish to mould is open except for special grade steel billets for which nitrogen shrouding is practiced. In sequence casting a maximum of two heats are cast successively. Total casting time for 18 tonnes is about 50-60 minutes.

Table 3.2 : Characteristics of Continuous Casting Machine at Haryana Concast, Hisar

Machine	
Supplier	ISPL, Bombay
Type	Curved Mould Billet Caster
Radius	4000 mm.
Ladle	
Capacity	20 tonnes
Refractory	High Alumina; Sliding Nozzle Plate-Magnesite; Nozzle-Zirconia
Teeming Modes	Mechanical Slide Gate Valve Manually Operated
Nozzle Diameter	Not Available
Tundish	
Capacity	1.2 tonnes
Refractory	Garnex Board; Nozzle - Zirconia
Nozzle Diameter	13 mm. for 100x100 mm. sq.
Strand	
Numbers	2
Centres	1200 mm.
Metallurgical Length	8.0 m.
Casting Speed	1.5 to 2.0 m./sec. for 100x100 mm. sq. 2.4 to 3.0 m./sec. for 120x120 mm. sq.
Mould	
Material	Water Cooled Chromium Plated Copper
Sizes	100x100 mm. sq. and 120x120 mm. sq.

le 3.2 (Contd.)

Tube Length	800 mm.
Lubricant	Mustard Oil
Stroke Length	12 mm.
Oscillation Frequency	150 Cycles/min.
Water Flow Rate	2.5 kg./cm^2 (1250 to 1400 kg./min.)
Water Inlet/Outlet Temperatures	$40^oC/48^oC$

ondary Cooling Zone

Total Length	6.25 m.
Number of Zones	Zone I (1.0 m.Long with 40 Spray Nozzles)
	Zone II (48 Spray Nozzles)
	Zone III (48 Spray Nozzles)
Water Flow Rate	180 to 200 lits./min.
Water Inlet/Outlet Temperature	Not Available

and Straightening — D.C. Drive Mechanically Operated Pinch Rolls

let

Cut-off	Manually by Gas Torch
Length	3.8 m. to 5.7 m.
Cooling	Walking Beam, Turn Over Bed

uence Casting — 2 heats

There is also a provision for macroetching of transverse sections of billets in the laboratory. The purpose of this is to assess the quality of billets in respect of porosity, blow holes and cracks, as well as cast structure.

At the time of our visit, low carbon steel billets were being cast and the plan for production of medium-to-high carbon steel billets was uncertain. Hence only eight 200 to 250 mm long billet sections of low carbon steel were collected. From these only 4 were selected for the present study. The specifications and related casting data are presented in Table 5.2.

CHAPTER 4

PHYSICAL AND CHEMICAL EXAMINATION OF BILLET SECTIONS

4.1 Sulphur Printing of Longitudinal Sections of Billets

4.1.1 Literature review

Sulphur printing is a macrographic method of examining the state of sulphur distribution in steel. It is also capable of uncovering the outlines of original dendrites(58). Amongst a wide variety of methods, only the sulphur print is used widely today to study heterogeneity of steel products, like castings and rolled or forged objects.

In steel nearly all the sulphur is present in the form of sulphide inclusions, such as MnS and FeS. These get precipitated due to the very low solubility of sulphur in solid steel. The distribution of these sulphides is influenced by steelmaking processes, especially the method of casting of liquid steel.

Various techniques of sulphur printing have been discussed in the literature(58-61). The basic technique used even today with minor variations was developed by Baumann in 1906(59). In the sulphur printing method, a photographic paper soaked with sulphuric acid is adhered to the polished steel surface to be printed. After a few minutes, the paper is peeled off the surface and subsequently it is washed in water, fixed, washed and dried. The chemical reactions taking place during printing are(60):

$$FeS\ (\text{inclusion}) + H_2SO_4\ (aq.) \rightleftharpoons FeSO_4\ (aq.) + H_2S\ (g) \quad ..4.1$$

$$MnS\ (\text{inclusion}) + H_2SO_4\ (aq.) \rightleftharpoons MnSO_4\ (aq.) + H_2S\ (g) \quad ..4.2$$

$$H_2S\ (g) + 2AgBr\ (emulsion) \rightleftharpoons Ag_2S\ (s) + 2HBr\ (g) \quad ..4.3$$

The reaction of the sulphuric acid with the sulphide regions of the steel produces hydrogen sulphide gas (H_2S), which reacts with the silver bromide in the paper emulsion, forming a characteristic brown or grey-black deposit of silver sulphide. These dark coloured areas of silver sulphide in the print show the mirror image of the precise location of sulphide inclusions on the prepared surface of the metal and hence the sulphur distribution in the sample.

A grouping or agglomeration of such silver sulphide areas indicates the presence of sulphur segregation, whereas a random dispersion of the spots denotes a more uniform, and perhaps less harmful, distribution of the sulphide inclusions. A classification of the sulphur distribution based on the results of sulphur printing is given in Table 4.1(61).

Sometimes the liberated H_2S gas can become entrapped in voids or holes on the steel surface(59). Thus, when the paper covers these open areas, trapped H_2S gas will often leave a brown colour on the paper, indicating the presence of a gross sulphide segregate. In interpreting the sulphur print, these areas must be recognised as cracks or holes rather than as sulphide segregation by comparing the sample surface with the sulphur print visually.

To make the sulphur printing method successful, following parameters should be taken into consideration.

(i) Surface finish of the sample

(ii) Surface finish of the photographic paper

(iii) Acid concentration

le 4.1 : Classification of Sulphur Segregation Patterns in Sulphur Prints(61)

ssification	Symbol	Summary
Normal segregation	S_N	Segregation normally observed in ordinary steel. The sulphur distribution increases from outer portion to centre of steel and is shown in sulphur printing paper with colour which is heavier in centre than outer portion. This colouring is particularly light in rimmed part of rimmed steel.
Inversed segregation	S_I	Sulphur distribution decreases from outer portion to centre of steel, therefore colouring in sulphur printing paper is lighter in centre than in outer portion.
Central segregation	S_C	Sulphur distribution concentrates in centre and colouring on sulphur printing paper is extremely heavy.
Dispersed segregation	S_D	Sulphur segregation appeared in dispersed state with heavy colour on sulphur printing paper.
Linear segregation	S_L	Sulphur segregation appeared in linear state with heavy colour on sulphur printing paper.
Columnar central segregation	S_{CO}	Segregation observed in section steel or the like. The central segregation appeared in columnar central state.

(iv) Soaking time

(v) Contact or adhesion time

A smooth and finely ground surface finish is required. Polished surfaces can be used but do not produce improved results(59). Indeed, paper slippage resulting in blurred images is more common with polished surfaces. The surface to be tested should also be free from foreign matter such as dirt, grease and oil. Otherwise spurious dark spots appear on printing paper. Cleaning with acetone, alchohol, or 1,1,1-trichloroethane has been recommended by Vander Voort(59). Grinding the surface on No.00 or No.000 emery paper and subsequent thorough washing will generally produce a surface finish satisfactory for the purpose, as has been reported by Kehl(60).

According to Vander Voort(59), bromide type photographic papers are better than chloride type papers. Although glossy bromide papers produce sharper prints, semimatte printing papers have been recommended in the literatures(58-60), so as to minimise the danger of slippage, and hence blurring of the image, when the paper is placed in direct contact with the specimen surface. The action of dilute acid on the gelatin of the paper tends to make it soft and slimy, this condition being decidedly worse on glossy paper than on semimatte paper. Single weight (i.e.thin) papers are preferred so as to make good contact with the specimen surface(59).

In the literature, acid concentrations varying between 1 and 5% (H_2SO_4 in water) have been mentioned. A 2% solution is used most often(59). A more dilute acid solution can be used for

printing large surfaces where some time is required to cover the sample surface with the paper.

Soaking times varying between 1 and 5 mins. have been mentioned. Three mins. soke time is widely employed(59). Longer soaking times can cause swelling of the gelatin surface of the paper, which produces poor results.

A 2 to 10 mins. time of contact between the emulsion side of the paper and the sample surface, depending on the sulphur content of the steel, has been mentioned in the literature. In general, the same contact time should be used for a majority of the steel samples so that print intensities can be compared. Five mins. contact time is usually preferred. For very low sulphur steels, a 10 mins. contact time is often employed after preetching of the sample surface(59).

Preetching the surface of steel samples with 10% HNO_3 acid in water often helps to obtain high quality sulphur prints(59). The preetch improves the image intensity and promotes contact adhesion. Steels with less than 0.01% sulphur give faint prints, and preetching produces a more distinct print. The best results can be obtained only on the first or second print made from a sample surface. When making several sulphur prints of the same sample, the surface should be ground each time to ensure that previous printing does not affect the quality of subsequent prints.This is time consuming and uneconomical.

To make copies more conveniently, various techniques have been reported in the literature. Several investigators have used transparent film to reproduce a reverse image of the sulphur

print. Others have carried out subsequent photography of the sulphur print. One possibility of making several prints from the sample with relative ease is to preetch the sample surface. It has been possible to obtain prints several times.

Under standardised conditions, a quantitative measurement of sulphur content can be made. For this purpose, O'Nell used a photomicrometer to examine his transparent sulphur prints and obtained quantitative measurements of sulphur content as a function of print density(59). An image analyser was used by Haggart et al(35), to quantify the semimacro (or spot) segregation in etch prints made by etching the steel sample surface with a $CuCl_2$-picric acid solution.

4.1.2 Sulphur printing procedure

The various objectives of sulphur printing in this investigation were:

(i) to know the nature and type of sulphur distribution, especially along the centreline, in longitudinal sections of continuously cast (CC) steel billets,

(ii) to correlate the morphology of the CC billets, i.e. extent of equiaxed zone, porosity, etc. with centreline sulphur segregation as discussed in Chapeter 2, and

(iii) selection of specific locations along the centreline for generation of drillings (i.e. samples) to be used for sulphur and carbon analysis purposes.

Altogether 11 longitudinal sections of CC billet samples, the details of which are presented in Tables 5.1 and 5.2, were employed for sulphur printing work.

To obtain the surface finish required for sulphur printing, several methods, such as hand polishing by emery papers, polishing by emery paper fitted in a rotating wooden block, etc. were tried. Out of these, the following procedure was selected. Longitudinal sections of thickness 22 to 25 mm. and of length 150 to 250 mm. were cut along the central axis of the billets. Fig.4.1 shows the scheme of sample cutting. Two wide faces of these cut sections were flattened by a shaping machine. The wide face corresponding to the central axis of billet was polished by surface grinder to obtain the required surface finish.

Several trials were carried out to standardise the method for imparting proper contact between paper and sample surface. Removal of the air bubbles entrapped between the sample surface and paper requires special care. Several trials were made. Finally, the following procedure was adopted. The polished surface was washed with soap solution to remove dirt, grease and oil and rinsed with running water, and then again cleaned with acetone and dried with a dryer. The sample was placed horizontally on a bench vice with the polished surface facing upward and levelling was ensured by a spirit level. A bromide photographic paper was soaked in 2% H_2SO_4 acid solution in water for approximately 3 to 4 mins. Excess acid was drained out from the soaked paper surface using blotting paper before laying it on the steel surface in order to prevent blurring of the image. The emulsion side of the paper was placed in direct contact with the polished surface. To ensure proper contact and to avoid formation of white spots on the print, air bubbles were carefully removed

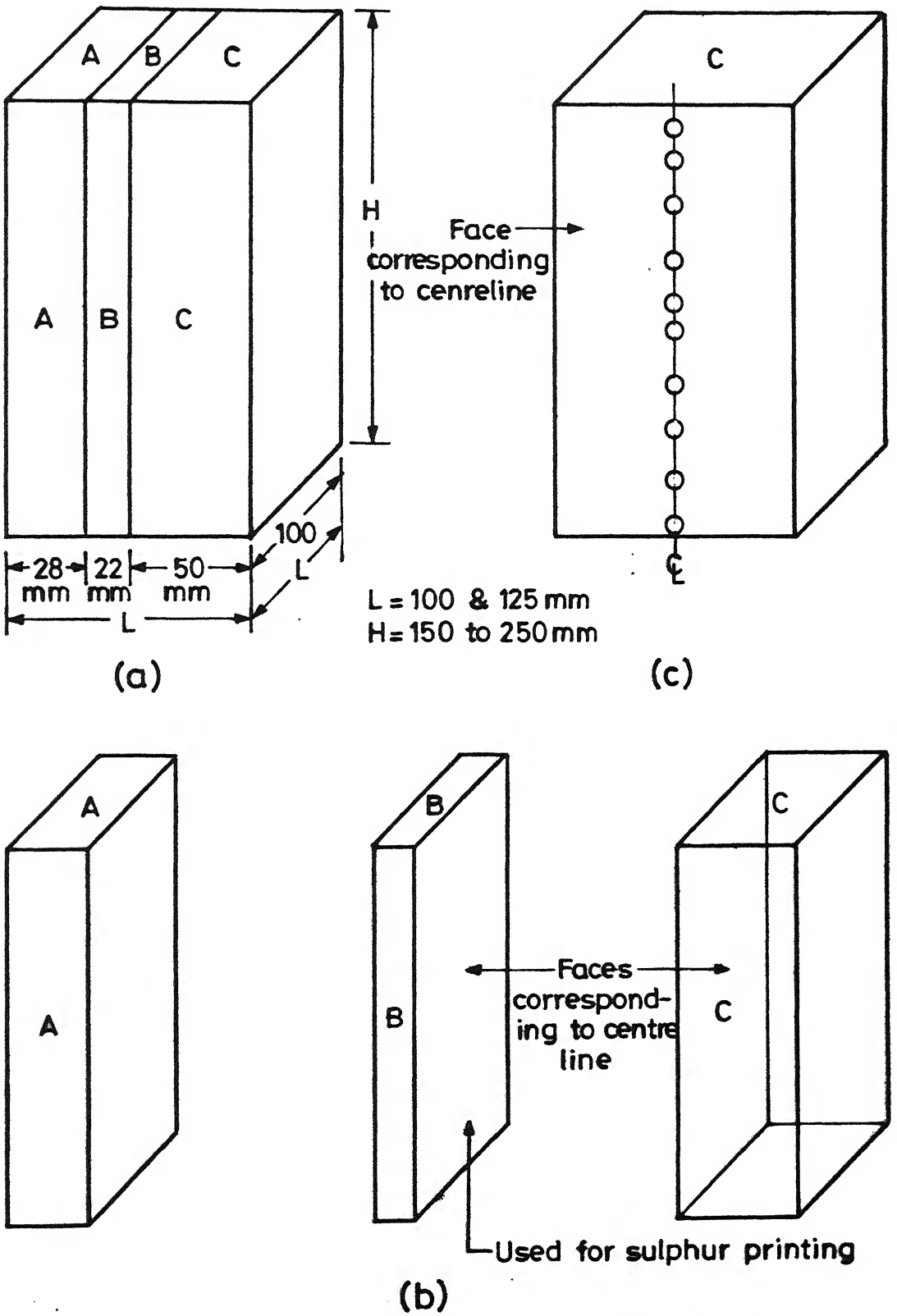

Fig. 4.1 Scheme of sample cutting: (a) billet sample

from the edges of the samples by using a smooth round bar. A moderate pressure was applied on the paper for 2 to 5 mins. depending upon steel composition by placing another smooth billet sample of almost the same size on the paper.

The paper was then taken off the surface of the sample carefully, and rinsed in clear running water. Then fixing was done in fixer solution for 15 to 20 mins. to make the developed image corresponding to exposed and unexposed areas, permanent. The fixer solution of sodium thiosulphate immediately dissolves the unaffected grains of silver bromide in printed paper. The print was again washed in running water for approximately 30 mins. and subsequently dried. It is advisable not to handle the print excessively before drying(59). The entire process was conducted under room illumination without damage to the paper. Strong sunlight, however, should be avoided.

4.1.3 Physical examinations

Physical examinations for various features, such as nature and extent of central porosity, bulging, cracks, blow holes etc. were made on the face corresponding to the central axis of the longitudinal billet samples. All observations were made after surface polishing. These observations are presented in Table 5.3.

4.1.4 Observations on sulphur prints

Each of the sulphur prints were examined with the aid of a magnifying glass to make various kind of observations including width of chill zone, nature and extent of equiaxed/columnar zone, nature and extent of centreline and

negative segregations, etc. All the observations made on billet samples from Tata Steel and Haryana Concast are presented in Tables 5.4 and 5.5.

4.1.5 Copying of sulphur prints

To make several copies of sulphur prints, many possibilities, such as repetition of the whole procedure etc. were tried. The former was feasible but it is time consuming. For the latter method, the colour of original print was too light to photographically prepare a good negative. So several attempts were made to obtain darker prints by varying parameters such as acid concentration (2 to 5%), soaking time (2 to 5 mins.), and contact time. But it was not possible to get darker sulphur prints without loosing contrast. Photocopying was another method of duplicating, and by adjusting photocopying machine after trials, it was possible to produce good quality copies of sulphur prints. Sample preetching, done with 10% nitric acid (HNO_3) in water, was also resorted to for making more than one sulphur prints. Preetching was also found to increase the image intensity of sulphur prints of some low carbon steel samples.

4.2 Determination of Sulphur and Carbon in Steel

There are several methods for determination of sulphur and carbon in steel. Basic principles and salient features of some of these methods have been reviewed by Roy(12). For sulphur determination in steel, Roy used the evolution method after some necessary modifications. The principle of the evolution method is

to convert all sulphur in the steel, present in the form of FeS and MnS, to an equivalent amount of H_2S gas by reacting the steel sample with hydrochloric acid. Liberated H_2S gas is absorbed in ammoniacal cadmium chloride ($CdCl_2$)solution and a yellow precipitate of cadmium sulphide (CdS) forms. Ammoniacal $CdCl_2$ solution is used because ammonia neutralizes the HCl acid which is produced due to the reaction(4.6) and thus prevents the solution of the precipitated CdS(62). The entire solution with precipitate of CdS is treated with an excess solution of iodine of known strength in the presence of HCl acid (1.16 sp.gr.). The excess of iodine is titrated back with a standard sodium thiosulphate ($Na_2S_2O_3$) solution. The amount of iodine solution consumed is a measure of the sulphur in the sample. The reactions involved in this process are:

$$FeS(s) + 2HCl(aq.) = FeCl_2(aq.) + H_2S(g) \quad ...4.4$$

$$MnS(s) + 2HCl(aq.) = MnCl_2(aq.) + H_2S(g) \quad ...4.5$$

$$H_2S(g) + CdCl_2(aq.) = CdS(s) + 2HCl(aq.) \quad ...4.6$$

$$CdS(s) + 2HCl(aq.) + I_2(aq.) = CdCl_2(aq.) + S(s) + 2HI(aq.) \quad ...4.7$$

$$2Na_2S_2O_3(aq.) + I_2(aq.) = Na_2S_4O_6(aq.) + 2NaI(aq.) \quad ...4.8$$

Percentage sulphur can be calculated as,

$$\%S = \frac{0.0016 \times V}{W} \times s$$

where, s = Strength of standard $Na_2S_2O_3$ solution used in Normality x 10

V = Volume of standard $Na_2S_2O_3$ solution consumed for sulphur i.e. difference between titration

of blank and sulphur containing solution, ml

W = Weight of the sample used, gm

The standard procedure requires a 5 gms. steel sample. However, by the drilling scheme for sample generation (section 4.3), it was not possible to generate samples of more than 2 gms. So, some modifications were necessary to accommodate this limitation. A standard $Na_2S_2O_3$ solution of strength N/20 was employed as against the recommended N/10 standard $Na_2S_2O_3$ solution. Accordingly the apparatus was modified(12). The reduction in strength of the standard sodium thiosulphate solution from N/10 to N/20 was done to minimise the error in reading the very small value of V corresponding to small sample weight. Other modifications made by Roy(12) are not being mentioned here. The accuracy and reproducibility of the modified method was assessed by Roy after extensive trials with many precautions.

For the present study, the evolution method standardised by Roy was again tried. Only one sample (No.5A) from Tata Steel was analysed by this method for quantitative sulphur segregation in the axial direction of longitudinal section of billet. Although this method was economical and fairly accurate, it was very time consuming. Therefore, it was decided to do analysis by the instrumental method such as automatic carbon and sulphur determinator. The latter offers the additional benefit of simultaneous carbon analysis as well.

National Metallurgical Laboratory (NML) kindly agreed to get the analysis done by their automatic Carbon and Sulphur

Determinator. This instrument analyzes both carbon and sulphur simultaneously. So, the rest of the samples as well as sample (No.5A) were then taken to Jamshedpur and analysed for both sulphur and carbon by this instrument. The theory and operation of this instrument is briefly noted below.

4.2.1 Carbon and sulphur determinator

The instrument being used at NML is a CS-444 carbon and sulphur determinator system (Fig.4.2) supplied by LECO Corporation, USA. The CS-444 system is a microprocessor-based instrument for a wide-range of measurements of carbon and sulphur content of metals, ores, ceramics and other materials. It consists of the CS-444 Determinator, the HF-400 Induction Furnace, a built-in balance, display monitor, printer and keyboard. Carbon determinations can be performed using one of the two selective ranges. Upto four separate calibration channels may be programmed. Specifications presented in Table 4.2. The automatic sample loader, autocleaner, and accelerator dispenser are ideal for high volume applications and reduce operating time.

Analysis begins by weighing out a sample (1 g nominal) into a ceramic crucible on the built-in balance. Accelerator material is added, the crucible is placed on the loading pedestal, and the ANALYZE key is pressed. Furnace closure and analysis is performed automatically. The sample is then purged with oxygen to drive off residual atmospheric gases. The induction furnace heats the sample, the sample material is combusted, and sample gases are released.

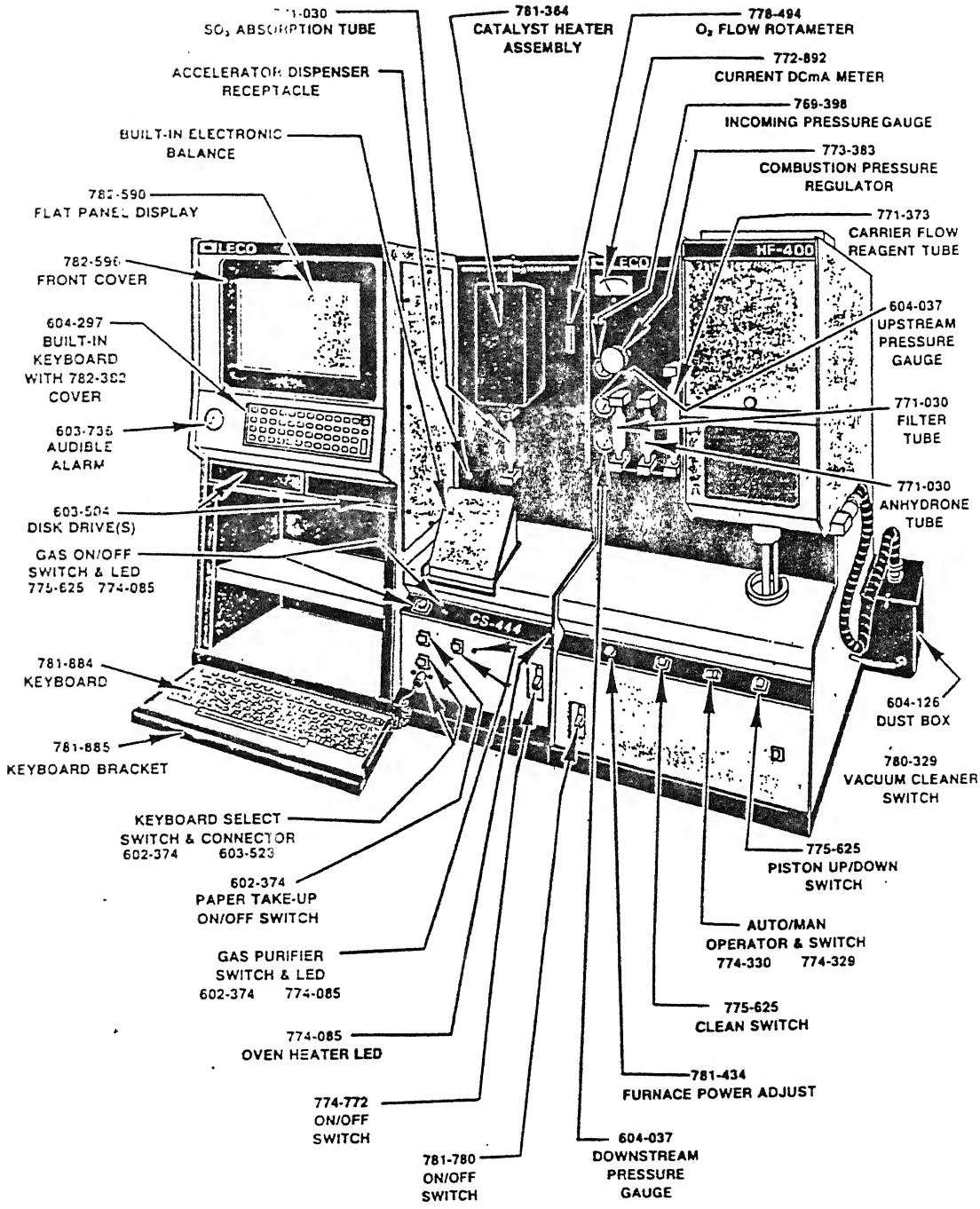

Fig.4.2 Automatic carbon and sulphur determinator (LECO CS-444)

ıble 4.2 : Specifications of Carbon and Sulphur Determinator at National Metallurgical Laboratory

ange 1 gm.*	
Carbon Low	0.00 - 0.5%
Carbon High	0.00 - 6.0%
Sulphur	0.00 - 0.35%
ccuracy**	
Carbon and Sulphur	± 0.3 ppm or ± 0.5% C and S present
recision	
Carbon and Sulphur	0.1 ppm
ensitivity	
Carbon and Sulphur	0.1 ppm
alibration	Gas dose or standards up to 200 analyses basis
nalysis Time	Nominal 40 sec., short cycle 25 sec.
mple Weight Range	0.00001 to 9.99999 gms.
lance Readability and epeatability	0.001 to 25 gms. ± 0.001 gm.
tection Method	Solid-state infrared absorption for both carbon and sulphur
emical Reagents	Anhydrous magnesium perchlorate($MgClO_2$), sodium hydroxide on impregnated clay, platinized silica gel, rare earth copper oxide, cellulose
ses Required	
Carrier Gas	Oxygen, 99.5% pure, 35 PSI (2.46 kg/cm^2)
Pneumatic Gas	Air, nitrogen or argon, source must be oil and water free, 40 PSI (2.81 kg/cm^2)
Optional Dosing Gas	Carbon dioxide, sulphur dioxide
rnace Type	Induction, 18 MHz, 2.2 kw

Range may be extended by reducing sample weight
Calibrated and conformance tested by gas dose analysis

Sample gases are swept into the carrier stream and transported to the infrared detection cells. Sulphur is measured as sulphur dioxide in the first IR cell. Carbon monoxide is converted to carbon dioxide in the catalytic heater assembly while sulphur trioxide is removed from the system in a cellulose filter trap. While gases flow through both the low and high range IR cells, carbon is measured as carbon dioxide in one cell only.

4.3 Drilling Scheme for Sample Collection

In the view of fluctuating nature of segregation profiles in longitudinal direction of billet samples, it was necessary to select a proper drilling scheme to study the quantitative aspect of centreline segregation of sulphur and carbon in steel billets in a better way. For this, it was required to consider the volume of the samples (i.e. drillings) and their positions along the axis of longitudinal section of billet samples. Accordingly a drilling scheme for sample generation was adopted after consulting the schemes proposed by many investigators(6,14,22,31)and original sulphur prints made on billet samples. A brief description of the same follows.

Drill diameter and depth of drill have been found to have a considerable effect on the analysis of solutes and therefore, on the magnitude of segregation ratios of solutes. Mori et al(6), Moore and Hamilton(14), and Shah and Moore(22) pointed out that larger the drill diameter and deeper the sample removed, greater was the effect of averaging out in composition. Mori et al gathered samples by drilling with a 3 mm. dia. drill to a depth

of 3 mm. to study the axial segregation of C and Mn in the 160 mm. sq. steel billets (0.85% C, $\Delta T = 50^{o}C$ and casting rate of 1.5 m./min.). Drilling made by 8 mm. dia. drill to a depth of 14 mm. were taken at 10 mm. interval by Moore and Hamilton to investigate axial segregation of C and S. Shah and Moore used a 8 mm. dia. drill with a 8 mm. depth to obtain 1 gm. sample per drilling to analyse both carbon and sulphur by an automatic carbon and sulphur determinator (LECO CS-344). In another investigation of carbon segregation in 200 mm. long steel billets, Iwata et al(31) collected drillings at 40 different positions along the centreline by drilling holes of 5 mm. dia. and 5 mm. deep at 5 mm. intervals.

Considering all these findings, a drilling scheme (see Fig.4.1) was selected to generate an adequate quantity of samples for analysis of carbon and sulphur. Fig.4.3 shows photographs of drilled surfaces. The different locations for drilling in axial direction were selected according to the sulphur print characteristics such as columnar bridges, white and dark regions of negative and positive segregations, respectively, etc. For seven samples (No.1 to 3 and Nos.4A, 4B, 5A and 5B) from Tata Steel, the drillings were made with a 8 mm. dia. drill to a depth of 8 mm. at different locations along the centreline direction of the billet samples (see Fig.4.3a). From these samples only the sample No.5A was analysed for sulphur by the evolution method as described in Section 4.2. For the samples (Nos. 6A, 6B, 7A and 7B), obtained from Haryana Concast, drillings were taken with a 4 mm. dia. drill to a depth of 8 mm. from different locations along

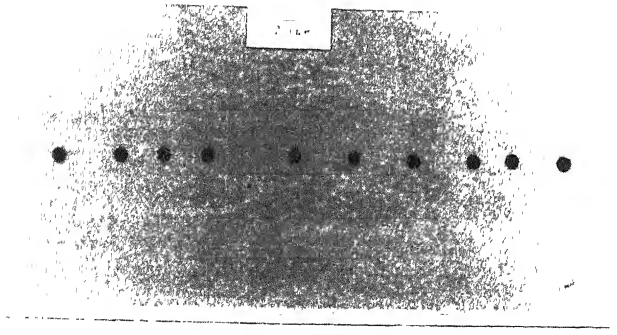

(a)

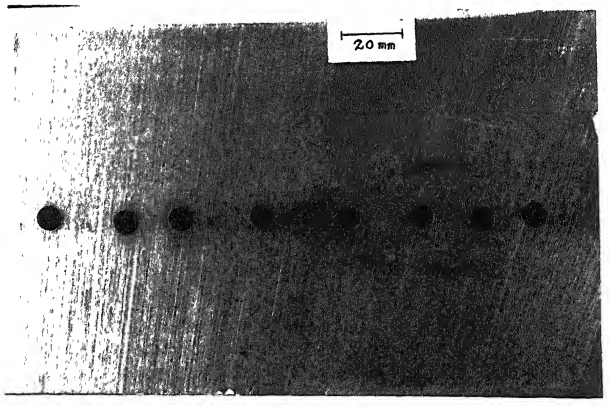

(b)

Fig. 4.3 Drilled surfaces along the centreline in longitudinal section of billet (a) 100x100 mm sq. and (b) 125x125 mm sq.

the direction of the billets (see Fig.4.3b). All 11 billet samples were analysed to determine both carbon and sulphur by an automatic carbon and sulphur determinator (sec.4.2). This method needed a lesser quantity (approximately 1 gm.) of sample than the evolution method which needed approximately 2 gms. of sample.

The surface used for drilling was washed with dilute hydrochloric acid, clear running water and acetone, and then dried. Apart from this, drillings were collected on a polyethylene sheet to avoid contaimination of carbon if paper was used. Clean plastic vials with proper identification marks were employed to store the drillings.

CHAPTER 5

RESULTS AND DISCUSSIONS

In the present investigation, 11 billet samples were studied. These samples were collected at Tata Steel and Haryana Concast. The specifications and casting details of the same are presented in Tables 5.1 and 5.2.

5.1 Physical Examination of Billets

Physical examination was carried out on longitudinal sections of the billet samples. The scheme of sample preparation has already been discussed in Chapter 4 (Sec.4.1.2) and illustrated in Fig.4.1. First, polished surfaces of billet samples were examined for central porosity, cracks, blowholes etc. Table 5.3 presents the results of observations made. These polished surfaces were then subjected to sulphur printing and various kinds of observations were made. Tables 5.4 and 5.5 present the observations made on sulphur prints.

5.1.1 Quality of sulphur prints

As mentioned in Sec.4.1.1, various techniques of sulphur printing were attempted to obtain the best quality prints. Parameters such as surface finish of the samples, glossiness of the photographic paper, acid concentration, soaking time, and contact time were varied. The standard procedure adopted has been described in the Sec.4.1.2. Standardisation of procedure was very important so as to meet the various objectives

Table 5.1 : Specifications and Casting Details of Billet Samples Collected at Tata Steel (12)

Sample No.	Heat No.	Steel Grade	Composition+,wt.%					LD Tapping Temp. °C	Ladle Temp. °C		Tundish Temp. °C	Sample Position++
			C	S	P	Mn	Si		Before Purging	After Purging		
1*	M38849	SWR	0.83	0.032	0.030	0.65	0.225	1720	1610	1570	1505	towards start of casting
2*	M38818	SWR	0.62	0.026	0.029	0.69	0.237	1730	1610	1555	1510	towards start of casting
3*	M38822	SWR	0.68	0.030	0.030	0.68	0.205	1725	1620	–	1575	–
4A**	M38935	11/14C (Si killed MS)	0.12	0.028	0.033	0.68	0.217	1720	1690	1636	1575	towards start of casting
4B**	M38935	11/14C (Si killed MS)	0.12	0.028	0.033	0.68	0.217	1720	1690	1636	1570	towards end of casting
5A**	M38910	11/14C (Si killed MS)	0.14	0.033	0.046	0.84	0.209	1700	1625	–	1570	towards start of casting
5B**	M38910	11/14C (Si killed MS)	0.14	0.033	0.046	0.84	0.209	1700	1625	–	1550	towards end of casting

* Sample of 125x125 mm sq.section
** Samples of 100x100 mm sq.section
\+ Composition based on lollypop samples taken after the final adjustment of composition at the purging station
++ All samples collected from strand No. 6

ıble 5.2 : Specifications and Casting Details of Billet Samples Collected at Haryana Concast

ımple No.	Heat No.	Steel Grade	Composition,wt.%					Furnace Tapping Temp.,°C	Ladle Temp. °C		Tundish Temp.	Sample Position
			C	S	P	Mn	Si		Before Purging	After Purging		
A*	BD982 (N_2 gas Purging)	Low Carbon MS	0.08 (f)	0.048 (f)	0.032 (f)	0.48 (f)	0.09 (f)	1685	1630	1615	1540	beginning of 1st billet
›B*	BD982 (N_2 gas Purging)	Low Carbon MS	0.08 (f)	0.048 (f)	0.032 (f)	0.48 (f)	0.09 (f)	1685	1630	1615	1500	beginning of 17th billet
7A*	BD992 (Ar gas Purging)	Class-2 Forge	0.175 (l)	0.04 (l)	0.029 (l)	0.88 (l)	0.18 (l)	1660	1620	1575	1535	beginning of 2nd billet
7B*	BD992 (Ar gas Purging)	Class-2 Forge	0.175 (l)	0.04 (l)	0.029 (l)	0.88 (l)	0.18 (l)	1660	1620	1575	1495	beginning of 28th billet

f Composition of lollypop samples taken from furnace

l Composition of lollypop samples taken from ladle

* All samples of 100x100 mm sq.section

** All samples collected from strand No. 1 of CONCAST machine.

of sulphur printing in the present investigation. Figs.5.1 to 5.15 present the sulphur prints (original or copy).

According to literature, two basic techniques of sulphur printing are:(i) technique as invented by Baumann and (ii)sulphur printing with preetching (Sec.4.1.1). Following these two techniques sulphur prints were made and a comparison between the quality of both the methods is discussed below.

Figs.5.1 and 5.4 show the sulphur prints made without preetching, and Figs. 5.2 and 5.5 show sulphur prints with preetching of the same samples. A better contrast between dark and light areas, and hence more resolution of segregation patterns may be noted in the former than in the latter. In sulphur prints of preetched samples, a prominent yellow background formed which led to reduction in the contrast and hence less clarity. Apart from this, in the technique involving preetching, the images of cast structure were not sharp and sometimes clearly visible outlines of dendrite crystals get broken into parts in the sulphur prints as compared to that in the sulphur prints made without preetching. The similar problem was faced also with the strings of inclusions. This may be due to the roughness of polished surface developed as a result of preetching with 10% nitric acid. There is also the possibility of removal of some inclusions during preetching. Nevertheless, this method of sulphur printing with preetching was a good alternative to make 2 to 3 more sulphur prints from the same sample without polishing the surface again and again. Only fresh preetching was required each time.

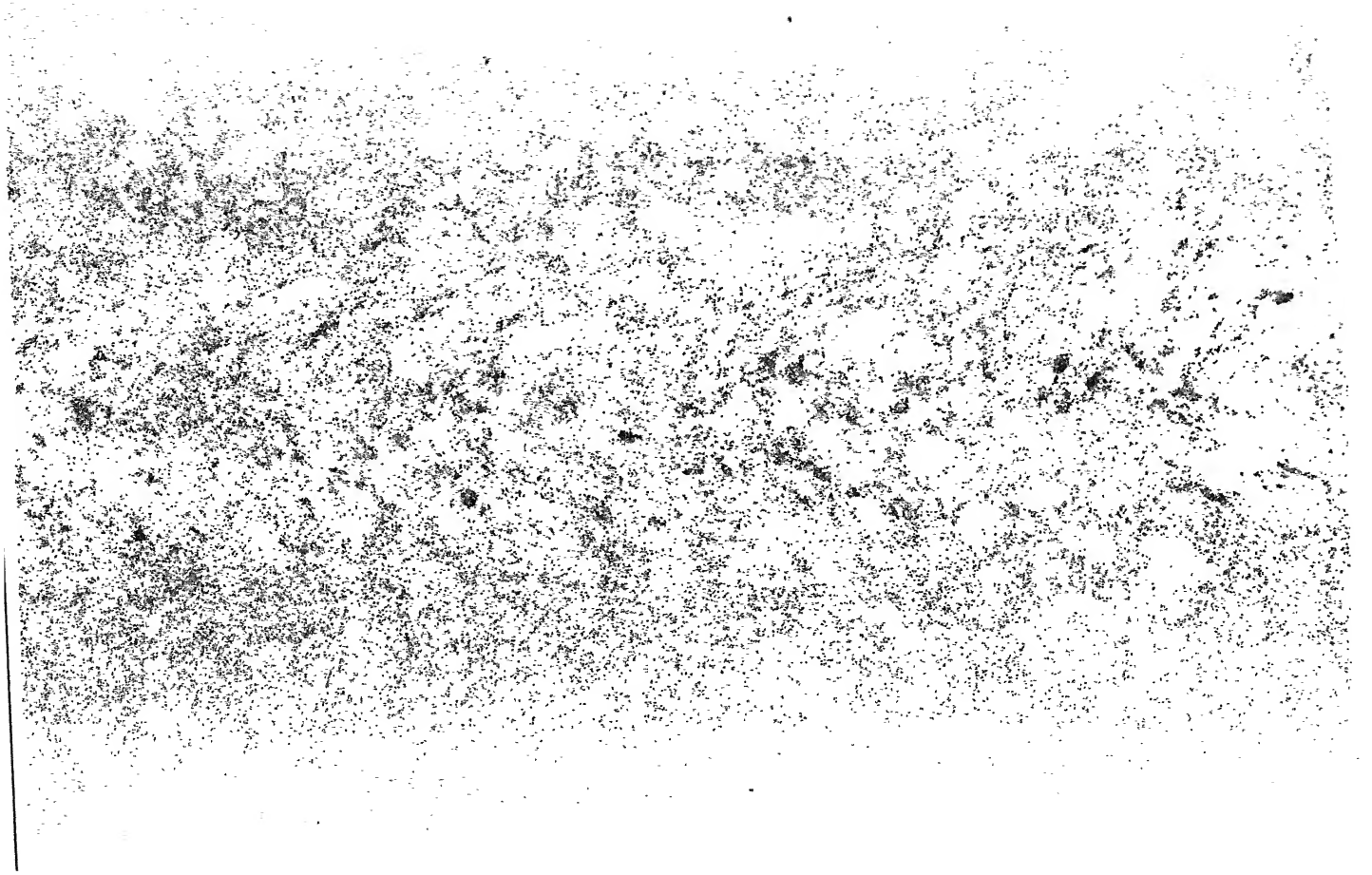

Fig.5.1 Sulphur print of longitudinal section of sample 1

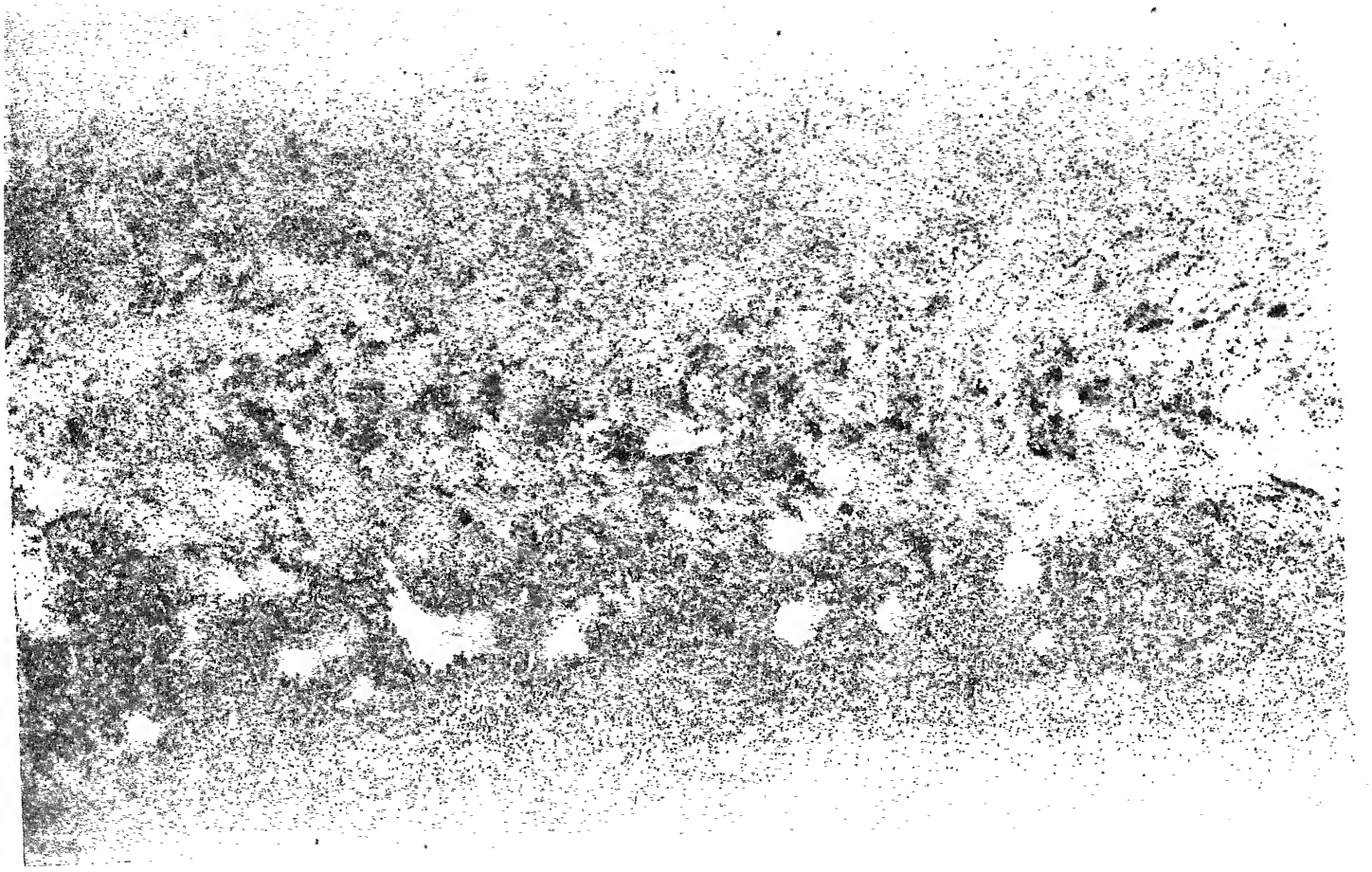

Fig.5.2 Sulphur print of preetched sample 1

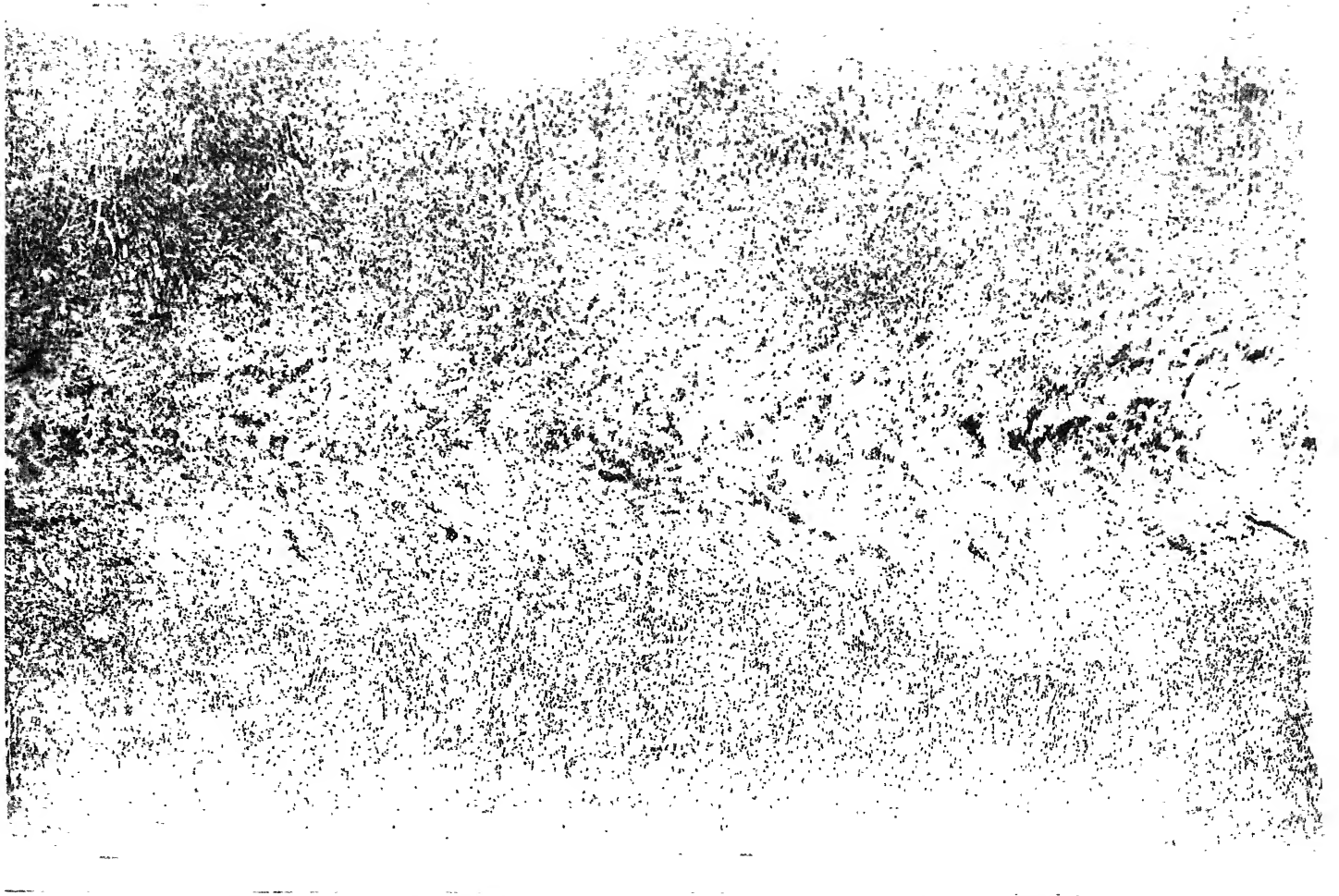

Fig.5.3 Photocopy of sulphur print of sample 1

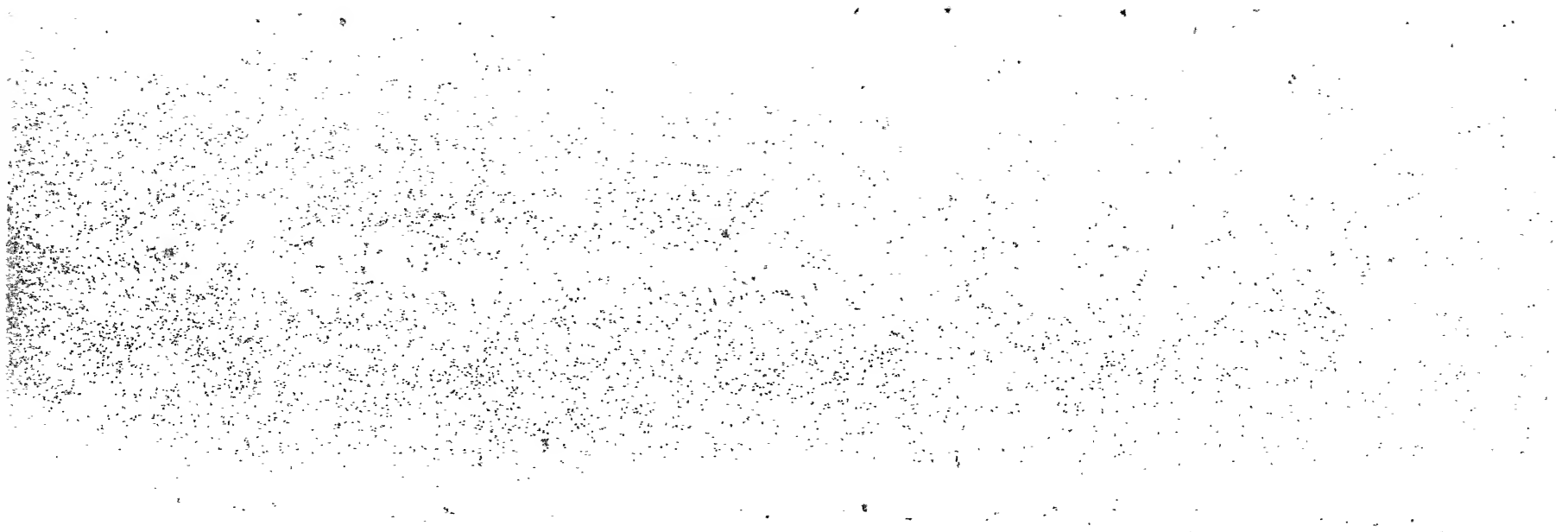

Fig.5.4 Sulphur print of longitudinal section of sample 4A

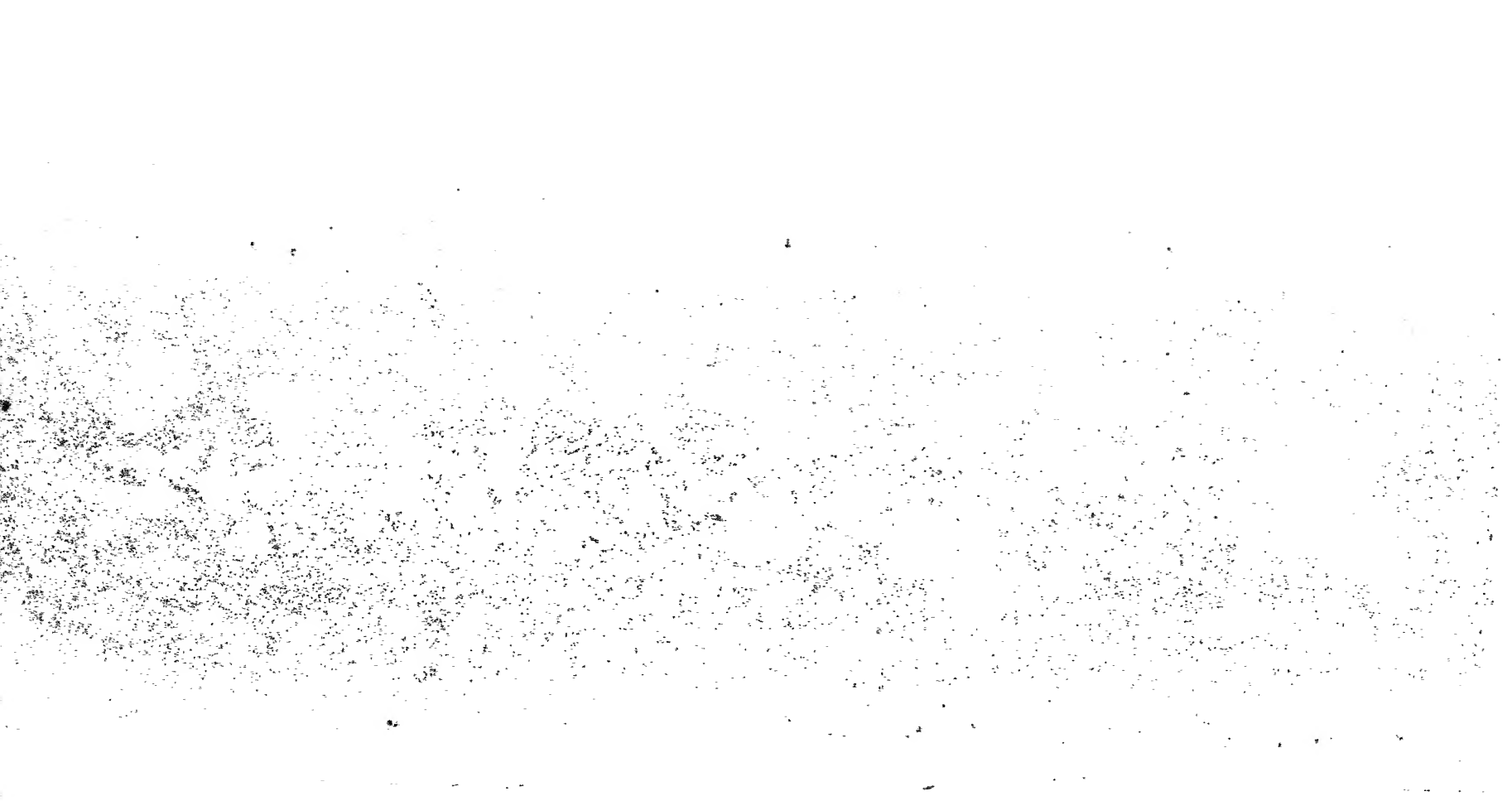

Fig.5.5 Sulphur print of preetched sample 4A

Fig.5.6 Photocopy of sulphur print of sample 4A

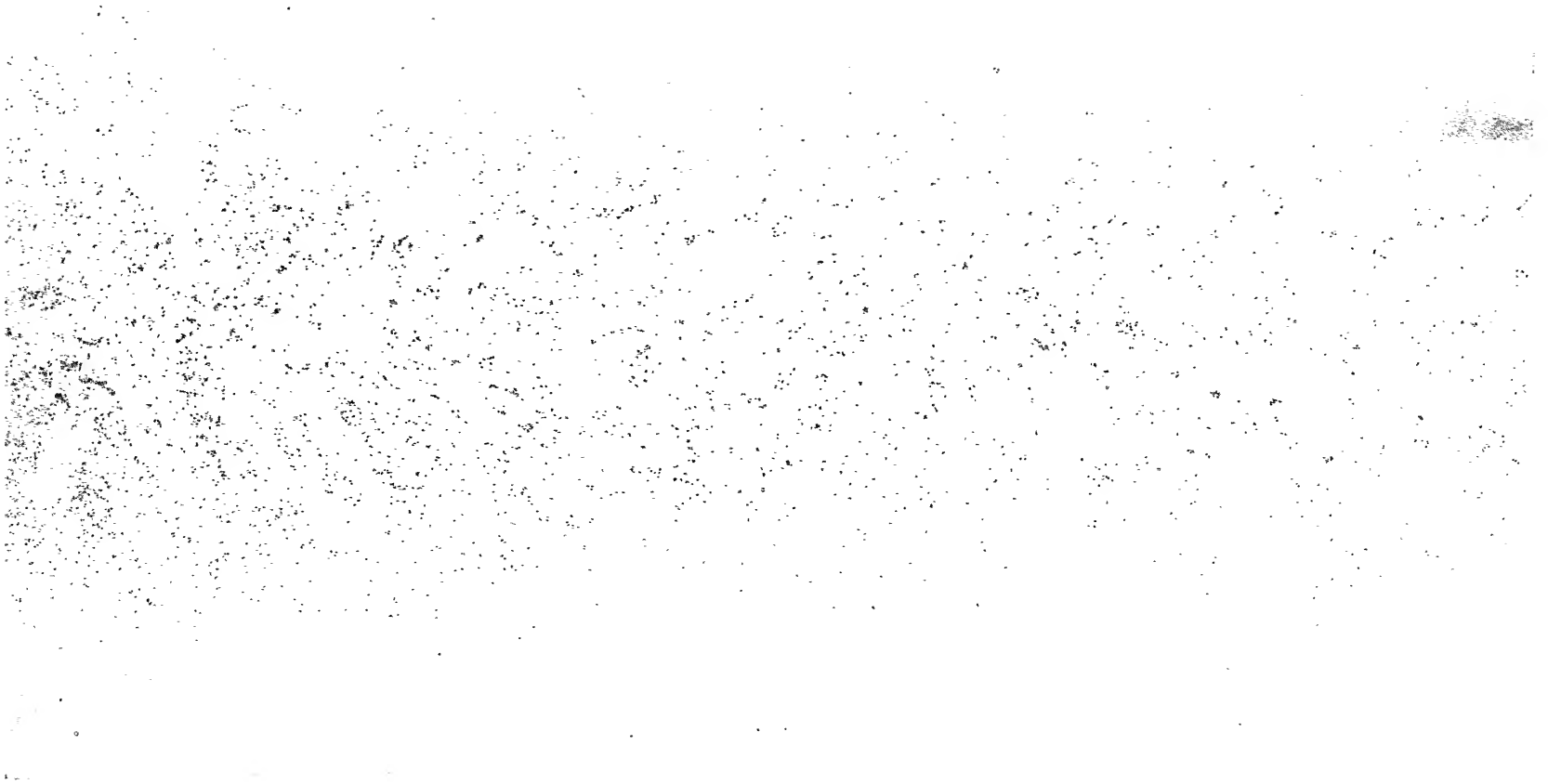

Fig.5.7 Sulphur print of longitudinal section of sample 2

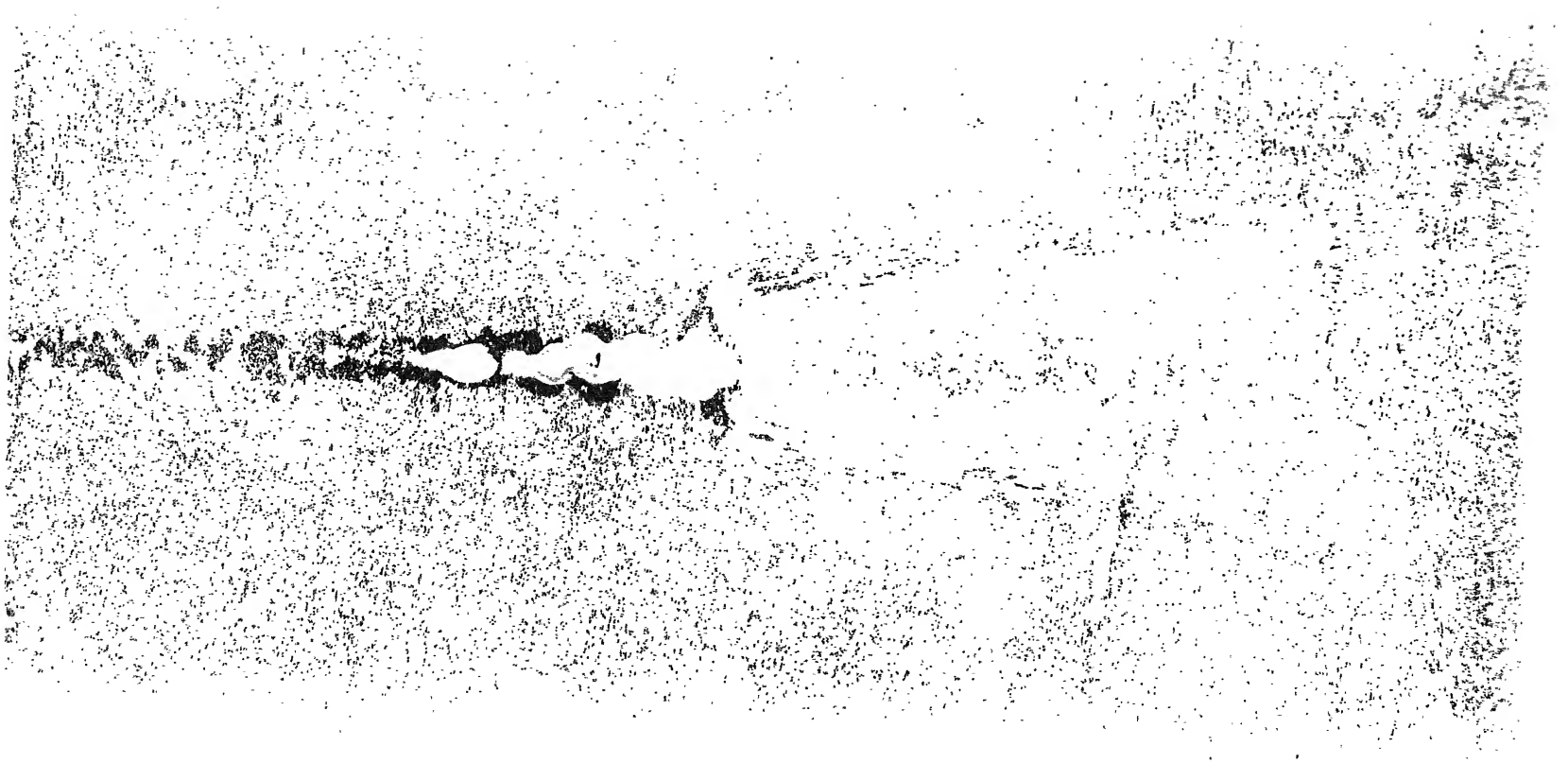

Fig.5.8 Photocopy of sulphur print of sample 3

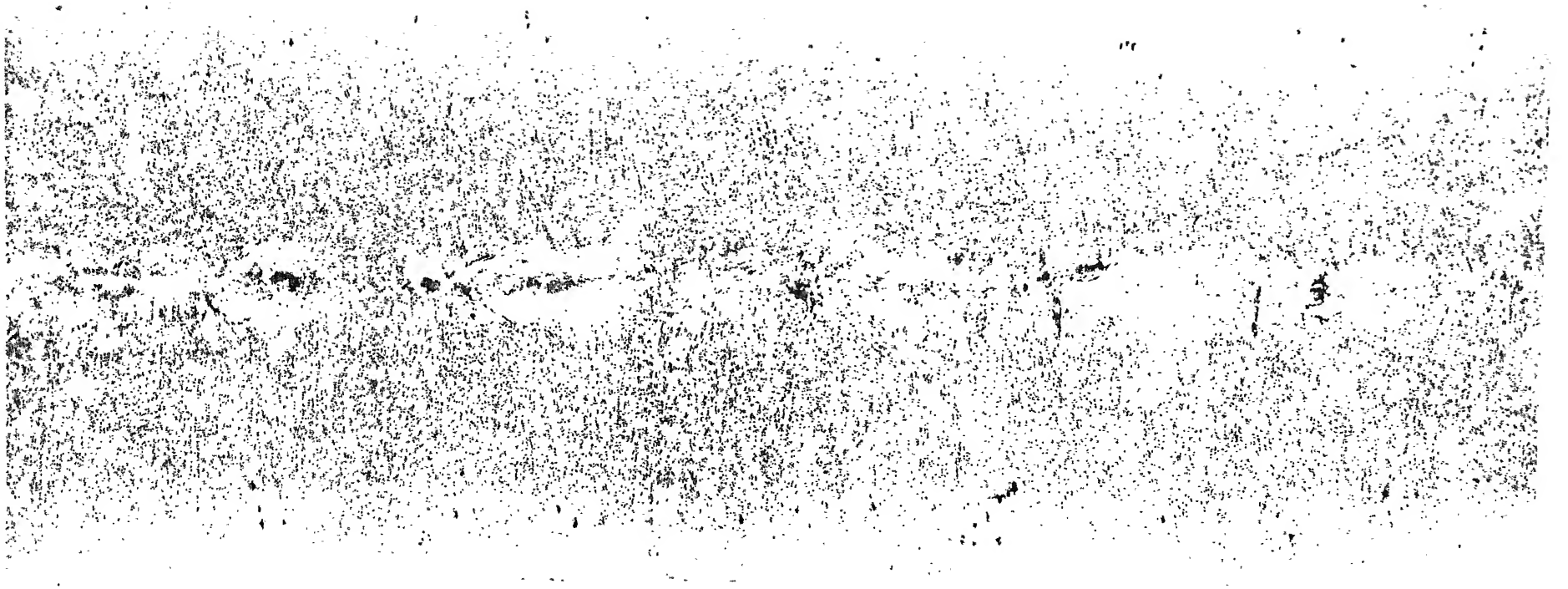

Fig.5.9 Photocopy of sulphur print of sample 4B

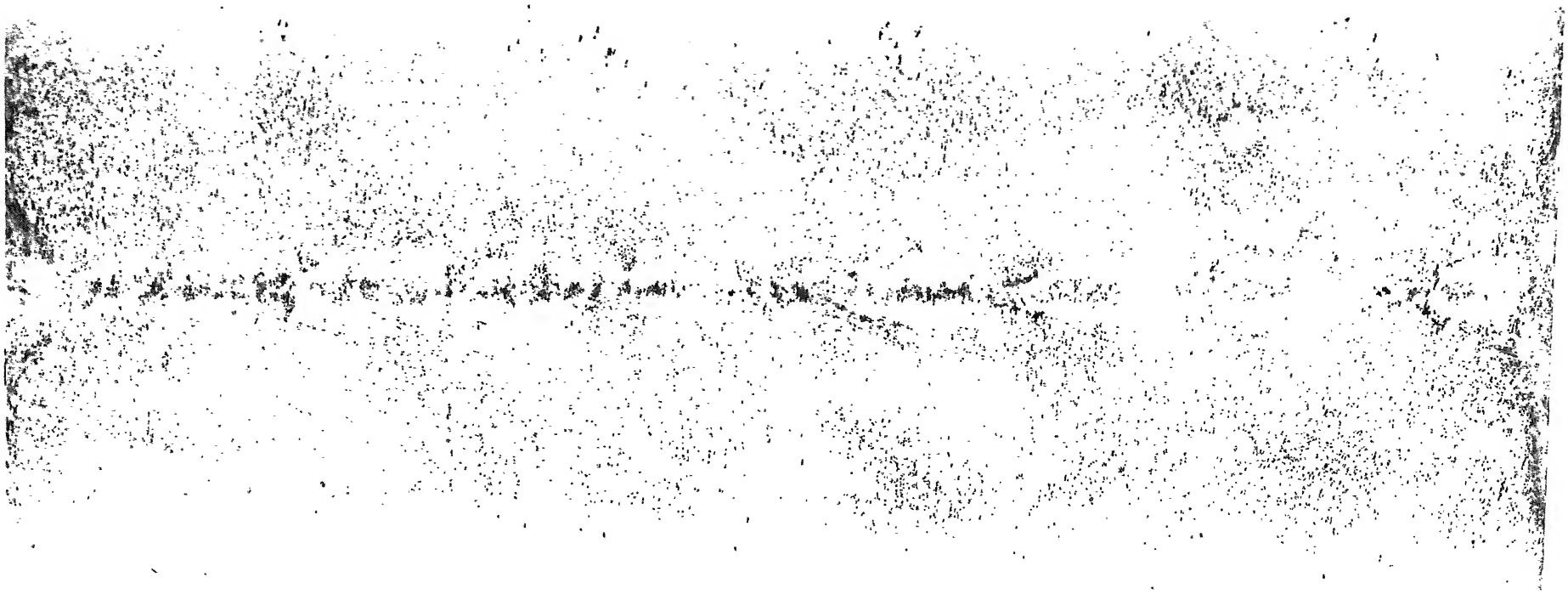

Fig.5.10 Photocopy of sulphur print of sample 5A

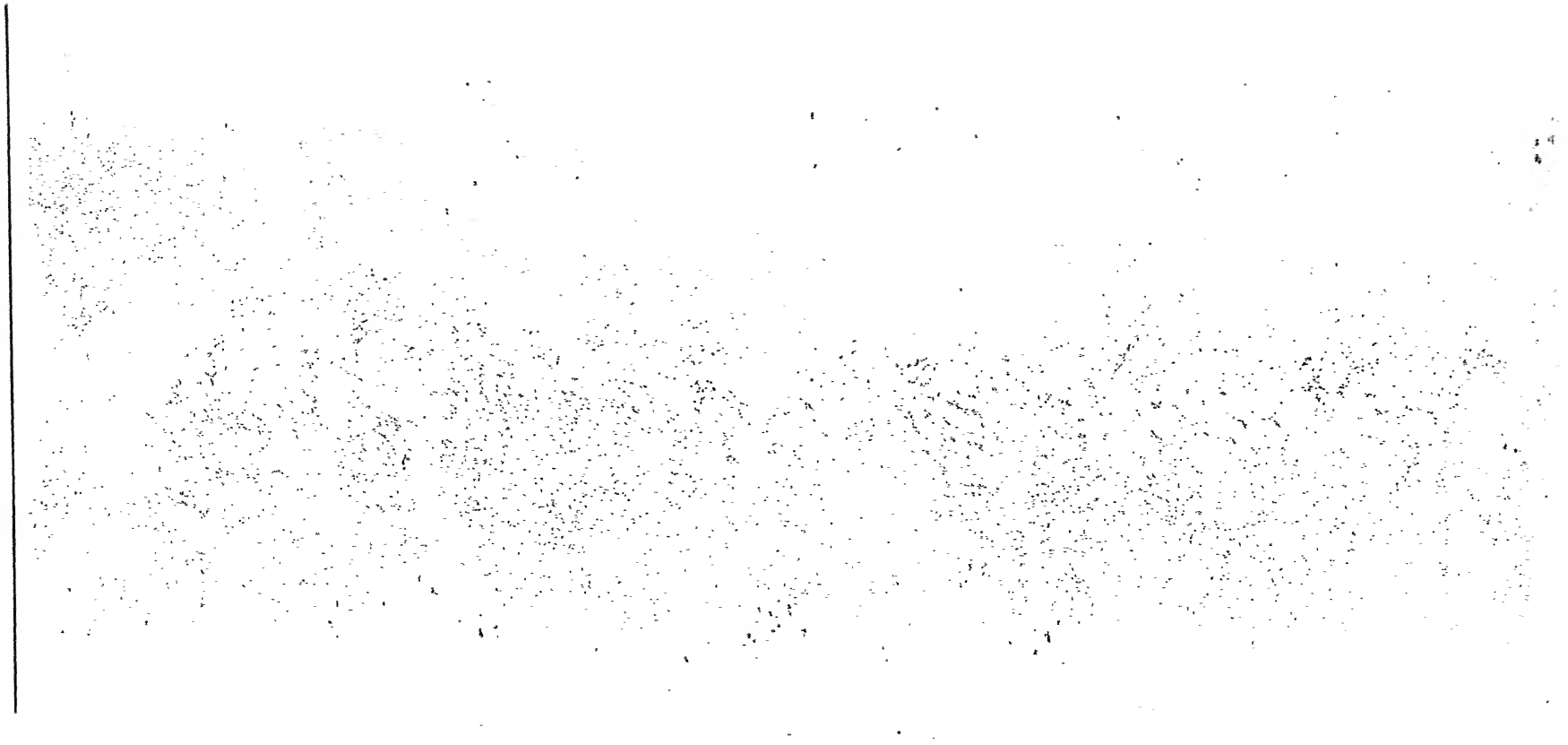

Fig.5.11 Sulphur print of longitudinal section of sample 5B

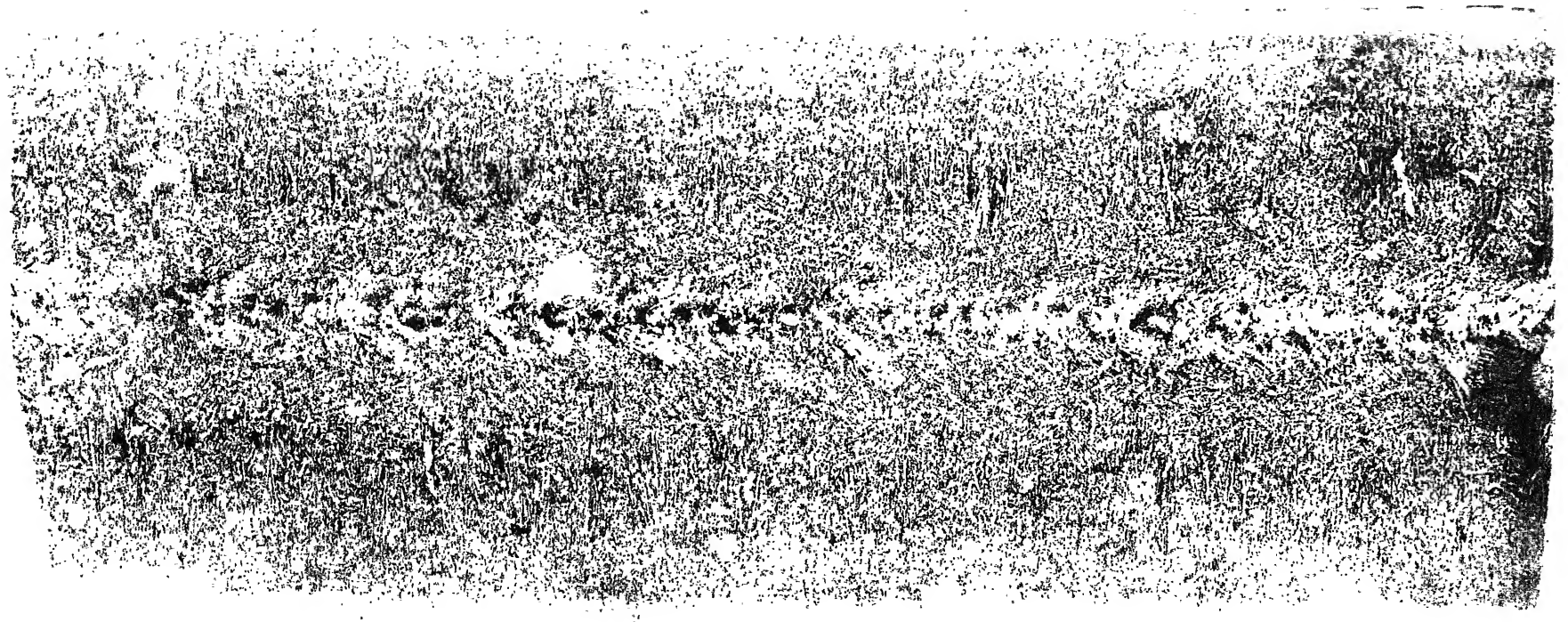

Fig.5.12 Photocopy of sulphur print of sample 6A

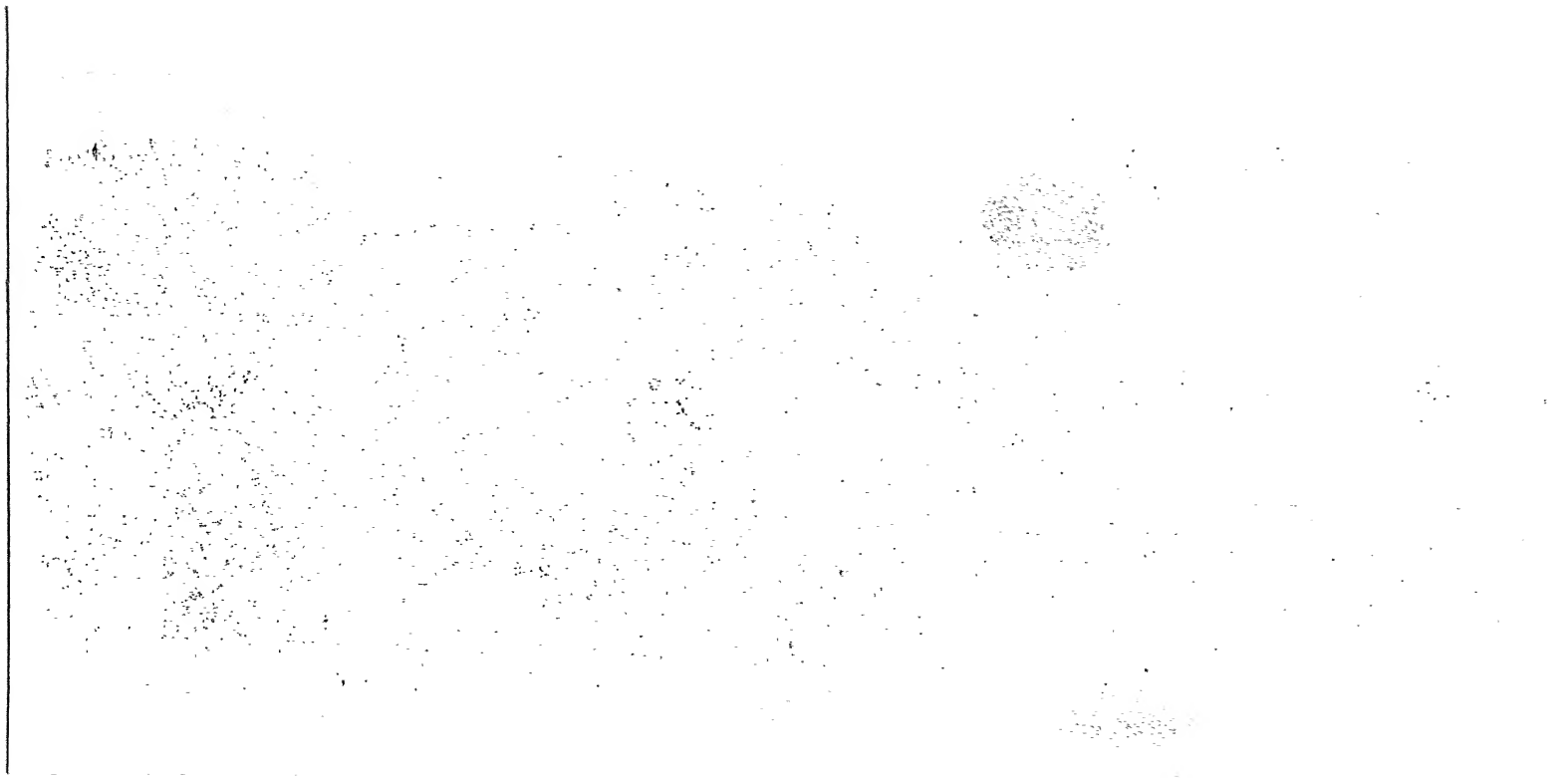

Fig.5.13 Sulphur print of longitudinal section of sample 6B

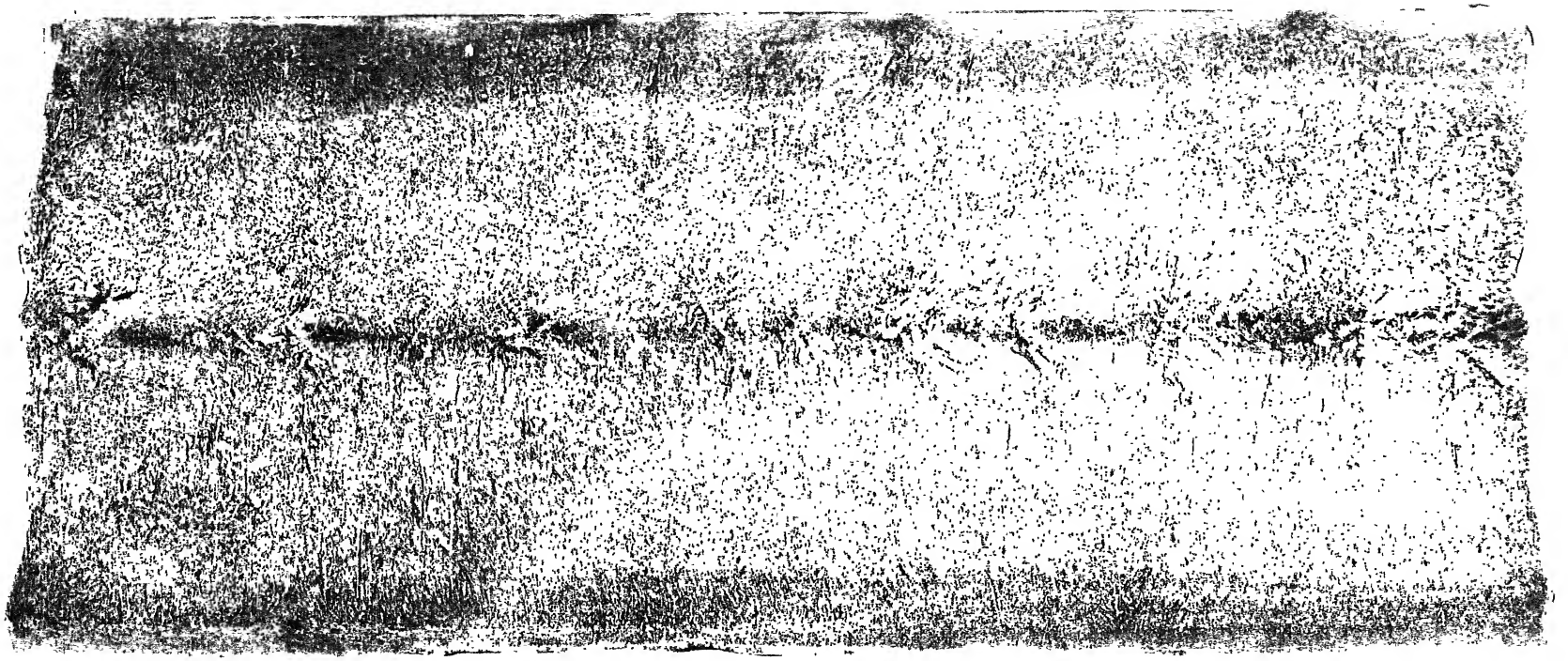

Fig.5.14 Photocopy of sulphur print of sample 7A

Fig.5.15 Photocopy of sulphur print of sample 7B

As mentioned earlier in Chapter 4 (Sec.4.1.5) photography of the sulphur prints was not possible due to lack of contrast and light colour of the prints. It was also found to be difficult to prepare many sulphur prints of the same sample properly without spending lot of time and efforts. Therefore, photocopying of the sulphur prints was attempted and was found to be satisfactory. Figs.5.1 and 5.4 and Figs.5.3 and 5.6 present the sulphur prints and corresponding photocopies of these, respectively. A comparison of these two kinds of prints reveals that the photocopies provide a superior picture of the segregation patterns such as V-bands, U-bands, etc. around the axis of the billets. On the other hand, they do not reveal the grain structure away from the axis as well as the original sulphur prints do. This is because of the nature of the photocopying process where spots or areas above a certain darkness only get reproduced. Rest of the areas or spots remain white in the photocopies. Since around the centreline segregation, bands or spots are darker and more massive in nature, they were reproduced with a better contrast during copying.

Therefore, it is concluded that photocopying of sulphur prints in a good quality automatic photocopying machine is capable of revealing the segregation patterns around the centreline of the billet samples better than the original prints. Therefore, it was decided to use this technique for reproduction of many copies of the original sulphur prints wherever necessary.

5.1.2 Observations on longitudinal section of billets

All 11 billet samples were cut according to

the scheme discussed in Sec.4.1.2 and illustrated in Fig.4.1, in order to prepare the required longitudinal faces corresponding to the centreline. These wide faces were used after polishing for two purposes: (i) observation on polished surfaces, and (ii) for sulphur printing.

5.1.2.1 Observations of polished surfaces

Table 5.3 presents the observations made on polished surfaces of the billet samples along the centreline direction. It also gives the values of the tundish superheats (ΔT), which is the difference between the temperature of molten metal in the tundish and the liquidus temperature of that particular grade of the steel. Liquidus temperatures were calculated using the following formula (**63**).

$$T_l\ (^{o}C) = 1537 - 88\,[\%C] - 25\,[\%S] - 5\,[\%Cu] - 8\,[\%Si] - 5\,[\%Mn] - 2\,[\%Mo] - 4\,[\%Ni] - 15\,[\%Cr] - 18\,[\%Ti] - 2\,[\%V] - 30\,[\%P] \qquad ...5.1$$

where [%] means weight percentage of an element in steel.

From Table 5.3, it may be noted that for the billet samples collected at Haryana Concast, the superheat values were very small and for two samples these turned out to be negative. Since this is not possible, these values are considered to be unreliable and would henceforth be ignored. The superheat values of samples collected at Tata Steel were considered to be reasonable by Roy(12) and these values are being accepted during discussions.

Only one sample (4A) of Tata Steel contains blowholes near chill zone. Other samples did not exhibit visible blowholes and

Table 5.3 : Physical Examination on Polished Surfaces of Billets

Sample No.	Superheat (ΔT), ^{o}C	Nature and Extent of Central Porosity	Cracks or Blowholes
1	48	little; very fine pores	nil
2	36	appreciable only in top part of the sample; small pores	nil
3	105	large, prominent only in bottom part of the sample	nil
4A	55	appreciable; small pores dispersed in V- shape	blowholes near chill zone
4B	50	almost nil; very fine pores in bottom part of the sample	nil
5A	53	little; small pores distributed along centreline	nil
5B	33	nil	nil
6A	-	little; fine pores distributed along centreline	nil
6B	-	nil	nil
7A	-	little; small pores distributed along centreline	nil
7B	-	nil	nil

7A, cast at relatively high superheats, whereas samples 6B and 7B, which were cast at low superheats, exhibited no porosity at all. This observation is also in agreement with the literature (Sec.2.5).

5.1.2.2 Observations on sulphur prints

All the 11 longitudinal sections of billet samples were subjected to sulphur printing to observe the various features of centreline segregation such as V-bands, U-bands, V- lines, white bands. Sulphur printing also reveals the cast structure and its various features like chill zone, nature and extent of columnar/equiaxed zone, bridging etc. Tables 5.4 and 5.5 present the various observations made on Tata Steel and Haryana Concast billet samples, respectively. The prints were also consulted for selection of locations along the centreline for drilling of samples to be used for quantitative analysis of carbon and sulphur (Sec. 4.2). Following are the discussions of observations on sulphur prints presented in Table 5.4 for samples collected at Tata Steel.

(i) **Width of chill zone :** Width of chill zone varied between 5 to 10 mm. (approximately) and it was independent of superheat and section size in almost all samples. However, for sample 3, cast at high superheat, the width of chill zone was less. This observation is expected from theory.

(ii) **Nature and extent of equiaxed/columnar zone :** In samples 2 and 5B, cast at relatively low superheats, equiaxed zone was found to be dominant. At a very high superheat (sample 3), coarse and extended columnar crystals were dominant

ble 5.4 : Observations of Sulphur Prints of Longitudinal Sections of Billets from Tata Steel

mple No.	Width of Chill Zone (mm,approx)	Nature and Extent of Equiaxed Zone	Width of Central Segregated Zone (mm, approx.)	Nature and Extent of Positive Centreline Segregation	Nature of V-segregation	Special Features
1	8-10	significant; small and coarse columnar crystals	15-20	dispersed broadly; significant	broad and conspicuous V-lines	negative segregation not discernible; few columnar bridges
2	8-10	dominant; less columnar crystals	15-30	less dispersed; significant	broad and conspicuous V-lines	negative segregation in bottom part; insignifcant columnar bridges
3	6-7	coarse and large columnar crystals dominate in general; few coarse equiaxed crystals inside U-line	8-40	slightly dispersed; prominent	prominent U-band	negative segregation inside U-line; extensive columnar bridges in bottom part of the sample

able 5.4 (Contd.)

4A	5-7	insignifi-cant; fine and extended columnar crystal dominate in general	10-15	dispersed slightly; significant	dull band of V-lines closely spaced	negative segregation inside V-lines; few columnar bridges; blowholes near chill zone
4B	not distin-guishable	insignifi-cant; small and lengthy columnar crystals dominate in general	8-10	narrow and prominent	fine V-lines widely spaced	negative segregation inside V-lines;appre-ciable columnar bridges
5A	5-6	insignifi-cant; large columnar crystals dominate in general	5-15	narrow and prominent	fine V-lines at reasonably close and uniform spacing	negative segregation inside V-lines;appre-ciable columnar bridges
5B	5-7	dominant	not discer-nible	widely dispersed; not prominent	fine band of V-lines; not easily dis-cernible	unrevealed negative segregation; insignifcant columnar bridges

Table 5.5 : Observations of Sulphur Prints of Longitudinal Sections of Billets from Haryana Concast

Sample No.	Width of Chill Zone (mm,approx)	Nature and Extent of Equiaxed Zone	Width of Central Segregated Zone (mm, approx.)	Nature and Extent of Positive Centreline Segregation	Nature of V-segregation	Special Features
6A	5-8	insignifi-cant; small columnar crystals dominate in general	15-18	narrow and dispersed; prominent	V-line widely spaced	negative segregation inside V-lines; few columnar bridges
6B	5-6	insignifi-cant;fine and large colum-nar crystals dominate in general	8-10	narrow and widely dis-persed; prominent	not dis-cernible	unrevealed negative segregation; appreciable columnar bridges
7A	very small	insignifi-cant;large and very fine columnar crys-tals dominate in general	15-18	narrow and less dis-persed; prominent	fine band of V-lines widely spaced	negative segregation inside V-lines; few columnar bridges
7B	6-7	dominant; almost no columnar crystals	35-40	narrow; insignif-cant	regular band of fine V-lines closely spaced	negative segregation inside V-band, no columnar bridges

everywhere, but not in the region inside the U- line, which was occupied by coarse equiaxed crystals around the centreline. In other samples 1, 4A, 4B, and 5A, cast at moderately high superheat, columnar crystals were dominant in general. All these observations are in conformity with literature (Sec.2.5) that larger the superheat, larger is the extent of columnar zone.

(iii) **Width of central segregated zone :** An irregular pattern of central segregated zone with large variation in its width was observed in almost all samples. However, sample 4B exhibited more or less uniform pattern with very less variation in the width of central segregated zone.

(iv) **Nature and extent of positive centreline segregation zone :** There was clear trend of this zone towards becoming narrow and prominent with increasing superheat in almost all samples.

(v) **Nature of V- segregation :** In samples 4A, 4B, 5A and 5B, V- segregation bands were observed whereas in samples 1,2 and 3, broad and conspicuous V- segregation lines were observed. It appears that difference in section size may be the cause of this difference in behaviour. Samples 4A, 4B, 5A, and 5B were 100x100 mm. sq., whereas samples 1,2 and 3 were 125x125 mm. sq. size.

In sample 3, a prominent U- band was observed with coarse columnar crystals extended across the U- line and coarse equiaxed crystals inside the U- line. Mori et al(6) (Sec.2.4) also have reported similar morphological features associated with U- bands. Presence of negative segregation between the V- lines was observed in all samples except in sample 1, where it was not

discernible. Similar white bands have also been reported in literature.

(vi) **Bridging :** Tendency of formation of more columnar bridges with increasing superheat in all samples was observed. More the superheat, more is the growth of columnar crystals and hence more bridging, as mentioned in the literature (Sec.2.3.2).

Following are the discussions on observations presented in Table 5.5 for samples obtained from Haryana Concast. As mentioned earlier, absolute values of superheat were unreliable here hence only relative values amongst the samples were meaningful.

(i) Width of chill zone : In samples 6A, 6B and 7B, width of chill zone was almost the same (5 to 8 mm.) and this little variation in the width was independent of superheat. However, sample 7A cast at relatively high superheat, revealed very small width of chill zone.

(ii) Nature and extent of equiaxed/columnar zone : Columnar crystals were dominant in all the samples except in sample 7B in which equiaxed zone was predominant. In sample 7A, cast at relatively high superheat than sample 7B, columnar crystals were dominant. This was again in agreement with literature (Sec.2.5).

(iii) Width of central segregated zone : Small variation in the width was observed in all samples. However, sample 6B cast at low superheat showed very narrow width of central segregated zone.

(iv) Nature and extent of positive centreline segregation : With the increasing superheat, positive centreline segregation zone was found to become narrow and prominent in all the samples. This behaviour pattern is consistent with that of Tata Steel samples.

(v) Nature of V- segregation : V- lines of varous kinds of distribution were observed in all samples, except in the sample 6B, cast at low superheat. This behaviour pattern is in contrast with Tata Steel samples of same size (100x100 mm. sq.) which exhibited V- bands rather than V- lines. V- shaped negative segregation was observed in the all samples except in the sample 6B.

5.2 Centreline Segregation of Carbon and Sulphur

In the present investigation, the purpose of the chemical analysis was to determine the nature and extent of the centreline segregation in billets. The evolution method as standardised by Roy(12) was tried for analysis of sulphur in one sample (5A) from Tata Steel. Although this method was fairly accurate, it was time consuming. After availability of an automatic carbon and sulphur determinator at National Metallurgical Laboratory, it was decided to do analysis of sulphur as well as carbon by this instrument. The results obtained by this instrument were reliable. Moreover both carbon and sulphur could be determined. The drilling scheme adopted for sample collection has been discussed in Chapter 4 (Sec.4.3). Table 5.6 presents the results of analysis of drillings.

Table 5.6 : Carbon and Sulphur Contents of Drill Samples Along the Axis of Longitudinal Sections of Billets

Location	Sample 1 Nominal Composition (Wt%) C = 0.83, S = 0.032			Sample 2 Nominal Composition (Wt%) C = 0.62, S = 0.026		
	Length (mm.)	Wt% C	Wt% S	Length (mm.)	Wt% C	Wt% S
a	0	0.880	0.025	0	0.670	0.018
b	28	0.838	0.024	22	0.671	0.023
c	61	0.844	0.026	40	0.655	0.022
d	94	0.848	0.031	62	0.686	0.023
e	113	0.867	0.031	87	0.673	0.019
f	133	0.841	0.029	123	0.667	0.021
g	163	0.829	0.035	149	0.720	0.024
h	-	-	-	177	0.789	0.024
i	-	-	-	202	0.575	0.020
j	-	-	-	216	0.705	0.025

	Sample 3 Nominal Composition (Wt%) C = 0.68, S = 0.030			Sample 4A Nominal Composition (Wt%) C = 0.12, S = 0.028		
a	0	0.723	0.025	0	0.429	0.026
b	26	0.731	0.038	30	0.413	0.035
c	45	0.729	0.030	42	0.426	0.032
d	66	0.697	0.027	57	0.420	0.032
e	90	0.753	0.036	77	0.430	0.030
f	119	0.733	0.034	105	0.429	0.029
g	145	0.587	0.024	120	0.446	0.026
h	163	0.797	0.023	138	0.450	0.032
i	186	0.593	0.027	151	0.456	0.033
j	-	-	-	175	0.467	0.030
k	-	-	-	199	0.482	0.033
l	-	-	-	211	0.480	0.030

able 5.6 (Contd.)

ocation	Sample 4B Nominal Composition (Wt%) C = 0.12, S = 0.028			Sample 5A Nominal Composition (Wt%) C = 0.14, S = 0.033		
	Length (mm.)	Wt% C	Wt% S	Length (mm.)	Wt% C	Wt% S
a	0	0.154	0.027	0	0.163	0.050
b	19	0.144	0.033	46	0.149	0.031
c	40	0.138	0.034	72	0.158	0.049
d	61	0.144	0.034	91	0.143	0.065
e	80	0.144	0.029	114	0.155	0.046
f	100	0.142	0.035	147	0.170	0.045
g	119	0.143	0.033	172	0.201	0.045
h	137	0.144	0.032	184	0.227	0.049
i	157	0.143	0.034	216	0.216	0.049
j	179	0.144	0.030	-	-	-
k	197	0.119	0.027	-	-	-
l	215	0.147	0.034	-	-	-
	Sample 5B Nominal Composition (Wt%) C = 0.14, S = 0.033			Sample 6A Nominal Composition (Wt%) C = 0.08, S = 0.048		
a	0	0.163	0.043	0	0.161	0.095
b	23	0.159	0.056	16	0.164	0.087
c	39	0.136	0.037	30	0.176	0.094
d	67	0.138	0.033	45	0.163	0.085
e	82	0.147	0.042	58	0.192	0.085
f	103	0.134	0.040	73	0.189	0.096
g	114	0.143	0.046	89	0.170	0.092
h	130	0.137	0.045	111	0.168	0.097
i	146	0.136	0.046	125	0.163	0.088
j	160	0.131	0.045	146	0.170	0.092
k	188	0.129	0.043	167	0.172	0.097
l	200	0.137	0.046	180	0.187	0.100
m	-	-	-	202	0.192	0.106
n	-	-	-	221	0.178	0.091

Table 5.6 (Contd.)

Location	Sample 6B Nominal Composition (Wt%) C = 0.08, S = 0.048 Lenght (mm.)	Wt% C	Wt% S	Sample 7A Nominal Composition (Wt%) C = 0.175, S = 0.040 Lenght (mm.)	Wt% C	Wt% S
a	0	0.124	0.077	0	0.163	0.055
b	11	0.113	0.080	18	0.203	0.071
c	37	0.115	0.092	27	0.195	0.068
d	53	0.132	0.096	40	0.192	0.045
e	70	0.124	0.094	56	0.175	0.057
f	91	0.123	0.087	77	0.169	0.056
g	112	0.104	0.079	94	0.198	0.062
h	130	0.127	0.106	112	0.215	0.066
i	160	0.115	0.088	122	0.199	0.056
j	172	0.105	0.081	134	0.190	0.061
k	185	0.125	0.101	148	0.209	0.062
l	-	-	-	162	0.193	0.058
m	-	-	-	184	0.174	0.055
n	-	-	-	195	0.198	0.059

Location	Sample 7B Nominal Composition (Wt%) C = 0.175, S = 0.040 Lenght (mm.)	Wt% C	Wt% S
a	0	0.168	0.043
b	18	0.166	0.044
c	31	0.172	0.031
d	52	0.171	0.038
e	72	0.166	0.038
f	93	0.171	0.043
g	122	0.177	0.042
h	138	0.179	0.046
i	152	0.179	0.044
j	173	0.168	0.043

5.2.1 Nature of segregation profiles

From the analysis results, segregation ratios for carbon and sulphur were calculated using the following formula,

Segregation ratio of solute i (r_i)

$$= \frac{\text{composition of solute i at the drill position (wt\%)}}{\text{Nominal composition of solute i (wt\%)}} \quad \ldots 5.2$$

Nominal compositions were obtained from analyses of molten steel in the plant as presented in Table 5.6. The segregation ratios of carbon and sulphur are denoted as r_C and r_S respectively. Figs.5.16 to 5.26 present the profiles of r_C and r_S along the centreline in the longitudinal sections of all 11 billet samples.

The fluctuating nature of the segregation profiles were observed in all samples. It is consistent with literature findings (Sec.2.4), and is due to alternating positive and negative segregation bands along the centreline of continuously cast products. As the sulphur prints reveal these segregation bands were not uniform along the centreline. The drill diameters were 8 mm. in Tata Steel samples and 4 mm. in Haryana Concast samples. Therefore the drillings included both positive as well as negative segregation regions.

In view of non-uniformity along the centreline, average composition of one drilling is not expected to have any correlation with other drillings. That is why the profiles are to be treated as discrete points joined by straight lines rather

than smooth curves.

Samples 4A and 4B were from the same heat and hence same nominal composition. However, the r_C values of carbon in sample 4A was abnormally large. This was an exceptional case, as in all other samples both the sulphur and carbon profiles followed similar trend (either intersecting or very near to each other). The maximum segregation ratios for both carbon and sulphur were more than 1 in general. This was in agreement with many investigators(6,20,22,31) in the literature and is generally expected. However, in sample 2 maximum r_S which is denoted as $r_{S,max.}$ was 0.98 only. Similarly in sample 4A, maximum r_C (denoted as $r_{C,max.}$) was 4.2. The reasons for these discrepancies, particularly in sample 4A were not clear. The analyses of drillings were checked more than once and there was no problem in obtaining reproducibility.

5.2.2 Comparison of segregation profiles with sulphur prints

In Figs.5.16 to 5.26 the characteristics of each location (indicated by symbols a,b,c,d.....), as revealed by sulphur prints, are also presented below each profile. A rating system is proposed to correlate the characteristics of each location as revealed by sulphur prints with segregation ratios determined from chemical analysis. In this rating system, 1 corresponds to the location predominently dark, 3, predominently white, and 2, in between 1 and 3.

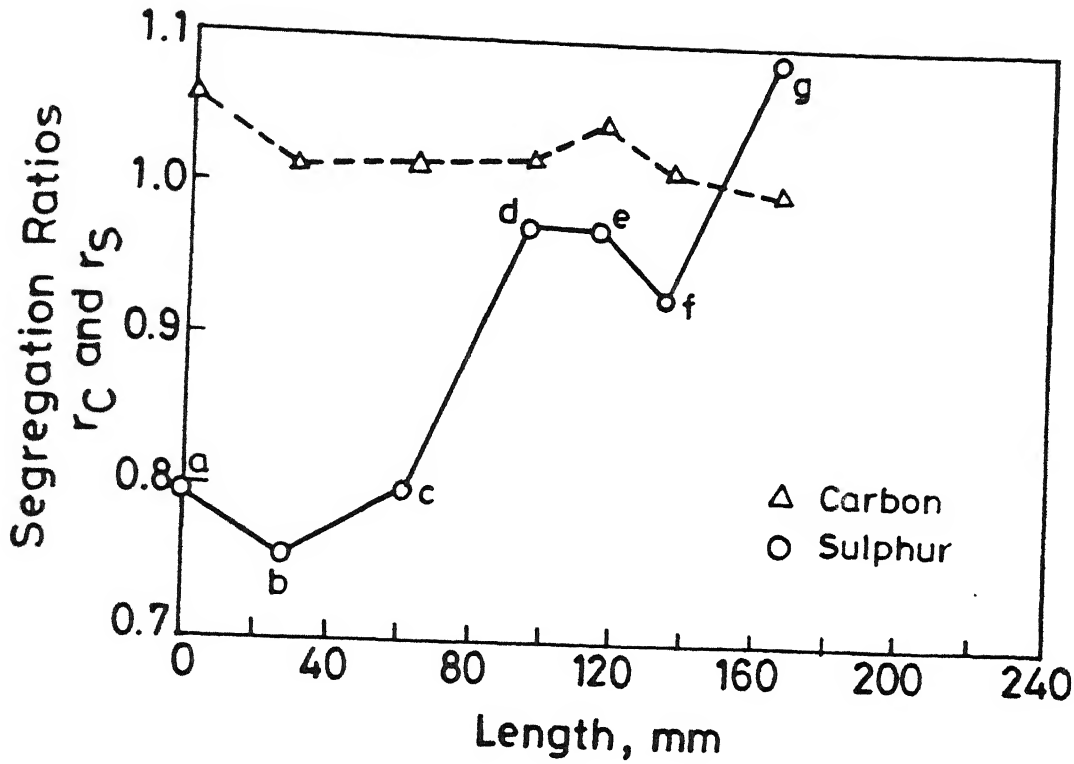

Fig.5.16 Segregation profiles for carbon and sulphur along the centreline of sample 1.

Location	Rating	Characteristics	Matching
a	2	light spot inside V-line	N
b	1	predominantly dark spot with columnar bridge	N
c	2	light black spot inside V-line	Y
d	2	black spot with fine porosity	N
e	1	predominantly dark spot	Y
f	3	predominantly white spot inside V-line	Y
g	1	predominantly dark spot	Y

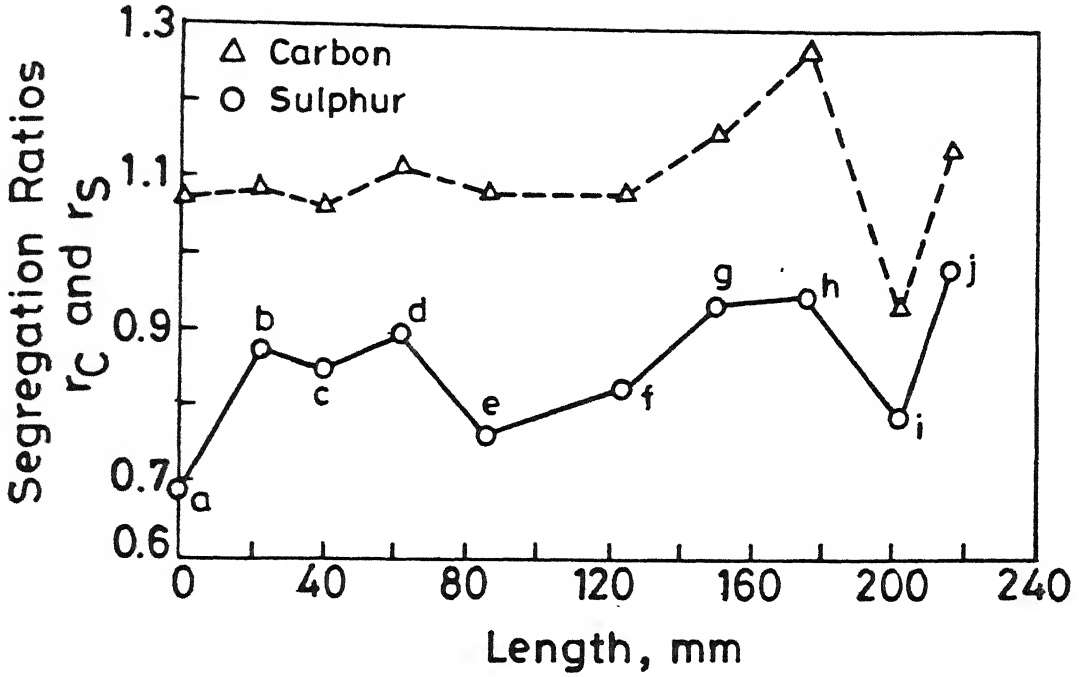

Fig. 5.17 Segregation profiles for carbon and sulphur along the centreline of sample 2.

Location	Rating	Characteristics	Matching
a	2	light spot with porosity	N
b	2	dark spot with porosity	N
c	3	predominantly white spot	Y
d	1	predominantly dark spot with porosity	Y
e	2	dark spot inside V-line	N
f	2	black spot inside V-line	Y
g	2	dark spot	Y
h	3	predominantly white spot near V-line	N
i	3	predominantly white spot inside V-line	Y
j	1	predominantly dark spot	Y

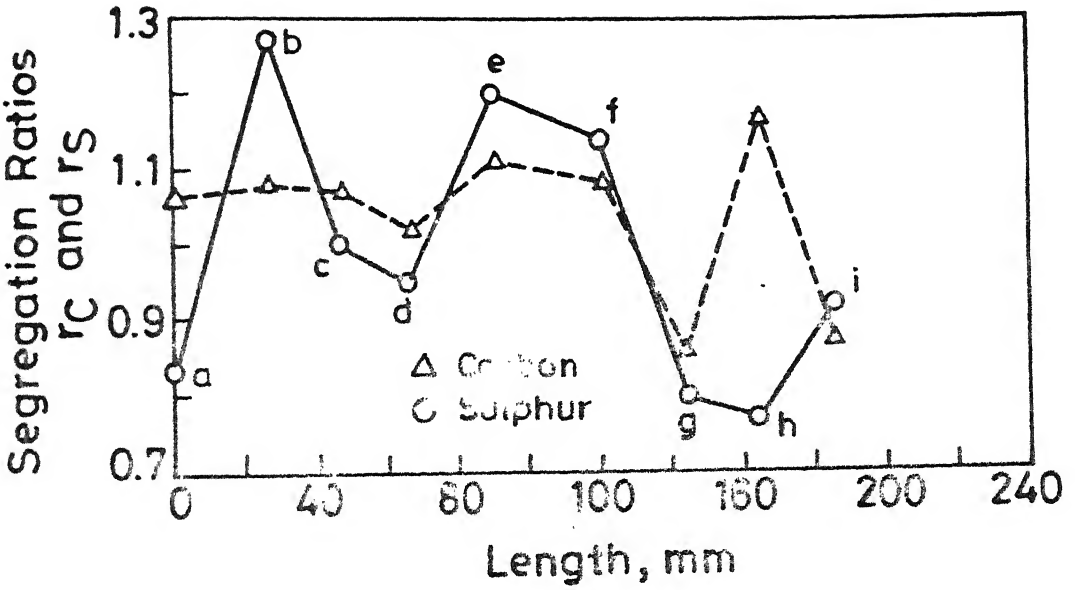

Fig.5.18 Segregation profiles for carbon and sulphur along the centreline of sample 3.

Location	Rating	Characteristics	Matching
a	2	faint dark spot with columnar bridge	N
b	3	predominantly white spot	N
c	3	predominantly white spot with columnar bridge	Y
d	3	predominantly white spot	Y
e	3	predominantly white spot at closed end of V-line	N
f	2	black spot with pipe	N
g	1	predominantly dark spot with columnar bridge	Y
h	1	predominantly dark spot	N
i	1	predominantly dark spot with columnar bridge	Y

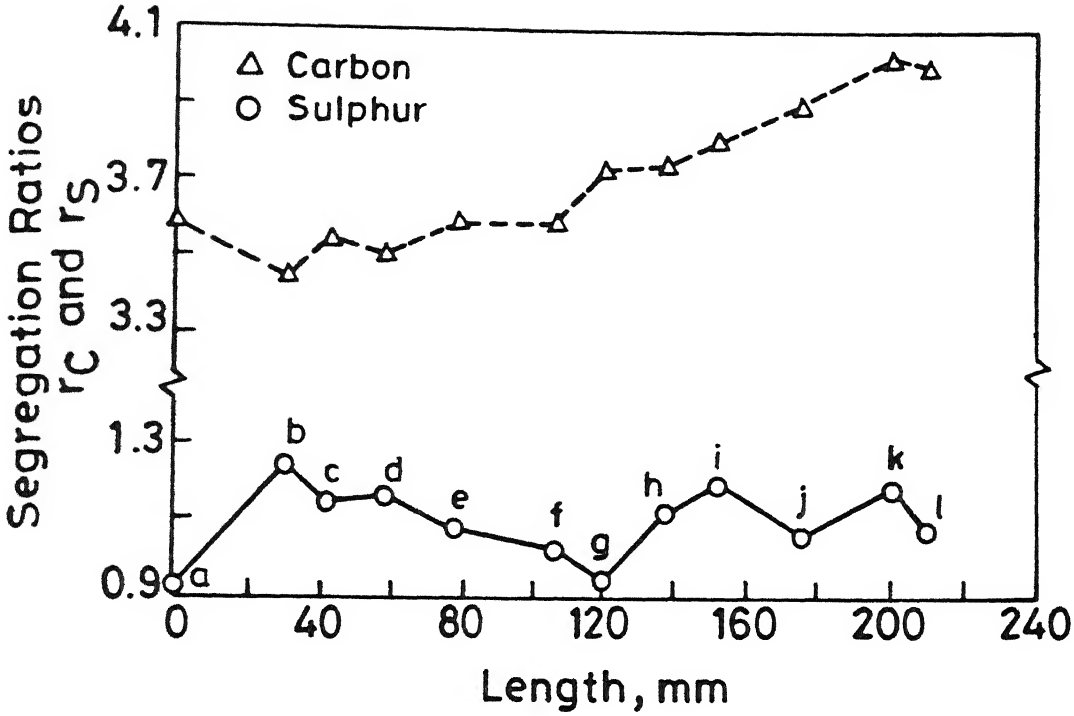

Fig.5.19 Segregation profiles for carbon and sulphur along the centreline of sample 4A.

Location	Rating	Characteristics	Matching
a	3	predominantly white spot with columnar bridge	Y
b	1	predominantly dark spot with columnar bridge	Y
c	3	predominantly light spot insie V-line	Y
d	2	light spot with columnar bridge inside V-line	N
e	3	predominantly white spot with columnar bridge and porosity	N
f	2	white spot inside V-line with porosity	Y
g	3	predominantly white spot inside V-line with appreciable porosity	Y
h	2	dark spot with porosity	Y
i	1	predominantly dark spot inside V-line with columnar bridge and porosity	Y
j	2	white spot inside V-line with porosity	N
k	2	white spot inside V-line with columnar	N

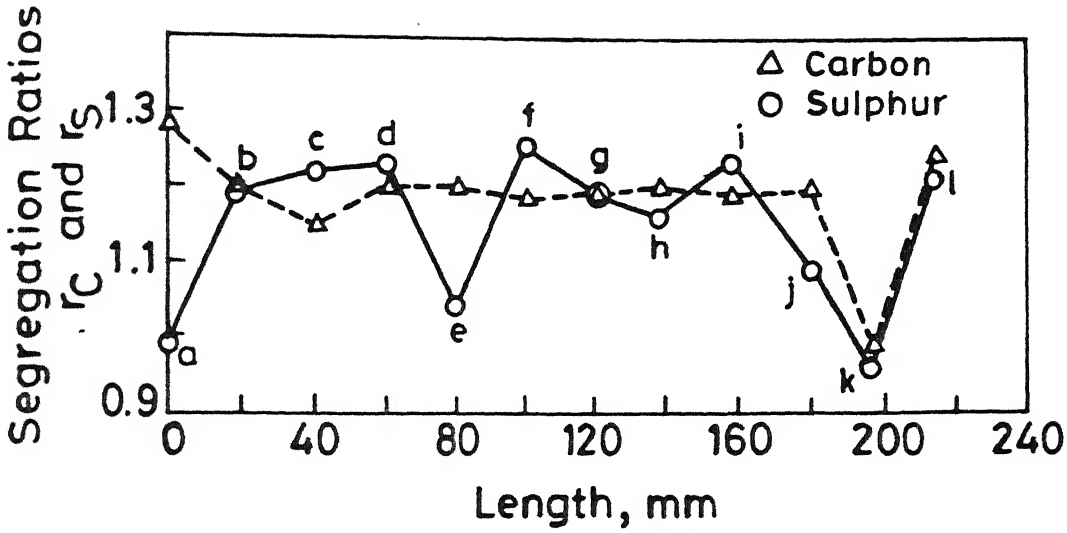

Fig. 5.20 Segregation profiles for carbon and sulphur along the centreline of sample 4B.

Location	Rating	Characteristics	Matching
a	3	predominantly white spot with columnar bridge	Y
b	2	dark spot at closed end of V-line	Y
c	3	predominantly light spot	N
d	2	predominantly dark spot at closed end of V-line	N
e	3	predominantly white spot	Y
f	1	predominantly dark spot with columnar bridge at closed end of V-line	Y
g	3	predominantly white spot	N
h	3	predominantly white spot inside V-line	Y
i	2	dark spot with porosity	N
j	1	predominantly dark spot inside V-line	N
k	3	predominantly white spot outside V-line	Y
l	1	predominantly dark spot with porosity	Y

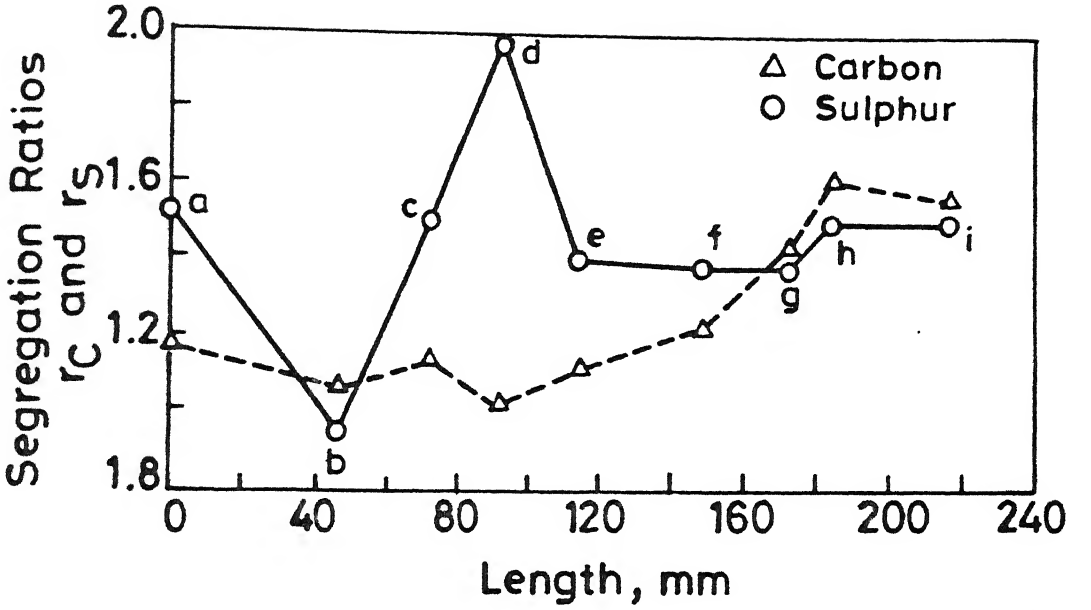

Fig. 5.21 Segregation profiles for carbon and sulphur along the centreline of sample 5A.

Location	Rating	Characteristics	Matching
a	3	predominantly white spot inside V-line with columnar bridge	N
b	2	white spot inside V-line	N
c	2	light spot	Y
d	1	predominantly dark spot	Y
e	2	dark spot with porosity and columnar bridge	Y
f	1	predominantly dark spot with porosity	N
g	3	predominantly white spot	Y
h	2	white spot inside V-line	N
i	1	predominantly dark spot	Y

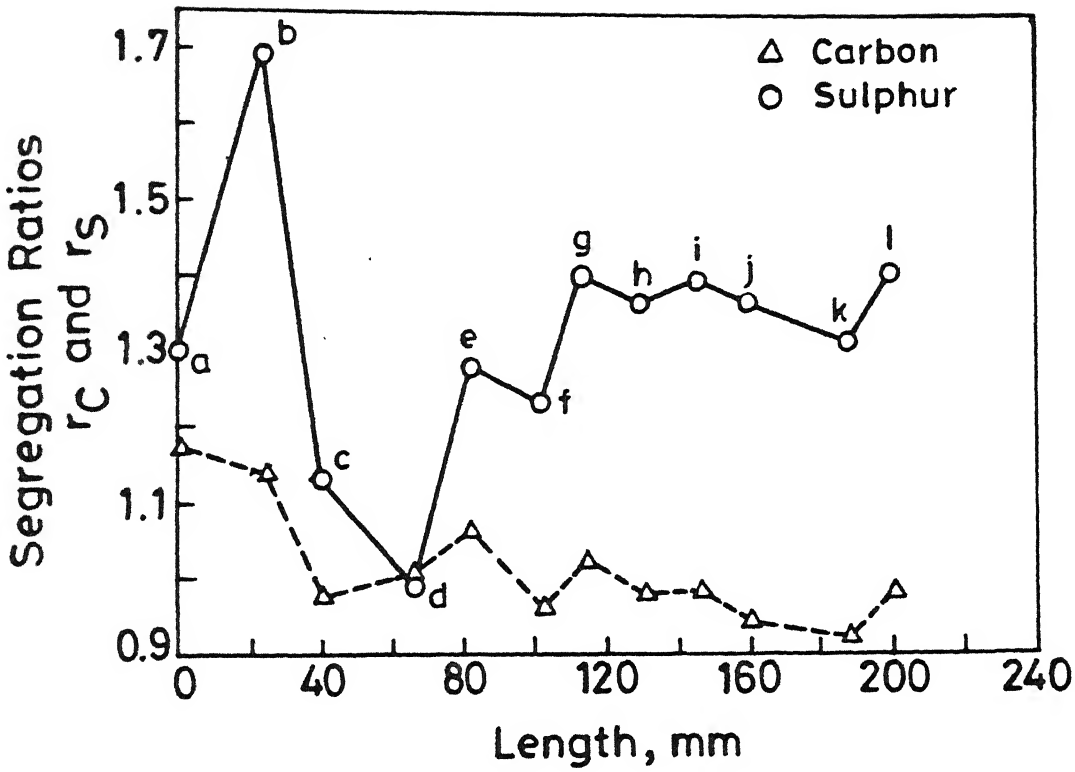

Fig.5.22 Segregation profiles for carbon and sulphu along the centreline of sample 5B.

Location	Rating	Characteristics	Matchin
a	3	predominantly white spot	Y
b	2	dark black spot	N
c	2	light spot inside V-line	Y
d	2	dark spot	N
e	1	predominantly dark spot	Y
f	3	predominantly white spot	Y
g	3	predominantly white spot inside V-line	N
h	3	predominantly white spot	Y
i	2	dark spot at closed end of V-line	N
j	2	dark spot at closed end of V-line	Y
k	3	predominantly white spot	Y
l	2	black spot at closed end of V-line	N

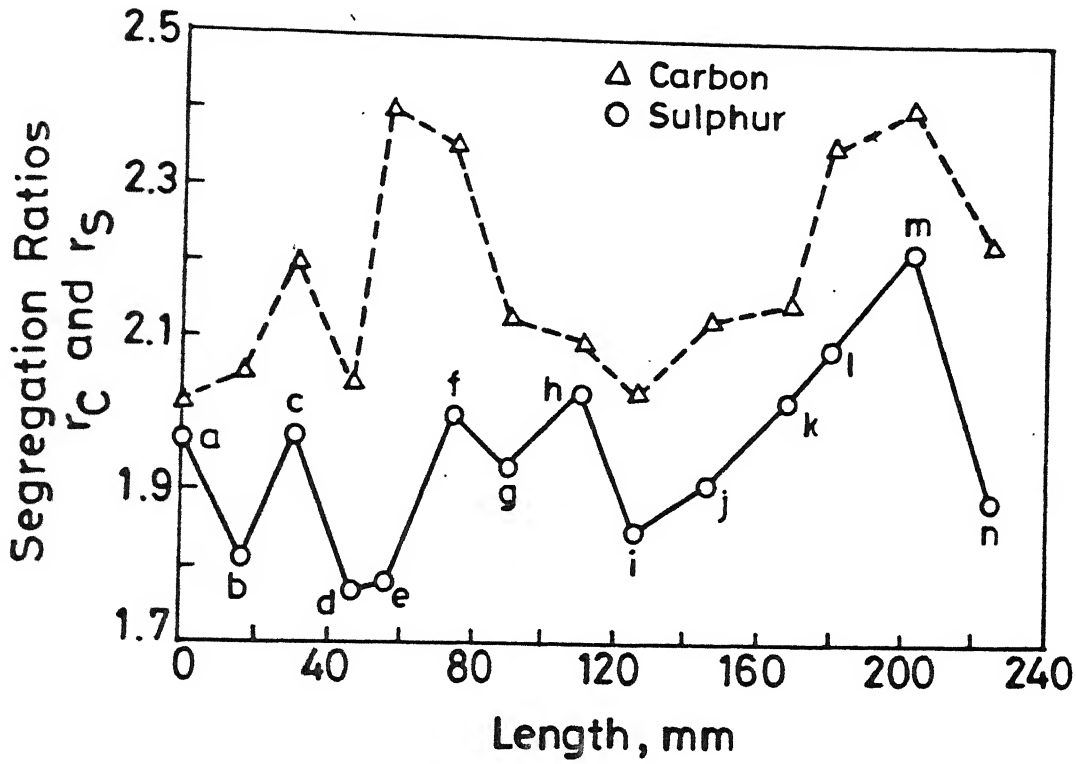

Fig. 5.23 Segregation profiles for carbon and sulphur along the centreline of sample 6A.

Location	Rating	Characteristics	Matching
a	1	predominantly dark spot inside V-line	Y
b	2	dark spot with columnar bridge	N
c	3	predominantly white spot with porosity	N
d	3	predominantly light spot inside V-line	Y
e	2	dark spot with porosity	Y
f	2	light spot with porosity at closed end of V-line	N
g	3	predominantly white spot	Y
h	1	predominantly dark spot with porosity	Y
i	1	predominantly dark spot	N
j	2	black spot	Y
k	1	predominantly dark spot	N
l	2	light spot	Y
m	1	predominantly dark spot with columnar bridge	Y
n	3	predominantly white spot inside V-line	Y

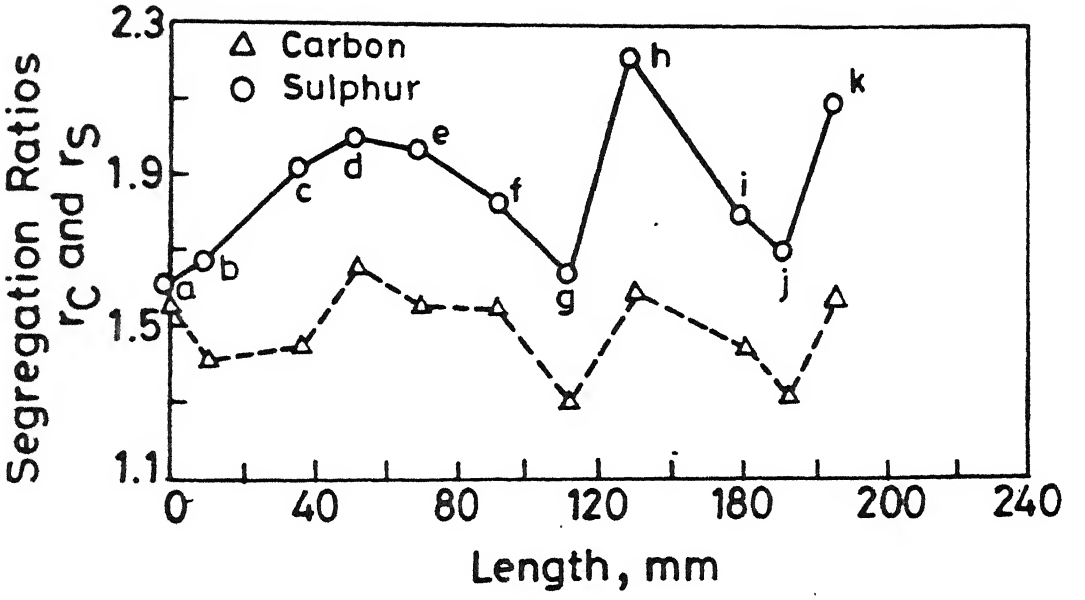

Fig.5.24 Segregation profiles for carbon and sulphur along the centreline of sample 6B.

Location	Rating	Characteristics	Matching
a	3	predominantly light spot with columnar bridge	Y
b	2	dark black spot	Y
c	2	dark balck spot with columnar bridge	Y
d	2	dark spot	N
e	2	dark spot with columnar bridge	Y
f	2	dark spot with columnar bridge	Y
g	1	predominantly dark spot	N
h	2	dark spot	N
i	2	light spot	Y
j	1	predominantly dark spot with columnar bridge	N
k	1	predominantly dark spot with columnar bridge	Y

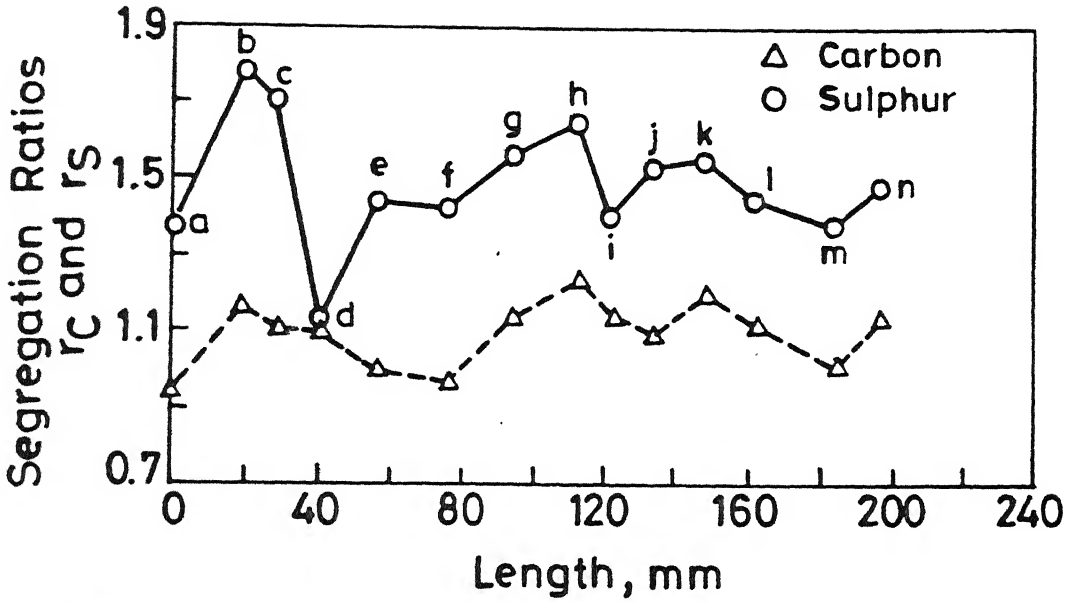

Fig.5.25 Segregation profiles for carbon and sulphur along the centreline of sample 7A.

Location	Rating	Characteristics	Matching
a	1	predominantly dark spot	N
b	1	predominantly dark spot with columnar bridge and porosity	Y
c	1	predominantly dark spot with columnar bridge	N
d	2	white spot inside V-line	N
e	2	dark spot	Y
f	3	predominantly white spot at V-line with porosity	Y
g	2	black spot with columnar bridge	Y
h	2	dark spot with porosity	N
i	1	predominantly dark spot	N
j	2	dark black spot at V-line with columnar bridge	Y
k	2	faint drak spot	N
l	2	dark spot	Y
m	3	predominantly dark spot inside V-line	Y
n	3	predominantly white spot at closed end of V-line	N

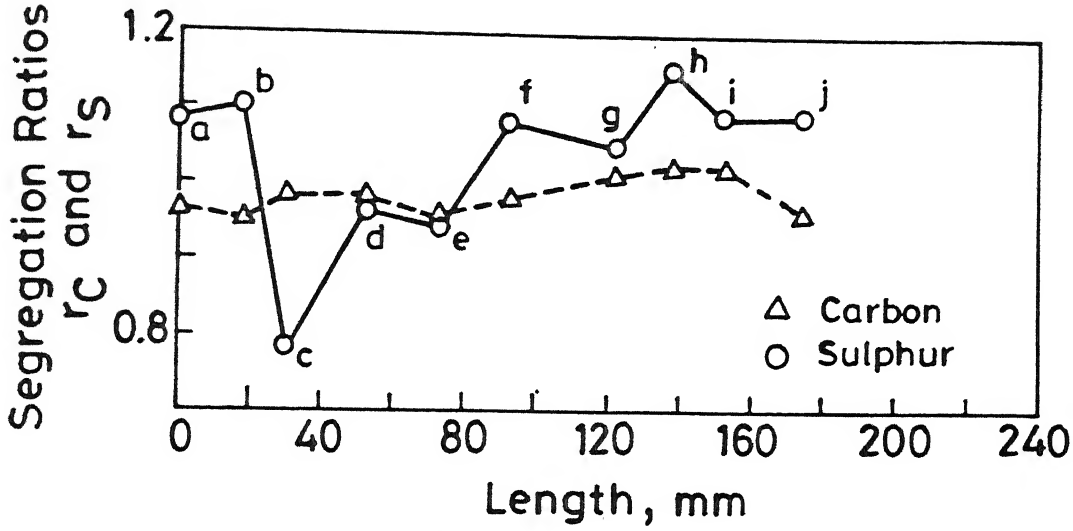

Fig. 5.26 Segregation profiles for carbon and sulphu
along the centreline of sample 7B.

Location	Rating	Characteristics	Matching
a	2	dark black spot	Y
b	1	predominantly dark spot	Y
c	3	predominantly light spot	Y
d	2	dark spot at closed end of V-line	N
e	1	predominantly dark spot at closed end of V-line	N
f	1	predominantly dark spot	Y
g	3	predominantly white spot inside V-line	Y
h	1	predominantly dark spot inside V-line	Y
i	1	predominantly dark spot	N
j	2	dark spot	Y

The comparison of the ratings with segregation ratios of sulphur and carbon is presented along with the figures of segregation profiles (Figs.5.16 to 5.26). The procedure adopted for comparison was as follows.

(i) If rating 1 corresponds to peaks in the sulphur profile then matching is denoted by 'Y' (meaning Yes).

(ii) If rating 3 corresponds to troughs in the sulphur profile then matching is denoted by 'Y' (meaning Yes).

(iii) If rating 2 corresponds to middle segregation ratios in the sulphur segregation profile then matching is denoted by 'Y' again.

(iv) In all other cases matching is denoted by 'N' (meaning No).

Since the rating system is on the basis of sulphur prints, this comparison was done only for sulphur segregation and not for carbon segregation. Following the procedure above, the total number of 'Y' is 70 and that of 'N' is 50. Therefore, the point analyses are showing some agreement with expectations from sulphur prints. However, there were mismatches too. The mismatching may be explained as due to the following reasons.

(i) Presence of even a small sulphide inclusion on the surface may produce a big dark spot (hence rating 1) due to the more spreading of H_2S gas.

(ii) Sulphur prints show distribution of sulphur on the etched surface only. Below the surface there might be inclusions of sulphides, pores or negative segregation zones. The drillings (8 mm. and 4 mm. diameter) were

made upto a depth of 8 mm. from the surface and hence some averaging out in the composition was involved.

5.2.3 Quantitative correlations

As mentioned in the literature (Sec.2.1), the extent of macrosegregation of different solutes would not be the same due to the different values of equilibrium partition coefficients (K_e) for each element. However, correlations are expected for centreline segregation of various elements at the same spot amongst elements due to some common factors such as movement of fluid and solid. Some empirical correlations were proposed by Kawamoto(14). These have already been presented in Fig.2.1 in Chapter 2.

Fig.5.27 presents the plot between r_C and r_S for low carbon steel samples (4A, 4B, 5A, 5B, 6A, 6B, 7A and 7B). The best fit line of Kawamoto(14) is also included. It may be noted that most of the data of present study were scattered around the literature line, and hence the present findings were qualitatively consistent with the literature report. The scatter is attributed primarily due to presence of precipitates such as sulphides and carbides. The extent of such compound formation are expected to be considerably different for carbon and sulphur.

However, in the literature there was no separate correlation between r_C and r_S for different grades of carbon steels. In the present investigation, a separate correlation was made for medium carbon and high carbon steel (samples 1,2 and 3). From Fig.5.28 it is clear that actual data points were not close to the literature line. No explanation for this mismatch is being

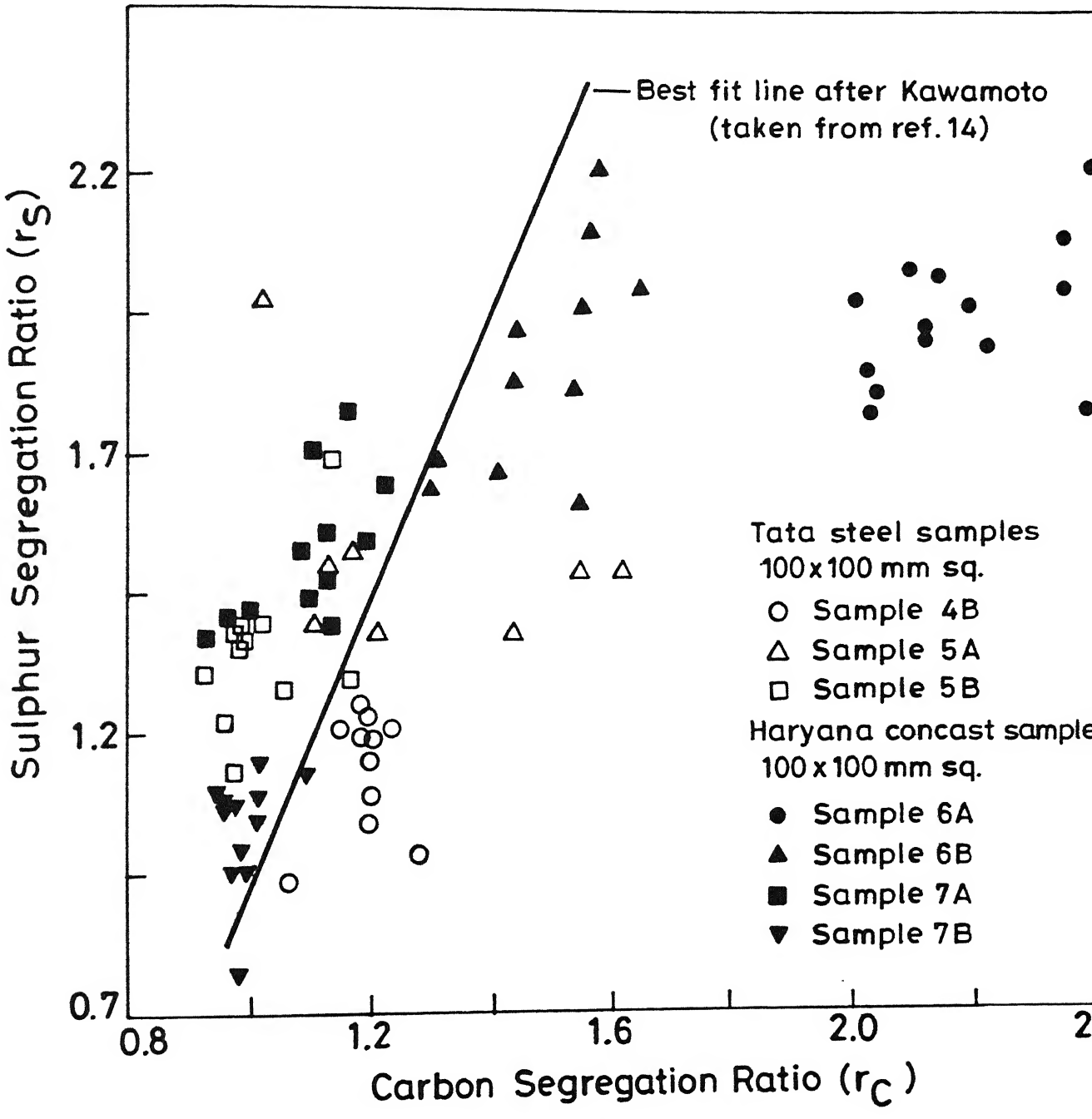

Fig. 5.27 Relationship between r_C and r_S for low carb steel samples.

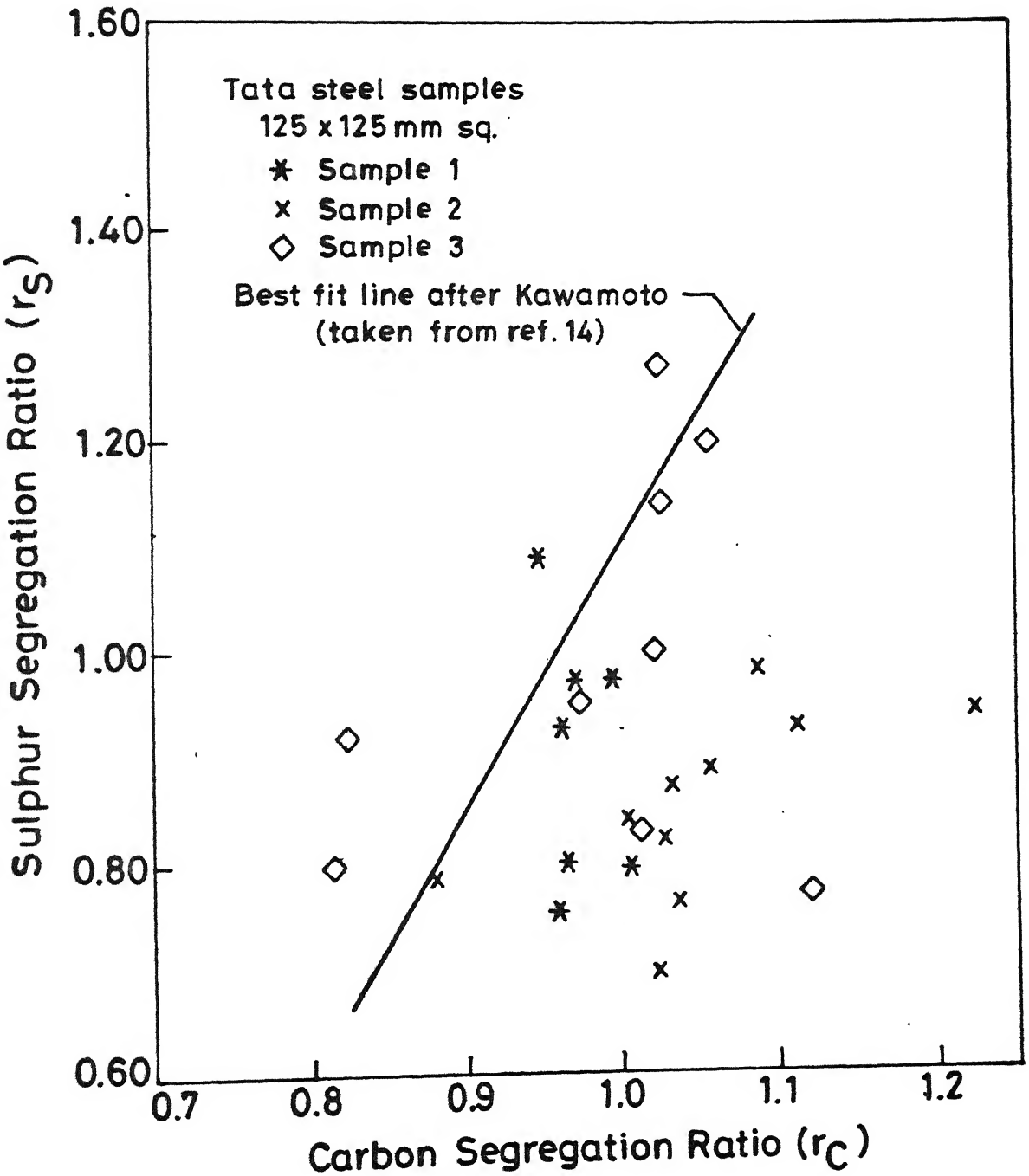

Fig.5.28 Relationship between r_C and r_S for high carbon steel samples.

provided. The data points are also limited.

Fig.5.29 shows a plot between $r_{C,max.}$ and $r_{S,max.}$ for all 11 samples. Most of the data are scattered around the literature line.

According to literature, more the superheat (ΔT), more is the extent of fluctuation in the segregation profiles of elements. As mentioned earlier (Sec.5.1.2.1), ΔT values for samples of Haryana Concast are unreliable. Hence only data for Tata Steel were plotted and no trend could be observed and data are very limited. Hence no attempt was made to correlate the extent of fluctuation in segregation profiles with superheat.

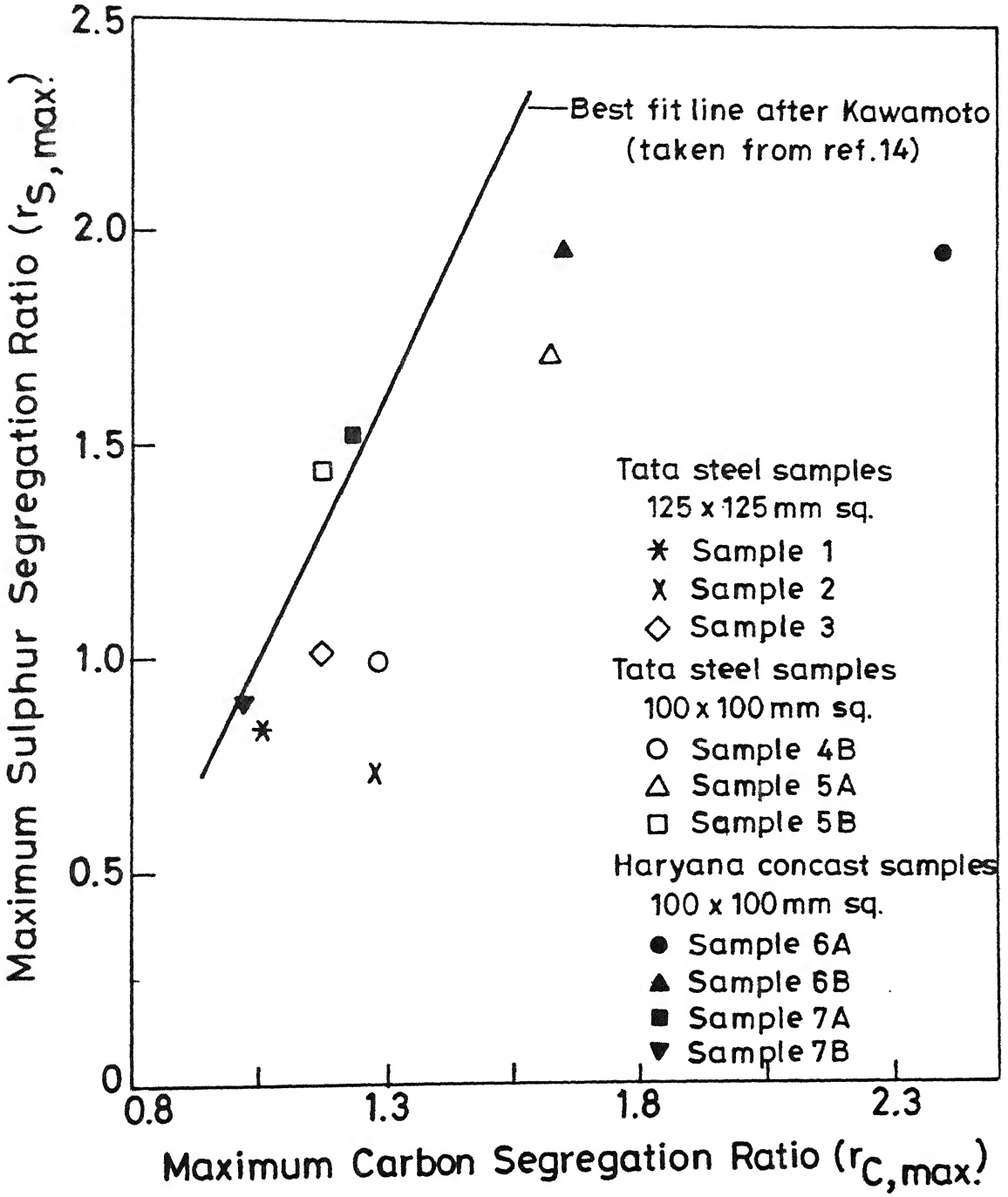

Fig.5.29 Relationship between $r_{C,max.}$ and $r_{S,max.}$

CHAPTER 6

SUMMARY AND CONCLUSIONS

The present investigation is concerned with macrosegregation along the centrelines of longitudinal sections of CC billet samples. The work consisted of :

(i) data and sample collection from steel plants,

(ii) study of longiitudinal sections of samples, sliiced through billet axes, using sulphur printing techniique and chemical analysis of carbon and sulphur.

Chemical analyses were carried out by an automatic carbon and sulphur determinator at the National Metallurgical Laboratory, Jamshedpur. Samples for analysis were collected by drilling selected spots on the centrelines of billet sections. A total of 11 samples of carbon steel billets, 100x100 mm. sq. and 125x125 mm.sq. section size and 150 to 250 mm. in length, obtained from Tata Steel and Haryana Concast were studied. Various kinds of observations were made on polished surfaces as well as sulphur prints. Based on the experimental results, following conclusions were made.

6.1 Physical Examinations of Billet Sections

(i) The quality of the sulphur prints made by Baumann's method was satisfactory as compared to those made after preetching of surface. Former reveals the segregation pattern as well as cast structure in a better way.

(ii) Photocopies of sulphur prints were better in revealing the centreline segregation as compared to the original prints.

(iii) Fine pores were observed in both Tata Steel and Haryana Concast samples, whenever superheat was modererately high. In one sample (No.3) cast at high superheat ($105^{o}C$), the centreline porosity took the form of a prominent central pipe.

(iv) Columnar zone was found to be dominant at higher superheats almost in all samples. Some samples cast at lower superheat revealed very large equiaxed zones.

(v) There was less variation in the width of the central segregated zone in the Haryana Concast samples as compared to the same in Tata Steel samples.

(vi) There was a trend of positive centreline segregation zone towards becoming narrow and prominent with increasing superheat in almost all samples.

(vii) At the same section size (100x100 mm. sq.), samples collected at Haryana Concast showed V- lines rather than V- bands as observed in the samples from Tata Steel. In one sample (No.3) with large superheat, a prominent U- band was observed. Samples of section size (125x125 mm. sq.) from Tata Steel revealed broad and conspicuous V- lines.

(viii) V- shaped negative segregation zones in between positive segration were observed in almost all samples.

(ix) Bridging appeared to be increasing with the increase in superheat in the samples collected at Tata Steel.

(x) Comparisons were made with literature reports wherever possible.

6.2 Segregation Profiles

(i) Carbon and sulphur segregation profiles were fluctuating in nature, and this observation was in conformity with the literature. Nature of profiles varied from billet to billet. An attempt was made to correlate sulphur prints with the corresponding centreline segregation data in a qualitative fashion.

(ii) Maximum segregation ratios for carbon (r_C) and sulphur (r_S) were 2.4 and 2.2 respectively. Minimum segregation ratios for C and S were 0.86 and 0.77, respectively. This excludes sample 4A which exhibited some abnormal results.

(iii) The correlation between r_C and r_S was in agreement with the literature for low carbon steels only.

(iv) No attempt was made for quantitative correlation with superheat of melt due to limited data and large scatter.

CHAPTER 7

SUGGESTIIONS FOR FUTURE WORK

(i) Correlations amongst centreline segregation of other elements e.g. manganese, phosphorous etc. can be studied at the same casting conditions in different types of continuously cast products.

(ii) Alloy steel can also be studied for the segregation behaviour of alloying elements.

(iii) A similar investigation can be conducted on blooms and slabs of different size and shape.

(iv) A quantitative study of segregation can also be made directly from the sulphur prints by using computer-aided image analyser.

(v) Influence of heat transfer, thermal conditions, and bulging and fluid flow on the segregation can be studied by using mathematical/physical modeling or by doing experiments like nailing, autoradiography etc.

REFERENCES

1. N. Islam, Metals and Materials, **5**, (July. 1989), p.392.
2. M.G. Brooks, Proc.of Conf.on Solidification Processing, The Institute of Metals, London, (1988), p.231.
3. J. Barbe et al, Cah.Inf.Tech.,**87**, (July.-Aug. 1990), p.653 (Metal Abstract No.51-1746-9011)
4. U. Chatterjee and S. Basu, Proc.of International Symposium on Modern Developments in Continuous Casting, IIM-SAIL, New Delhi, (Nov. 1988), p.259.
5. O.P. Nagpal and S.L. Narasimhan, in ref.4, p.39.
6. H. Mori et al, Trans. ISIJ, **12**, (1972), p.102.
7. J.J. Moore, Continuous Casting, ed. J.J. Moore, ISS-AIME, **3**, (1984), p.11.
8. L. Schmidt and H. Fredriksson, Ironmaking and Steelmaking, **2**, (1975), p.61.
9. R.W. Welburm and D.J. Naylor, Continuous Casting, International Conf. Proc., The Metals Society, London, (1985), p.13.1.
10. A. Ghosh, **Principles of Secondary Processing and Casting of Liquid Steel**, Oxford and IBH Publishing Co.Pvt.Ltd., New Delhi, (1990).
11. S. Myoshi, Continuous Casting of Steel, International Conf. Proc., The Metals Society, London, (1977), p.286.
12. T.K. Roy, M.Tech.Thesis, Dept. of Metallurgical Engg., IIT Kanpur, (1990).
13. M.C. Flemings, **Solidification Processing**, McGraw Hill Book

14. J.J. Moore and J.C. Hamilton, in **Continuous Casting of Small Cross Section**, ed. Y.V. Murty, AIME, (1981), p.75.

15. M.C. Flemings, Elliott Symposium Proceedings, (1990), p.253.

16. A. Ohno and H. Sōda, Trans. ISIJ, **10**, (1970), p.13.

17. M.C. Flemings and G.E. Nereo, Trans. TMS-AIME, **239**, (1967), p.1449.

18. K. Suzuki and T. Miyamoto, Trans. ISIJ, **14**, (1974), p.296.

19. D. Ameling et al, Steelmaking Proc., ISS-AIME, **69**, (1986), p.387.

20. P.K. Sung et al, Ironmaking and Steelmaking, **17**, (Jan. 1990), p.424.

21. J.P. Birat et al, Continuous Casting, International Conf. Proc., The Institute of Metals, London, (1985), p.18.1.

22. N.A. Shah and J.J. Moore, 5th International Iron and Steel Congress, TMS-AIME, (April 1986), p.791.

23. J.E. Lait et al, Continuous Casting, ed. J.K. Brimacombe, I.V. Samarsekera and J.E. Lait, ISS-AIME, 2, (1984), p.169.

24. H.S. Marr, International Symposium on Casting and Solidification of Steel, Commission of European Communities, IPC Science and Technology Press Ltd., Guilford, U.K., **1**, (1977), p.338.

25. T. Ohashi et al, Trans. ISIJ, **15**, (1975), p.571.

26. K. Miyamura et al. Trans. ISIJ, **24**, (1984), p.718.

27. H. Fredriksson and B. Rogberg, Continuous Casting of Steel, Proc. 4th International Iron and Steel Congress, The Metals Society, London, (1982), p.C3/1.

28. K. Miyazawa and K. Schwerdtfeger, Anch. Eisenhuttenwes, **52**, (1981), p.415.

29. A.O. Benscoter, Metallography and Microstructure, Metals Handbook, ASM, **9**, (1985), p.171.

30. N.N. Druzhinin et al, Steel in the USSR, **13**, (Sept. 1983), p.397.

31. H. Iwata et al, Trans. ISIJ, **16**, (1976), p.374.

32. T.K. Roy et al, Trans. IIM (In Press).

33. H. Tomono et al, Steelmaking Proceedings, **69**, ISS, USA, (1986), p.371.

34. N.I. Revtov et al, Steel in the USSR, **17**, (April 1987), p.164.

35. J.E. Haggart et al, Ironmaking and Steelmaking, **17**, (Feb. 1990), p.130.

36. K. Takeo and H. Iwata, Wire Journal, (Aug. 1971), p.32.

37. B.L. Bramfitt, in ref.29, p.623.

38. E.A. Kazachkov et al, Steel in the USSR, **15**, (Oct. 1985), p.469.

39. J.K. Brimacombe and K. Sorimachi, in ref.23, p.199.

40. F. Weinberg et al, Met. Trans. A, **10A**, (Dec. 1979), p.1923.

41. L. Pochmarski et al, Steel Times, (Oct. 1985), p.504.

42. A. Radjai et al, Trans. ISIJ, **26**, (1986), p.78.

43. R.A. Knights et al, Ironmaking and Steelmaking, **13**, (Jan. 1986), p.32.

44. G.J.W. Kor, Ironmaking and Steelmaking, **9**, (June 1982), p.244.

45. M. Kitamura et al, Steelmaking Conf. Proc., ISS-AIME, **63**, (1980), p.154.

46. M. Komatsu et al, 'Effect of Electromagnetic Stirring on Solidification Phenomena of Steels', p.143.

47. M.R. Bridge and G.D. Rogers, Met. Trans. B, **15B**, (Sept. 1984), p.581.

48. O.V. Nosochenko et al, Steel in the USSR, **15**, (June 1985), p.266.

49. O.V. Nosochenko et al, Steel in the USSR, **18**, (Nov. 1988), p.500.

50. D.W. Bruce et al, Proc. of Conf. on Solidification Processing, The Institute of Metals, London, (1988), p.228.

51. L.K. Chiang, Steelmaking Conf. Proc., **72**, ISS, (1989), p.81.

52. T. Masaoka et al, in ref.51, p.63.

53. M. Suzuki et al, in ref.51, p.115.

54. H. Hattori et al, in ref.51, p.91.

55. T. Komai et al, in ref.33, p.363.

56. O.V. Abramov et al, Steel in the USSR, **15**, (April 1985), p.168.

57. V.M. Parshin et al, Steel in the USSR, **15**, (April 1985), p.171.

58. K. Mills, in ref.29, p.624.

59. V. Voort, **Metallography Principles and Practices**, McGraw Hill Book Co., New York, (1984).

60. G.L. Kehl, **The Principles of Metallograpic Laboratory Practice**, 3rd edition, McGraw Hill Book Co., New York, (1949).

61. JIS Hand Book : **Ferrous Materials and Metallurgy**, Japanese Standards Association, Tokyo, (1973).

62. B.C. Agrawal and S.P. Jain, **A Textbook of Metallurgical Analysis**, 4th edition, Khanna Publisheres, Delhi, (1984).

63. B.G. Thomas et al, Met. Trans. B, **18B**, (March 1987), p.120.